Assessing the Impacts of DER on Customer Voltages Using Smart Meter-Driven Low Voltage Line Models

by

Yiqing (Yolanda) Wang

ORCID ID: 0000-0003-2423-2036

A thesis submitted to The University of Melbourne for the degree of

Master of Philosophy

August 2020

Department of Electrical and Electronic Engineering

Melbourne School of Engineering

This thesis is submitted for the total fulfilment of the degree

ABSTRACT

The rapid adoption of distributed energy resources (DER) in low voltage (LV) networks is driving the need for distribution companies to assess their impacts on customer voltages in any demand/generation condition (also known as what-if analyses). Although this can be done by running conventional power flow analyses, there are two main challenges. The first one is that LV line models (three-phase LV feeder lines and single-phase service lines) are needed. However, the corresponding impedances are often poorly recorded by distribution companies. In other words, the information is incomplete or not available. The second challenge is that, if such studies are needed for operational purposes (calculations in near real time), then implementing power flows to be run for hundreds of LV feeders can be a complex task for distribution companies.

Several studies have attempted to solve the challenges of impedance estimation and simplified voltage calculations, but there are still some gaps. Given the rollout of smart meters in many places, several works have exploited smart meter measurements to estimate impedances of LV line models. However, in most cases, the three-phase nature of LV feeders (i.e. the phase couplings) is not adequately considered; and thus, such approaches cannot cater for the needs of inherently unbalanced LV networks. For the voltage calculations, existing simplified methods are based on the single-phase voltage drop equations and an additional 'unbalanced factor'. Given that the 'unbalanced factor' is determined either empirically or using data-driven techniques that require large amounts of data, such methods cannot be precise or practical enough for their actual implementation by distribution companies.

This thesis proposes a practical approach to determine customer voltages (in what-if analyses) using smart meter-driven LV line models that adequately capture the effects among the three phases. Firstly, impedances (three-phase LV feeder lines and single-phase service lines) are estimated using linearised voltage drop equations and a regression technique. This process exploits historical time-series measurements from smart meters and at the head of the LV feeder and assumes that the customer connectivity and customer phase connection are known. Then, using the linearised voltage drop equations and the estimated impedances, simplified calculations of customer voltages can be carried out for what-if analyses (any demand/generation condition).

The proposed approach is demonstrated on realistic LV networks from Australia and the UK. Impedances are estimated considering realistic weekly historical meter measurements (i.e. active power, reactive power, and voltage magnitudes) with a 15-minute resolution (672 time steps). Voltage calculations (what-if analyses) consider weekly demand and generation profiles with 1-minute resolution (10,080 time steps). Results show a very good accuracy for most of the estimated impedances. More importantly, the calculated voltages are not only highly accurate but are also obtained much faster than with a power flow engine. Consequently, the findings suggest that the proposed approach is accurate and practical enough for its use by distribution companies.

This page is intentionally left blank.

DECLARATION

This is to certify that

1. the thesis comprises only of my original work towards the degree of Master of Philosophy except where indicated in the preface,
2. due acknowledgement has been made in the text to all other material used, and
3. the thesis is less than 50,000 words in length, exclusive of tables, maps, bibliographies, and appendices.

Yiqing (Yolanda) Wang, August 2020

This page is intentionally left blank.

PREFACE

This work was supported by The University of Melbourne. Publications listed below have been carried out in collaboration with Dr Michael Z. Liu (The University of Melbourne).

Publication included in this thesis – Peer reviewed Journal Paper and Conference Paper

[1] Y. Wang, M.Z. Liu, L.F. Ochoa, "Assessing the effects of DER on voltages using a smart meter-driven three-phase LV feeder model", Electric Power Systems Research, Accepted in 2020-05 (In Press).

[2] Y. Wang, M.Z. Liu, L.F. Ochoa, "Assessing the effects of DER on voltages using a smart meter-driven three-phase LV feeder model", 21st Power Systems Computation Conference PSCC 2020, 2020-06/07 29-3, p 8.

The part of the methodology used in this thesis is incorporated in the above paper [1, 2].

Dr Michael Z. Liu provided support with the three-phase linearised voltage drop equations.

Contributions by others to the thesis

"No contributions by others"

Statement of parts of the thesis submitted to qualify for the award of another degree

"None"

This page is intentionally left blank.

DEDICATION

To Jun and Fujian,

my wonderful and loving parents.

Thank you for raising me into the person I am today.

This page is intentionally left blank.

ACKNOWLEDGEMENTS

I would like to express my deepest gratitude to my supervisor Prof. Luis F. Ochoa for his continuous supervision and support throughout the ups and downs of my MPhil. His guidance and feedback over the past years have positively influenced my way of thinking as an engineer and as a mature person.

Furthermore, I would like to thank my friends and colleagues within the Power & Energy Systems group at the University of Melbourne: Arthur, Michael, Dillon, Andreas, William, Kyri, Yue, Han, Guanchi, and Mehdi.

This page is intentionally left blank.

TABLE OF CONTENTS

This page is intentionally left blank.

LIST OF FIGURES

This page is intentionally left blank.

LIST OF TABLES

This page is intentionally left blank.

ABBREVIATIONS

AC	Alternative Current
ADMD	After Diversity Maximum Demand
APE	Absolute Percent Error
BES	Battery Energy Storage
DC	Direct Current
DER	Distributed Energy Resources
DoD	Depth of Discharge
EVs	Electric Vehicles
Li-ion	Lithium Ion
LV	Low Voltage
MLR	Multiple Linear Regression
NEM	National Electricity Market
OLS	Ordinary Least Squares
PMU	Phasor Measurement Unit
PV	Solar Photovoltaic
V2G	Vehicle-to-Grid

Symbols

L	Three-phase Lines
S	Single-phase Service Lines
N	Buses
Φ	Phases
V	Voltage Magnitudes of Three-phase Lines
v	Voltage Magnitudes of Smart Meters
Θ	Voltage Angles
T	Time
p	Active Power of Smart Meters
q	Reactive Power of Smart Meters
P	Active Power of Three-phase Lines
Q	Reactive Power of Three-phase Lines
R^s	Self-resistance of Three-phase Lines
R^m	Mutual-resistance of Three-phase Lines
X^s	Self-reactance of Three-phase Lines
X^m	Mutual-reactance of Three-phase Lines
r	Resistance of Single-phase Service Lines
x	Reactance of Single-phase Service Lines
$\vec{I}$	Current of Three-phase Lines
$\vec{\imath}$	Current of Single-phase Service Lines

1 INTRODUCTION

The reduction of carbon emissions has been one of the significant challenges of the 21st century. This year, 2020, began with devastating wildfires in Australia, which showed the whole world how climate change is disrupting economies, decreasing the diversity of plants and animals, and threatening human health [1].

Over the past few years, many countries around the world have been making efforts to combat climate change and move toward a carbon-neutral economy by adopting renewable energy [2]. For example, globally, the total solar PV generation has increased by about 187% in the last five years, from 251kWh in 2015 to 720kWh in 2019 [3]. Driven by the declining costs of advanced technologies and expensive electricity bills, there has been an exponential growth in distributed energy resources (DER) in residential low voltage (LV) electricity networks [4].

The main DER are residential photovoltaic (PV) systems, residential battery energy storage (BES) systems, and electrical vehicles (EVs) [5]. The rapid adoption of DER introduces significant challenges for distribution companies to cope with voltage issues in LV networks. Therefore, before tackling these issues, assessing the effects of DER on customer voltages in LV networks (i.e., to perform what-if analyses, in an operational environment, for intended DER injections) is extremely valuable for distribution companies. Although voltages can be determined by running conventional power flow analyses, the main challenges are the lack of knowledge of the underlying LV network model and the complex implementations. Thus, to practically calculate customer voltages (i.e. in what-if analyses), it is necessary to solve these challenges.

To this end, Section 1.1 of this chapter provides an understanding of the characteristics of traditional LV networks, background of DER and smart meters, and the impacts of the high penetration of DER on LV networks. Given the technical issues caused by DER, it is important to perform what-if analyses to understand the extent of DER impacts on LV networks. Section 1.2 discusses that among the main challenges in assessing the extent of DER impacts are the lack of the knowledge of the underlying network model and the complex implementations of power flow analyses. Furthermore, the research questions of the thesis, the main contributions

of the thesis and the publications are presented in Sections 1.3-1.5, respectively. Finally, an outline and abstract of all the chapters of the thesis is given in Section 1.6.

1.1.1 Low Voltage Networks: From Load-Only to Distributed Energy Resources-Rich and Observable

The traditional LV network is a simple load-only network without observability. Along with the growth of DER and smart meters, LV networks have become more complex (i.e. a large number of various DER with different behaviours) and more observable. This section provides an understanding of the characteristics of traditional LV networks, background (current status and technical aspects) of DER and smart meters, and the impacts of DER on traditional LV networks. Given the technical issues caused by DER, this section highlights the importance of performing what-if scenarios to understand the extent of DER impacts on LV networks.

1.1.2 Traditional Low Voltage Networks: Load-Only, No Observability

The traditional network hierarchy (Figure 1-1) is such that the electricity generated from power plants travels from transmission (e.g. 500kV) to distribution networks (e.g. 11kV) before it reaches LV networks (e.g. 400V) [6, 7]. It should be noted that different countries and regions may have different voltage levels, and the commonly used voltages for three-phase LV networks are in the range of 208V to 433V (line to line voltages) [8, 9]. For example, in Australia and European countries, the nominal voltage is required at 400V with a tolerance range that varies per country [10, 11].

In many countries or regions (e.g. Australia, Europe and Asia), LV networks usually have multiple radial LV feeders that are connected with one or more three-phase distribution transformers. These LV feeders, in turn, supply electricity to several customers through service lines [12]. For example, in Figure 1-1, one distribution transformer connects with two LV feeders (blue lines) and three service lines (red lines). LV feeders are usually three-phase, four-wire systems (i.e. three conductors and one neutral) [11]. On the other hand, the characteristics of service lines depend on types of connected customers. Residential loads usually connect with LV feeders via single-phase, two-wire service lines, and commercial or industrial loads need a two-phase or three-phase power supply. Without load, voltages are balanced on the three-phase LV feeders (i.e. the phase shift between any two conductors is 120^{o}) [11, 12]. However, in practice, given the loading and locational diversity of customers, three phases are usually unbalanced. This causes residual currents to go through the neutral wire, and thus, the

phase shift cannot be kept as 120º. Consequently, three-phase LV feeders are inherently unbalanced [11, 12].

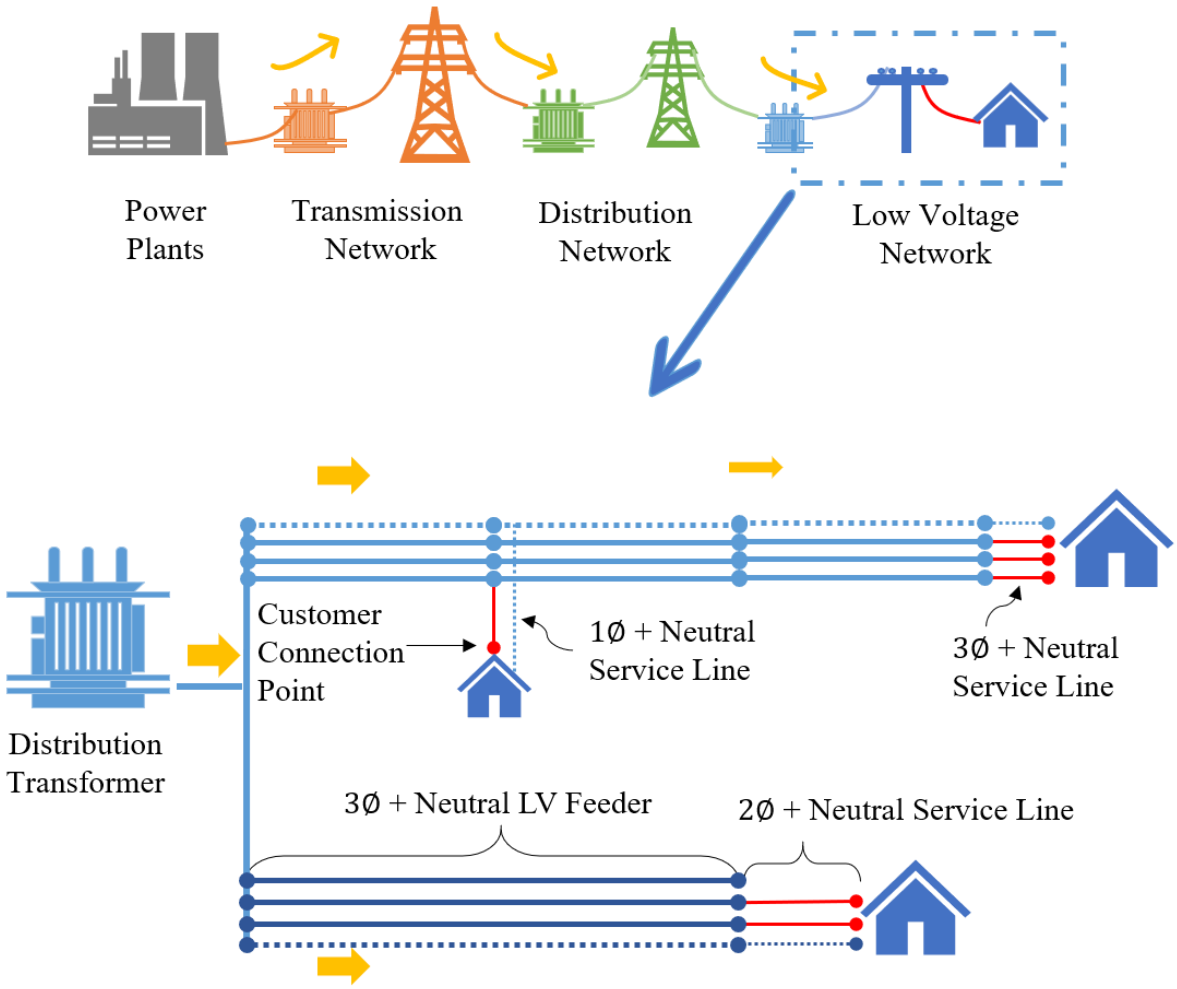

Figure 1-1. A traditional power system

In practice, LV networks are owned and operated by distribution companies [13]. Although the design of LV networks considers multiple technical constraints, such as the power flow, power losses, voltage drop, system earthing, and fault calculations, etc., two key considerations [12, 14, 15]:

- The voltage limits at the customer connection points; and
- The thermal capacity of network assets (i.e. distribution transformers and LV lines).

The network assets must be sized to accommodate the peak demand to ensure integrity. Given that different customers usually have their peak demand at different times, using the After Diversity Maximum Demand (ADMD) to determine the peak demand is the common practice

within distribution companies [16, 17]. ADMD is often derived from the aggregated yearly peak demand divided by the number of customers served by the network. For example, the maximum demand for customer $i \in I$ over a year is P_i, and the total maximum demand for all the customers is $\sum_i^I P_i$, and thus, the ADMD is determined by $\sum_i^I P_i \, / I$. However, it is worth mentioning that this approach cannot cater for future photovoltaic (PV)-rich LV networks. For instance, in Australia, a typical value of ADMD is 3kW [18]. If many customers install 5kW solar PV systems, during the low-demand period (e.g. 0.5kW), the reverse power flow may cause the LV feeder overloaded. The challenges and impacts of PV systems will be further discussed in a later section.

1.1.3 More Observability: Smart Meters

Traditional LV networks do not have monitoring devices, and customers' electricity consumption is recorded in conventional accumulation meters (with dial display) over defined periods. This type of meter needs readers to manually record and update the data, which is ineffective [19-21]. On the other hand, with the development of advanced technologies, conventional meters are gradually replaced by single-phase, two-phase, and three-phase smart meters (with digital display) [22, 23]. For example, in some European countries (e.g. Italy, Sweden, Finland, etc.), the penetration of smart meters is higher than 80%. In addition, in Australia, 2.8 million smart meters have been placed in almost all households across the state of Victoria [24].

In contrast with conventional meters, smart meters enable two-way communications between connected customers and distribution companies, which significantly increases the observability of LV networks [25]. It allows distribution companies to quickly detect and provide responses to a series of faults, such as power outage and phase to ground faults [23]. Furthermore, smart meters can automatically record customers' data at the customer connection points within an interval of time (e.g. 30 minutes) [25], including the voltage magnitude, the active and reactive power. One of the multiple benefits of smart meters is that they provide a large number of measurements, which can help distribution companies to have a better understanding of customer behaviour and develop analytical models (e.g. load forecasting). Hence, many distribution companies are increasingly interested in leveraging smart meter data [26]. However, currently, smart meters are mainly used for conventional applications (e.g. improving load forecast [27]) and providing more accurate electricity bills [19, 20, 26].

1.1.4 Distributed Energy Resources

DER represents the behind-the-meter assets that can provide electricity or manage demand [5]. The main three types of DER are residential photovoltaic (PV) systems, battery energy storage (BES) systems, and electrical vehicles (EVs), which changes the way customers consume electricity [5]. Traditionally, customers rely on electricity from power plants. However, more and more customers adopt residential PV systems to generate electricity for self-consumption, and the surplus energy can be stored in BES systems and EVs for latter usage. Although this thesis focuses on residential solar PV systems, the proposed approaches to calculate voltages in what-if scenarios are applicable to any DER technology. Therefore, this section provides an understanding of the current status, future trends, and technical information of these three types of DER.

1.1.4.1 Residential Solar PV Systems

Mainly due to the reduction in solar PV panel prices and, in some cases, the increase in electricity costs, there has been a rapid growth in residential solar PV system installations worldwide [2, 3, 28]. For example, in Australia, until now, the total installations of residential solar PV systems are more than 2.4 million (total of 8GW), with 10 million households. And it is approximately eight times higher than that recorded in 2010 [29]. This places Australia as one of the countries with the highest penetration of residential solar PV systems (i.e. around 25%) [30].

A grid-connected solar PV system (Figure 1-2) has two main types of elements: PV panels and PV inverters [31-33]. Whenever sunlight falls on PV panels, solar cells can convert solar energy to electricity in the form of direct current (DC). Given most of the home appliances work in alternating current (AC), PV inverters need to convert DC to AC electricity. If there is excess electricity from PV systems, the surplus energy will be measured by meters and exported into the power grid [32, 33]. On the contrary, if there is insufficient electricity from PV systems, customers will need to import electricity from the grid.

In Australia, the sizes of PV systems are regulated by local distribution companies to avoid jeopardizing the operation of LV networks [34]. The size of a PV system generally depends on the household phase connection. For a single-phase household, it can only connect with single-phase PV systems. The most popular single-phase PV system is 6.6kW with a 5kW inverter, which is cost-effective and meets network requirements [35]. If a large PV system is needed

(e.g. 10kW), the size of the inverter can be increased as long as the maximum 'export limit' meets 5kW per phase [36]. For a three-phase household, the PV system can be single-phase, two-phase, and three-phase. The three-phase PV systems allow customers to have the larger size of PV systems (e.g. up to 30kW) [36, 37].

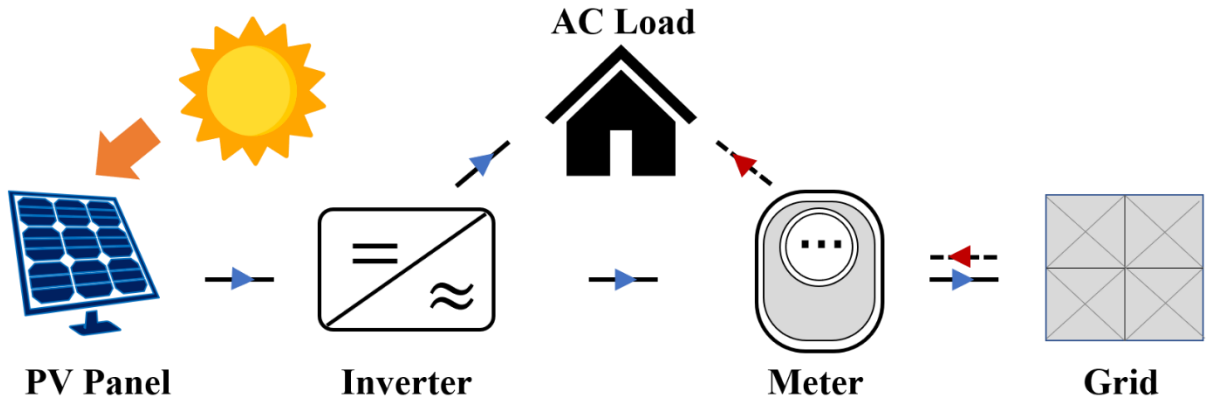

Figure 1-2. A grid-conected PV system

1.1.4.2 Other Residential Technologies

Given that PV systems only generate electricity during daylight hours, customers that use most of their electricity at night can barely self-consume their own generation. To store the surplus solar energy for later use and reduce electricity bills, customers are adopting BES systems and EVs [38]. Although the most common type of batteries is the lead-acid battery, the most recent commercially available BES systems and EVs use lithium-ion (Li-ion) technology [39, 40]. Given the cost reduction of batteries and the growth of government incentives, there will be an increasing number of BES systems [31] and EVs [41, 42]. Currently, Australia is one of the countries which has installed many residential BES systems, and it expects to install one million BES by 2025 [43, 44]. However, the sales of EVs in Australia have been modest, even though there is an increasing uptake of EVs globally [42].

EVs are, in general, loads. But vehicle-to-grid (V2G) technology allows EVs to perform the same function as that of BES systems in the charging and discharging process [42, 45, 46]. A battery can be charged with surplus solar energy during the day, or it can be charged by the power grid when electricity is cheaper. Then, the stored energy in the battery can be discharged for shaving the peak demand or backup power during a blackout [39].

In terms of residential batteries, there are three main aspects: the battery capacity, depth of discharge (DoD), and power [47, 48]. Firstly, the battery capacity represents the maximum energy stored in a battery. Secondly, DoD indicates usable storage capacity. The higher the DoD, the more the stored energy can be used. Lastly, the power of the battery presents how fast the energy can be charged/discharged at any time. Both BES and EVs can be compatible with single-phase, two-phase, and three-phase power supply. The capacity of BES systems is usually in the range of 1.2-14kWh, and the continuous power is between 0.26kW and 5kW [40, 47, 49]. On the other hand, the battery size of EVs is mostly in the range of 28-100kWh [50]. It should be noted that injections from both BES and EVs will follow the limits established for the corresponding single-, two-, or three-phase connections of the customers.

1.1.5 Impacts of Distributed Energy Resources on Low Voltage Networks

As mentioned in Section 1.1.1, traditional LV networks are designed for unidirectional power flow to accommodate the peak demand. Given the increasing number of DER in LV networks, distribution companies are growingly interested in understanding their technical impacts on LV networks [51, 52]. This section discusses the impacts of the high penetration of DER on LV networks. Given the technical issues caused by DER, it is important to perform what-if analyses to understand the extent of DER impacts on LV networks.

1.1.5.1 Residential Solar Photovoltaic Systems

Solar PV systems can provide electricity to customers during the day, and excess energy can be injected into the grid. This effect is referred to as *reverse power flow* (green arrows in Figure 1-3). The greater the electricity generated by PV systems, the higher the level of the reverse power flow in LV networks, especially during low demand periods. A large amount of reverse power flow may have negative impacts on LV networks or even on higher voltage-level networks [53-55]. Two main technical issues are overvoltage and asset congestion.

Firstly, excessive PV generation (e.g. during low demand periods) can introduce reverse power flow and causes voltage rises for the customers with PV systems. Thus, the significant reverse power flow may result in overvoltage (voltages violate the upper voltage limit). Secondly, given that network assets have a specific thermal capacity, a large amount of reverse power flow may also cause assets to become overloaded.

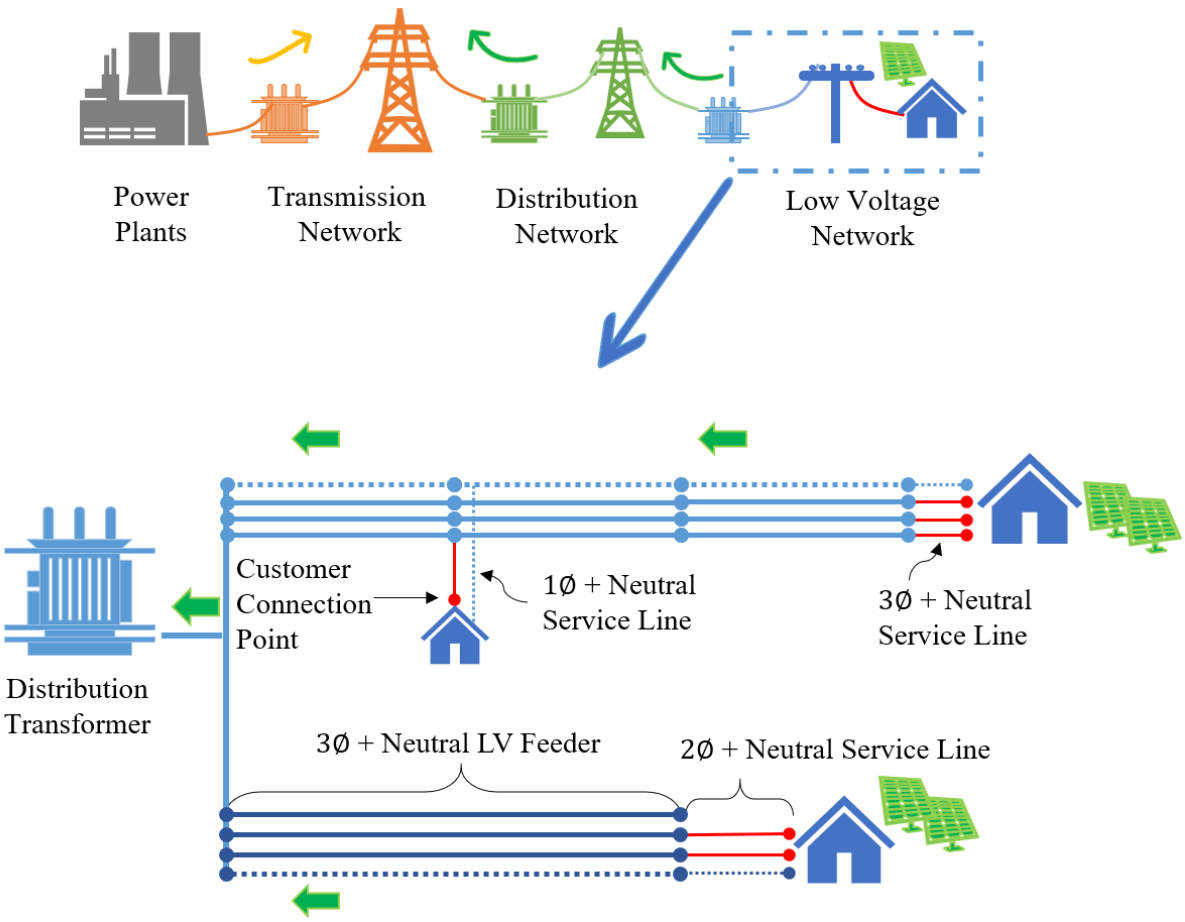

Figure 1-3. A current/future power system with PV systems

Although both violations may occur in LV networks, studies in [52, 56] have found that problems are primarily related to voltage rise. Because of this, most studies have mainly focused on mitigating voltage rise issues [55, 57]. Hence, efforts are necessary to tackle voltage rise issues in LV networks that have PV systems. Consequently, given that distribution companies are responsible for ensuring network integrity, they need to be able to effectively perform what-if analyses to first understand the extent of PV impacts on voltages before taking action to avoid voltage violations [51-61].

1.1.5.2 Other Residential Technologies

In contrast to residential solar PV systems, BES systems and EVs (with V2G technology) participate as both generators and loads. However, given the complexity and cost of V2G, EVs are likely to be only loads in the near future [62]. Theoretically, the adoption of BES systems and EVs can mitigate the above-mentioned technical issues (i.e. voltage violations and overload) by storing

surplus solar energy at peak PV generation periods. However, in practice, there are some challenges as introduced below.

On the one hand, commercially available BES systems with off-the-shelf-control (e.g. the Tesla Powerwall 2 [63]) are not necessarily effective to charge during the peak PV generation periods [64]. Therefore, the amount of reverse power flow and the main technical issues caused by PV systems may not be effectively reduced. Furthermore, considering that BES systems can provide many other grid services (e.g. respond to price spike), additional demand or generation in networks may cause voltage violations and overloading [64, 65].

On the other hand, based on the impact analysis in [66], the increasing penetration of EVs can slightly reduce the voltage rise and thermal issues caused by PV systems. The problems remain because the peaks of EV demand (e.g. 9 pm) and PV generation (e.g. 1 pm-4 pm) are not in the same period. Also, at the peaks of EV demand, a significant voltage drop may occur on LV networks [66-68]. Moreover, the impacts of EVs on both voltages and thermal overloading have been assessed in [67], and it has found that various LV networks may have different technical issues at different EV penetration levels.

Thus, when BES and EVs participate as generators, their injections create reverse power flows and causes voltage rises across LV networks. In contrast, when BES and EVs act as loads, voltage drop issues can also occur. Consequently, distribution companies must perform what-if analysis (i.e. any demand or generation of DER) to know the impacts of DER on voltages in LV networks.

1.2 Challenges in Low Voltage Networks

Given that the voltage violation is the main issue in DER-rich LV networks, distribution companies first need to calculate customer voltages in any demand/generation condition (i.e. what-if analysis) for either the operational or planning purpose.

From the operational perspective, DER might need to be actively managed by distribution companies (directly or indirectly [61]). In this context, distribution companies need to understand how to respond to the customers' intended demand/generation for the next time interval (e.g. 1 minute). Whether the intended operation causes voltage violations or not needs to be assessed. To achieve this, distribution companies need to calculate voltages before accepting all the customers' intended operation. If the calculated voltage is within the permissible range, the intended operation

is accepted. If voltage violations occur, distribution companies will take action to manage DER and to avoid issues. On the other hand, for the planning purpose, distribution companies can calculate voltages in terms of any demand/generation of DER before accepting the new connection request. Thus far, being able to calculate customer voltages in any demand/generation condition is key for distribution companies to make the most appropriate decisions [69, 70]. However, this thesis only focusses on the operational perspective.

Extensive research has been carried out in the literature about three-phase power flow analyses to assess the impacts of DER on customer voltages in any demand/generation condition [52, 58, 59, 61]. But to have accurate results, these approaches require the knowledge of networks: impedance of LV line models (i.e. three-phase LV feeder lines and single-phase service lines), customer connectivity, and customer phase connection. The impedances of LV line models must be adequately modelled to cater for inherently unbalanced LV networks. However, the first challenge in the impact analyses is the limited knowledge of the underlying LV network model. In practice, distribution companies do not have readily applicable LV network models, and existing models are often poorly/incompletely recorded.

Furthermore, from an operational perspective (to assist the active management of DER), distribution companies would benefit from fast and practical power flow calculations. However, running conventional three-phase power flow analyses can be complex to implement. Thus, the second challenge in the impact analyses is the complex implementations of power flow analyses.

1.2.1 Limited Knowledge of Low Voltage Networks

The limited knowledge of underlying LV networks has made that traditional model-based impact analyses are challenging to implement in practice. Many works have been investigating the impedance estimation of LV line models (i.e. three-phase LV feeder lines and single-phase service lines), customer connectivity, and customer phase connection [71-84]. Thanks to smart meter measurements, methods developed in [71, 72] and [73] can accurately estimate the customer connectivity and the customer phase connection in unbalanced three-phase LV networks, respectively. However, it is still very challenging to adequately estimate impedances of LV line models because of the phase couplings of three-phase LV feeder lines.

Many impedance estimation approaches are based on knowing the customer connectivity and customer phase connection [74-81]. For instance, the method in [74] can estimate the impedance of a single three-phase LV feeder line by using the phasors of three-phase bus

voltages and line currents from a phasor measurement unit (PMU)-based technique. However, the high cost of a PMU makes it difficult to be applied in LV networks, and it is not a technology adopted by distribution companies [75, 85]. On the contrary, all the other works have estimated impedances by exploiting smart meter measurements. These smart meter-driven approaches depend on the complexity of LV networks (from a single [76, 77] to multiple LV feeder lines [75, 78-81]) and the availability of smart meters (from full [75, 79, 80] to limited observability [78, 81]). One of the most advanced works [81], has considered a more realistic condition, which requires that meter measurements are only available at customer connection points and at the head of the feeder. It has used a non-linear optimisation approach to estimate impedances of multiple LV line models, but it did not differentiate the three-phase LV feeder lines and single-phase service lines. More importantly, there are no phase couplings involved in the feeder impedance estimation, and thus, the approach can only be used to estimate impedances of single-phase service lines in real LV networks.

Furthermore, compared with the above approaches, the methods in [82-84] rely on little network knowledge. Different from the first two works in [82, 83], the study in [84] differentiate three-phase LV feeder lines and single-phase service lines. However, Watson et al. [84] also noted the significant challenge in determining the impedance for each service line. Thus, an average impedance was used for all service lines in LV networks based on the voltage correlation analyses. In addition, for three-phase LV feeder lines, the phase couplings were not considered either. Consequently, thus far, impedance estimation of different types of LV line models (i.e. three-phase LV feeder lines and single-phase service lines) has been the most difficult part, which needs to be solved.

1.2.2 Complex Implementations of Power Flow Analyses

Power flow analyses determine customer voltages by solving non-linear equations [86-88]. The computation time depends on the types of the underlying LV line models, the time steps of demand/ generation profiles [67]. Given that LV networks may have hundreds and thousands of nodes, running power flow analyses is complex to implement for operational purposes (to assist the active management of DER). Thus, distribution companies require accurate but fast and practical simplified three-phase voltage calculation algorithms that can be easily implementable to effectively assess the impacts of DER on voltages in LV networks.

To simplify the voltage calculation, several approaches in the literature have been suggested based on the single-phase voltage drop equation [69, 89-91]. Given that unbalances across phases are not involved, these methods use an ‘unbalanced factor’ to correct the single-phase voltage drop equation. In [89-91], an empirically determined ‘unbalanced factor’ has been used to modify the linearised single-phase voltage drop equation. However, the problem is that the empirical value cannot be used in any network at any time, and thus, this approach cannot assess the impacts of DER on customer voltages in what-if analyses (different demand/generation combinations) in real LV networks (dozens to hundreds per primary substation). Furthermore, the method in [69] uses non-linear regression analyses and a machine learning technique to train the 'unbalanced factor'. The trained 'unbalanced factor' was applied to a non-linearised single-phase voltage drop equation. However, the training process requires a large amount of historical smart meter measurements (i.e. half or one year), which is still not practical. Consequently, thus far, the existing approaches cannot effectively assess the impacts of DER on voltages when performing what-if scenarios.

1.3 Research Questions

The increasing number of DER is driving distribution companies to assess customer voltages in what-if analyses. However, this task can be challenging in LV networks due to the limited knowledge of the impedances of LV line models (i.e. three-phase LV feeder lines and single-phase service lines) and the complexity from implementing power flow analyses. Given that smart meters have rolled out in many regions, the main research question to be addressed in this thesis and corresponding sub questions are listed as follows:

- Can we assess the impacts of DER on customer voltages in what-if analyses using smart meter-driven LV line models (i.e. three-phase LV feeder lines and single-phase service lines)?
    - What is the minimum requirement for the impedance of three-phase LV feeder lines to adequately capture the three-phase unbalanced characteristics of LV networks?
    - What smart meter data can be used for impedance estimation?
    - Except for customer connection points, which point of three-phase LV feeders needs to be metered for impedance estimation?

- What are the requirements of the underlying network topology (i.e. customer connectivity and customer phase connection) for the impedance estimation?
- What methods can be used to exploit historical smart meter data?
- Without using three-phase power flow analyses, how can we quickly and accurately determine customer voltages in any demand/generation condition (i.e. what-if analysis)?

1.4 Main Contributions of the Thesis

This section summarises the main and original contributions of this thesis.

- The first contribution is the proposed impedance estimation approach. It uses historical time-series measurements (i.e. the voltage magnitude, active power, and reactive power) from smart meters and at the head of the feeder to estimate the impedances of LV line models (i.e. the three-phase LV feeder lines and the single-phase service lines). Crucially, the phase couplings are considered in three-phase LV feeder line models.
- The second contribution is the proposed accurate but fast and practical simplified three-phase voltage calculation algorithms that can be easily implementable to effectively assess the impacts of DER on customer voltages.
- The third contribution is that the proposed approach has been used on realistic Australian and UK LV networks for both impedance estimation and voltage calculations. It is worth highlighting that realistic demand/generation data are used to emulate smart meter measurements.

1.5 Publications

The section contains the list of journal papers and conference papers.

1.5.1 Journal Papers

Y. Wang, M.Z. Liu, L.F. Ochoa, "Assessing the effects of DER on voltages using a smart meter-driven three-phase LV feeder model", Electric Power Systems Research, Accepted in 2020-05 (In Press).

1.5.2 Conference Papers

Y. Wang, M.Z. Liu, L.F. Ochoa, "Assessing the effects of DER on voltages using a smart meter-driven three-phase LV feeder model", 21st Power Systems Computation Conference PSCC 2020, 2020-06/07 29-3, p 8.

1.6 Thesis Outline

There are five chapters in this thesis, and a corresponding summary of each chapter is provided.

Chapter 2 - LV Line Models, Impedance Estimation and Voltage Calculation

Chapter 2 first presents the characteristics of different LV line models and discusses how adequacy they are for running unbalanced three-phase power flow analyses. It also summarises the existing literature and the research gaps concerning smart-meter driven impedance estimation approaches. Lastly, the state-of-the-art voltage calculation approaches and the corresponding research gaps are presented.

Chapters 3 - Methodology

Chapter 3 provides the details of the proposed approach in this thesis aiming at calculating the customer voltages in any demand/generation condition using a smart meter-driven LV feeder and service line model (estimated impedances using a smart meter-driven approach). Firstly, it presents how to estimate the impedances of three-phase LV feeder lines and single-phase service lines based on measurements of smart meters and at the head of the feeder. This process uses linearised voltage drop equations and a multiple linear regression technique, and it assumes having knowledge of the customer connectivity and customer phase connection. Once having the impedances, it presents how to calculate customer voltages in what-if analyses. Instead of running power flow analyses, this approach uses the linearised voltage drop equations to determine customer voltages in any demand/generation of DER. Lastly, an example LV feeder (with service lines) is used to present the process of impedance estimation and customer voltage calculations.

Chapter 4 - Case Studies

Chapter 4 assesses the performance of the proposed approach, both in terms of the estimation accuracy of LV line impedances and customer voltages, on realistic Australian and UK LV

networks. In both cases, impedances are predicted by using weekly historical meter measurements, with a 15-minute resolution (672 time steps). On the other hand, weekly demand/generation profiles used for the voltage calculations in what-if analyses have a 1-minute resolution (10,080 time steps). Also, the time consumed by this proposed voltage calculation is compared with that of full power flow analyses. The results have demonstrated that the proposed methodology can quickly and accurately calculate customer voltages at any time.

Chapter 5 - Conclusions and Future Work

Chapter 5 concludes the main findings from the research contained in this thesis. Furthermore, it outlines the potential future works and improvements to the research.

The Appendix contains the information concerning the impact of each impedance variable on the customers' voltages, which is useful for a better understanding of this thesis.

This page is intentionally left blank.

2 LOW VOLTAGE LINE MODELS, IMPEDANCE ESTIMATION AND VOLTAGE CALCULATION

2.1 Introduction

As discussed in Chapter 1, distribution companies must perform what-if analyses to understand the impacts of DER on customer voltages in any demand/generation condition for either the operational or planning purpose. This thesis focuses on the former purpose, which requires that voltage calculations are accurate, fast, and easily implemented.

The accuracy of voltage calculations depends on the correctness of the underlying LV line models: the more precise the LV line models, the more accurate the voltages. Due to a range of reasons, such as the lack of knowledge about LV line models by distribution companies, LV line models have been simplified in different ways. Given the three-phase inherently unbalanced LV networks, the minimum requirements for any simplified LV line model need to be identified. Therefore, this chapter first presents the characteristics of different LV line models and discusses how adequate they are for real LV networks.

Furthermore, one significant challenge of calculating voltages is that the impedances of LV line models (i.e. three-phase LV feeder line and single-phase service line models) are poorly recorded and not radically available. Several works have investigated to estimate impedances, which depends on the availability of the certain measurements and techniques tailored for LV networks. Given the rollout of smart meters in several places, some of studies exploit smart meter measurements to estimate impedances. However, the problem is that they have not determined impedances for three-phase LV feeders with phase couplings and they cannot cater for inherently unbalanced LV networks. Thus, this chapter will also summarise the existing literature and the research gaps concerning smart meter-driven impedance estimation approaches.

Lastly, with correct impedances, voltages in LV networks can be accurately calculated by running power flow analyses. However, another challenge of calculating voltages is that it is complex to implement for operational purposes (to assist the active management of DER). Although some approaches have investigated to simplify the calculation, it is difficult for them

to analyse the unbalanced characteristics of LV networks. Thus, lastly, this chapter will summarise state-of-the-art voltage calculation approaches and the corresponding research gaps.

2.2 Low Voltage Line Models

This section presents the characteristics of full (exact) and simplified LV line models. Given the unbalanced nature of LV networks, the adequacy of various simplified models is discussed.

2.2.1 Full (Exact) Low Voltage Line Models

There are different voltage levels for LV networks around the world. For three-phase LV networks, voltages are in the range of 208 V to 433V (line to line voltages) [8, 9]. For example, in Australia and European countries, the nominal voltage is required at 400V with a tolerance range that varies per country [10, 11]. Although voltage levels are different, LV line models play the same important role, which is to carry electricity from secondary substations to customers [92].

In an LV network (e.g. Figure 2-1), LV line models (overhead or underground) consist of two types: LV feeder line model and service line model [92, 11]. Firstly, LV feeder line models deliver electricity from the substation to the local service area [92]. For example, there are two feeders in Figure 2-1. Feeder 1 (yellow glow) represents a main feeder, and Feeder 2 (blue glow) illustrates another main feeder but with a lateral. The LV feeder line model consists of three phases and one neutral wire (Figure 2-2), and its impedance is shown in Equation 2.1 [93, 94]. Here, $\hat{z}_{aa}$, $\hat{z}_{bb}$, $\hat{z}_{cc}$, $\hat{z}_{nn}$ and $\hat{z}_{gg}$, represent the self-impedance of phase A, phase B, phase C, the neutral wire and the grounding of the line, respectively. The remaining variables in Equation 2.1 are mutual impedances. For example, $\hat{z}_{ab}$ is the mutual impedance between phase A and phase B.

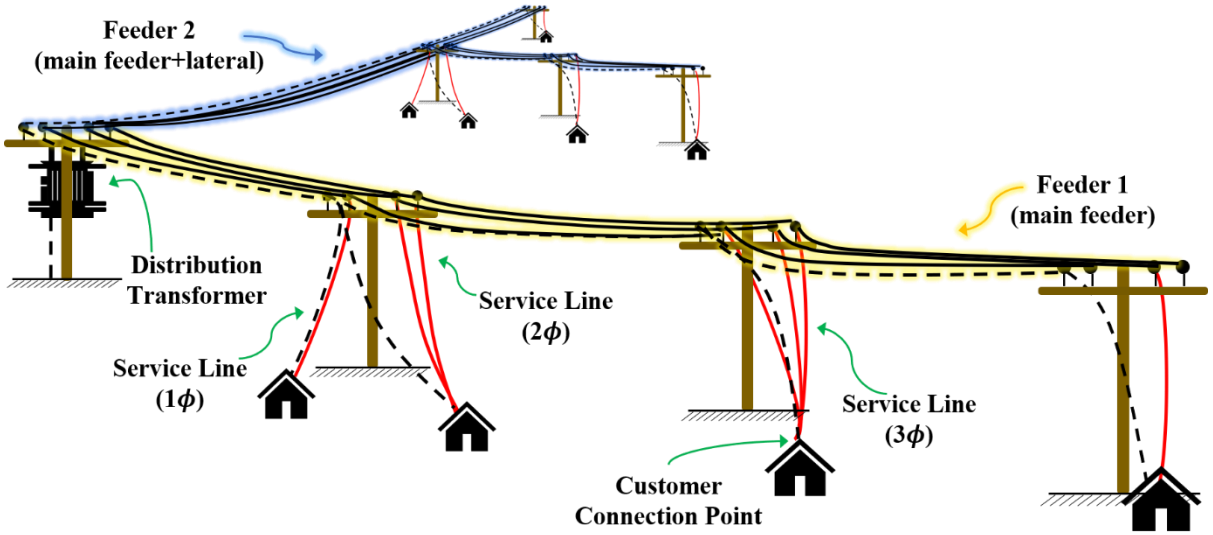

Figure 2-1. A general LV Network

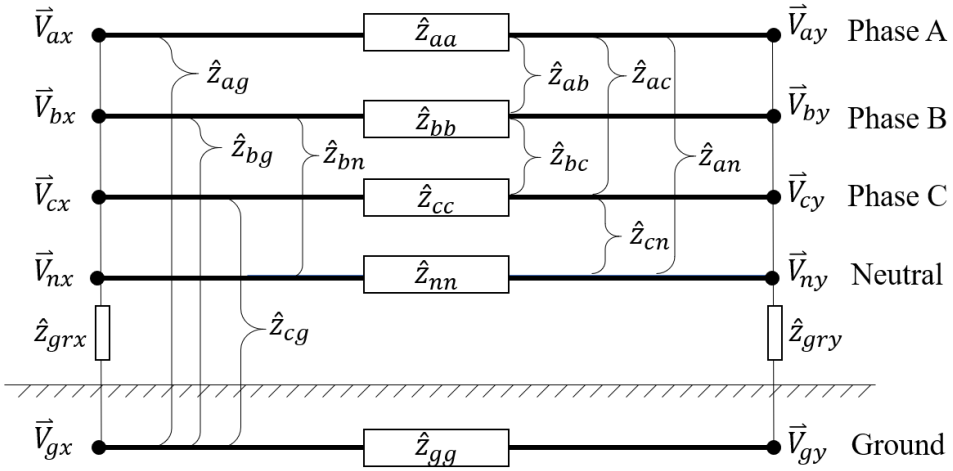

Figure 2-2. An exact three-phase four-wire line

$$\hat{z}_{5\times5}^{line} = \begin{bmatrix} \hat{z}_{aa} & \hat{z}_{ab} & \hat{z}_{ac} & \hat{z}_{an} & \hat{z}_{ag} \\ \hat{z}_{ba} & \hat{z}_{bb} & \hat{z}_{bc} & \hat{z}_{bn} & \hat{z}_{bg} \\ \hat{z}_{ca} & \hat{z}_{cb} & \hat{z}_{cc} & \hat{z}_{cn} & \hat{z}_{cg} \\ \hat{z}_{na} & \hat{z}_{nb} & \hat{z}_{nc} & \hat{z}_{nn} & \hat{z}_{ng} \\ \hat{z}_{ga} & \hat{z}_{gb} & \hat{z}_{gc} & \hat{z}_{gn} & \hat{z}_{gg} \end{bmatrix} \quad 2.1$$

Service lines connect local households with LV feeders in three different ways (i.e. single-phase, two-phase, and three-phase connections), as presented in Figure 2-1. If the service line does not connect with a certain phase, the corresponding row and column in Equation 2.1 will

have zero entries [93]. For example, in Australia, most of the local households are single-phase [11, 94]. Thus, it has one phase and one neutral wire, as shown in Figure 2-3, and its impedance is given by Equation 2.2. Here, $\hat{z}_{sl}$, $\hat{z}_{nn}$ and $\hat{z}_{gg}$, correspond to the self-impedance of the phase, the neutral wire and the grounding of the service line, respectively. The off-diagonal variables in Equation 2.2 are mutual impedances. For example, $\hat{z}_{sln}$ represents the mutual impedance between the phase and the neutral wire.

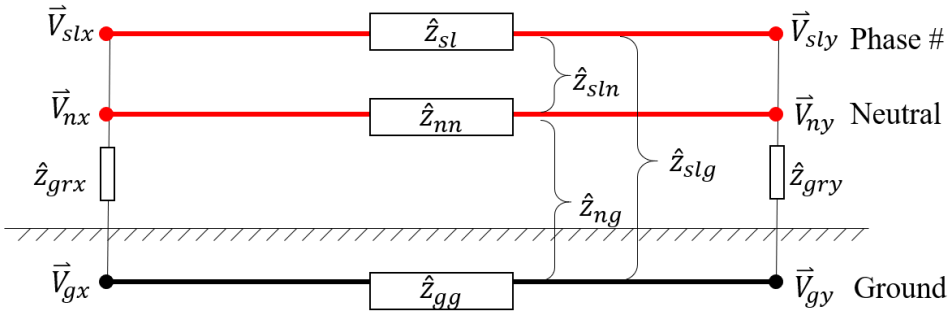

Figure 2-3. An exact single-phase two-wire line

$$\hat{z}_{2\times2}^{sl} = \begin{bmatrix} \hat{z}_{sl} & \hat{z}_{sln} & \hat{z}_{slg} \\ \hat{z}_{sln} & \hat{z}_{nn} & \hat{z}_{ng} \\ \hat{z}_{slg} & \hat{z}_{ng} & \hat{z}_{gg} \end{bmatrix} \quad 2.2$$

Impedance variables in Equations 2.1-2.2 can be denoted as $\hat{z}_{ij}$, where i and j represent any two conductors of the line. These impedance variables can be determined using the modified form of Carson's equations given in Equation 2.3, which is derived by setting the frequency and earth resistivity to 50 Hz and 100 Ω/m, respectively [95]. In Equation 2.3, when two conductors are the same (i.e. $j = i$), the self impedance is determined by the upper equation, where r_{ii} is the resistance (Ω/mile), and GMR_{ii} is the geometric mean radius (ft). In addition, when j is not equal to i, the mutual impedance is determined by the lower equation in Equation 2.3, where D_{ij} is the spacing between the two conductors (ft) [95]. It should be noted that the equation can be used to compute the self and mutual impedances of both overhead and underground lines. Full (exact) line models can be the most accurate model to be used in LV networks for power flow or short-circuit analyses.

$$\hat{z}_{ij} = \begin{cases} r_{ij} + 0.079 + j0.1\left(ln\frac{1}{GMR_{ij}} + 8.03\right)\Omega/\text{mile}, & j = i \\ 0.079 + j0.1\left(ln\frac{1}{D_{ij}} + 8.03\right)\Omega/\text{mile}, & j \neq i \end{cases} \quad 2.3$$

Moreover, it should be noted that LV networks are inherently unbalanced [71, 72, 96-99]. Households with various phase connections (i.e. single-phase, two-phase, and three-phase) randomly connect with three-phase LV feeders (with or without laterals). Given that customers usually have different demands/generation at any time in a day, the level of loading on each phase of the three-phase LV feeder is hardly the same. The unbalanced power causes unbalanced voltages on LV feeders, where the voltage magnitude of each phase and phase shifts between different phases are different, as shown in Figure 2-4. Using the exact LV line models in Equations 2.1-2.2, the unbalanced nature of LV networks (i.e. unbalanced voltages) can be accurately captured because of the consideration of the phase couplings.

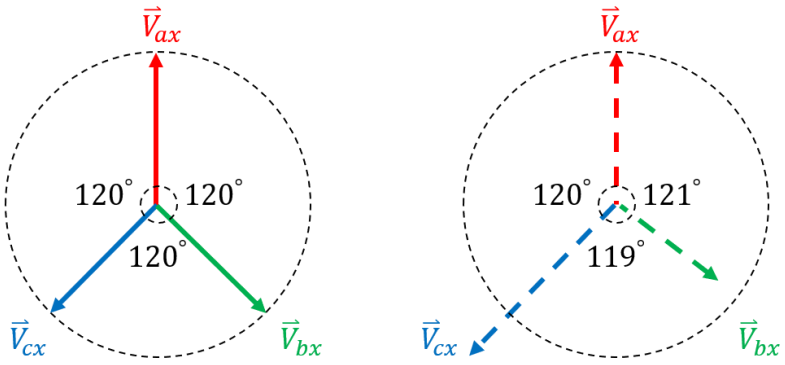

Figure 2-4. Illustration of balanced (left) and unbalanced (right) three-phase voltages

2.2.2 Simplified Low Voltage Line Models

Although exact LV line models can accurately determine voltages in LV networks, simplified models with reduced variables are often needed because of a few reasons [98]. One of the main reasons is the limited knowledge of LV line models (e.g. self and mutual ground impedances are not accurately known) [99]. Another main reason is that exact line models in large-scale networks can hinder fast system-wide parameter estimation and power flow analyses [98, 100]. To improve calculation efficiency, given the negligible effects of ground impedances, some works simplify the exact models from Equations 2.1-2.2 to Equations 2.4-2.5 [95, 101, 102].

In Equation 2.4, $\hat{z}_{aa}$, $\hat{z}_{bb}$, $\hat{z}_{cc}$ and $\hat{z}_{nn}$ represent the self-impedance of phase A, phase B, phase C and the neutral wire, respectively. The remaining variables in Equation 2.4 are the mutual impedances. In Equation 2.5, $\hat{z}_{sl}$ and $\hat{z}_{nn}$ are the self-impedance of the phase and the neutral wire, respectively. $\hat{z}_{nsl}$ (or $\hat{z}_{sln}$) indicates the mutual impedance between the phase and the neutral wire of the service line.

$$\hat{Z}_{4\times4}^{line} = \begin{bmatrix} \hat{z}_{aa} & \hat{z}_{ab} & \hat{z}_{ac} & \hat{z}_{an} \\ \hat{z}_{ba} & \hat{z}_{bb} & \hat{z}_{bc} & \hat{z}_{bn} \\ \hat{z}_{ca} & \hat{z}_{cb} & \hat{z}_{cc} & \hat{z}_{cn} \\ \hat{z}_{na} & \hat{z}_{nb} & \hat{z}_{nc} & \hat{z}_{nn} \end{bmatrix} \quad 2.4$$

$$\hat{Z}_{2\times2}^{sl} = \begin{bmatrix} \hat{z}_{sl} & \hat{z}_{sln} \\ \hat{z}_{nsl} & \hat{z}_{nn} \end{bmatrix} \quad 2.5$$

Moreover, Kron's reduction has been widely used to simplify LV line models determined in Equations 2.4-2.5. The reduction merges the neutral wire with the phase wires by assuming that the neutral wire directly connects with the ground, and the voltage drop across the neutral wire is zero [93, 101, 103]. For the three-phase line model, the reduced impedance $\hat{Z}_{3\times3}^{line}$ is given by Equation 2.6. Here, $\hat{Z}_{aa}$, $\hat{Z}_{bb}$ and $\hat{Z}_{cc}$, correspond to the self-impedance of phase A, phase B, phase C. The off-diagonal variables are the mutual impedances between two phases. In addition, for the single-phase service line model, the reduced impedance can be denoted as $\hat{Z}_{sl}$. The study in [101] has found that errors from Kron's reduction are extremely small when the network is not highly unbalanced.

$$\hat{Z}_{3\times3}^{line} = \begin{bmatrix} \hat{Z}_{aa} & \hat{Z}_{ab} & \hat{Z}_{ac} \\ \hat{Z}_{ba} & \hat{Z}_{bb} & \hat{Z}_{bc} \\ \hat{Z}_{ca} & \hat{Z}_{cb} & \hat{Z}_{cc} \end{bmatrix} \quad 2.6$$

In practice, sequence impedances (i.e. zero-sequence and positive-sequence impedances) are often used by distribution companies for line modelling as the knowledge of the couplings between sequences is not necessarily needed [95, 102, 104]. Instead, sequence impedances are derived as shown in Equation 2.7. The corresponding three-phase impedance is given by Equation 2.8, where three phases share the same self-impedance and mutual impedances. Compared with Equation 2.6, although Equation 2.8 has fewer variables, it cannot significantly

affect the accuracy of the voltage calculation [104]. Given that the mutual phase couplings are included in Equation 2.8, it can adequately analyse the three-phase unbalanced characteristics of LV networks. At the same time, the three-phase LV line model in Equation 2.8 has less impedance variables and, thus, can save computation time. Therefore, given that Equations 2.6-2.8 have phase couplings, they can be used to analyse the impacts of DER on a three-phase unbalanced LV network.

$$\tilde{Z}_{3\times3,seq}^{line} = \begin{bmatrix} \hat{Z}_s + 2\times\hat{Z}_m & 0 & 0 \\ 0 & \hat{Z}_s - \hat{Z}_m & 0 \\ 0 & 0 & \hat{Z}_s - \hat{Z}_m \end{bmatrix} \quad 2.7$$

$$\tilde{Z}_{3\times3}^{line} = \begin{bmatrix} \hat{Z}_s & \hat{Z}_m & \hat{Z}_m \\ \hat{Z}_m & \hat{Z}_s & \hat{Z}_m \\ \hat{Z}_m & \hat{Z}_m & \hat{Z}_s \end{bmatrix} \quad 2.8$$

However, some studies have reduced lines to be even simpler, as shown in Equations 2.9-2.10 [95, 102, 104]. These two equations have sole self-impedances and positive sequence impedances, respectively. These matrices can only be used for three single-phase lines and balanced LV feeder lines [102, 104]. Compared with the simplified three-phase LV line models with phase couplings (i.e. Equations 2.4, 2.6-2.8), using Equations 2.9-2.10 can cause substantial errors in determining voltages in unbalanced networks [102, 104]. Consequently, Equations 2.8 satisfies the minimum requirement for the impedance of three-phase LV feeder lines to adequately cater for the unbalanced characteristics of LV networks.

$$\tilde{Z}_{3\times3}^{line,opt1} = \begin{bmatrix} \hat{Z}_s & 0 & 0 \\ 0 & \hat{Z}_s & 0 \\ 0 & 0 & \hat{Z}_s \end{bmatrix} \quad 2.9$$

$$\tilde{Z}_{3\times3}^{line,opt2} = \begin{bmatrix} \hat{Z}_s - \hat{Z}_m & 0 & 0 \\ 0 & \hat{Z}_s - \hat{Z}_m & 0 \\ 0 & 0 & \hat{Z}_s - \hat{Z}_m \end{bmatrix} \quad 2.10$$

2.3 Low Voltage Line Impedance Estimation

Having adequate models of LV lines is necessary to be able to assess the impacts of DER on voltages in three-phase unbalanced LV networks. However, the challenge is that impedances are often unavailable or inaccurate. Although impedances can be identified by physical inspections, they require a considerable number of labour hours, especially in densely populated areas, which can be costly [75]. To solve this issue, several works [74, 76-84] have investigated different meter-driven impedance estimation approaches.

In [74], impedances are estimated by using the measurements from phasor measurement units (PMUs): phasors of three-phase of bus voltages and currents. However, the challenge is that PMUs are extremely expensive and hardly applied in LV networks [85]. On the other hand, given the growing adoption of smart meters in residential households, smart meter-driven impedance estimation approaches would be more practical. These meters typically record three types of time-varying data at customer connection points: active power, reactive power, and voltage magnitudes. Although these measurements have been used by a few works [76-84] to estimate impedances, there are some limitations. Therefore, this section discusses state-of-the-art smart meter-driven impedance estimation approaches, followed by a summary of the identified research gaps.

2.3.1 State-of-the-Art

State-of-the-art smart meter-driven impedance estimation approaches can be categorised by the level of complexity of their underlying LV line models.

Studies in [76, 77] have used a simple LV feeder model (in Figure 2-5), and the impedance between the secondary substation and the customer connection point has been estimated. In [76], meters were installed at the head of the feeder and a single customer connection point, which provides three pairs of values: active power (P_{sub}, P_{cust}), reactive power (Q_{sub}, Q_{cust}) and voltage magnitudes (V_{sub}, V_{cus}). The meter measurements are sent to the linearized voltage drop equation in Equation 2.11, and impedances ($R_{line} + jX_{line}$) are estimated by regression analyses. Furthermore, the method in [77] used 5-minute snapshots of smart meter measurements (P_{cust}, Q_{cust}, V_{cus}) at the household to estimate line impedances based on Equation 2.12. Here, the impedance was determined by the ratio of the changes in customer

voltages ΔV_{cust} to changes in customer currents $\Delta(P_{cust} + jQ_{cust})^*/\Delta V_{cust}{}^*$ by keeping the substation voltage constant.

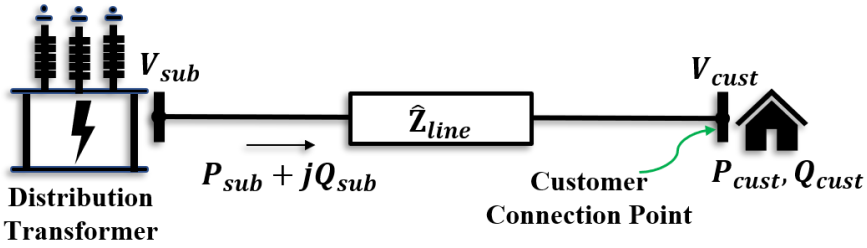

Figure 2-5. A simplified LV feeder model

$$V_{sub} - V_{cust} = R_{line} Re\left\{\left(\frac{P_{cust} + jQ_{cust}}{V_{cust}}\right)^*\right\} - X_{line} Im\left\{\left(\frac{P_{cust} + jQ_{cust}}{V_{cust}}\right)^*\right\} \quad 2.11$$

$$\hat{Z}_{line} = \frac{\Delta V_{cust}}{\Delta\left(\frac{P_{cust} + jQ_{cust}}{V_{cust}}\right)^*} \quad 2.12$$

Although these methods can correctly estimate the impedance, they have not considered adequate three-phase LV feeder line models with phase couplings. Thus, it can cause significant errors in determining voltages in real unbalanced LV networks. Most importantly, the above studies oversimplified the LV feeder model. In practice, multiple single-phase customers are unevenly allocated at different phases of three-phase LV feeder models through service lines; thus, voltages and power injections on three-phase buses along the three-phase feeder are hardly known. In short, the above two methods cannot be directly implemented in practice.

A few papers have considered more realistic LV network models (e.g. Figure 2-6), and they have estimated the impedances of each LV line [78-84]. These studies are grouped into two categories based on the availability of smart meters. In each group, requirements of the underlying network topology (i.e. customer connectivity and customer phase connection) are also outlined.

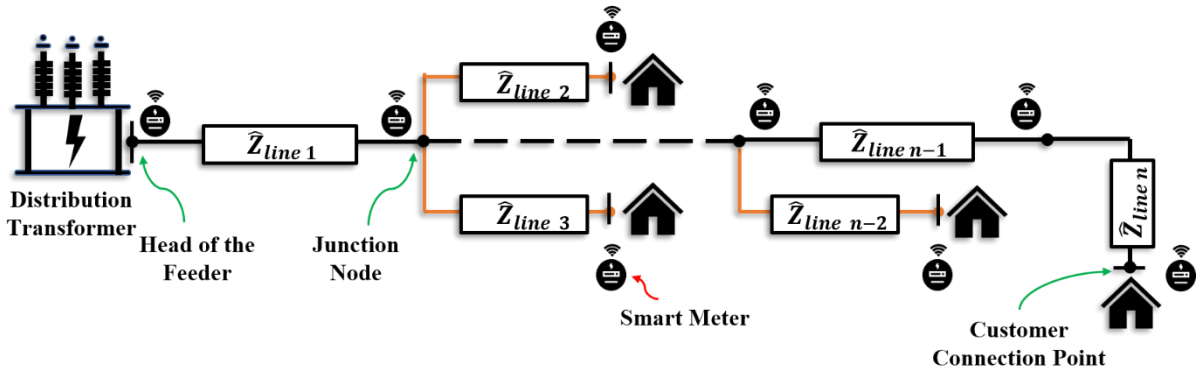

Figure 2-6. A more realistic LV feeder model with full observability

In the first category, several works [79, 80, 82] assume that smart meters are located at customer connection points, junction nodes and the head of the feeder, as shown in Figure 2-6. In contrast with [79] and [80], the approach in [82] does not rely on the full knowledge of the network topology [82].

In [82], the approach estimates the meter connectivity and the impedance between two meters. The connectivity refers to the relationship between two meters: parent-child and siblings, as shown in Figure 2-7. The method in [82] finds the best-fit impedance and meter connectivity based on the root mean square error of the residuals. Although this approach is accurate and efficient with the usage of the regression technique, it requires that the meters are at the same phase. This means that this method can only be used in the service area (service lines) of real LV networks.

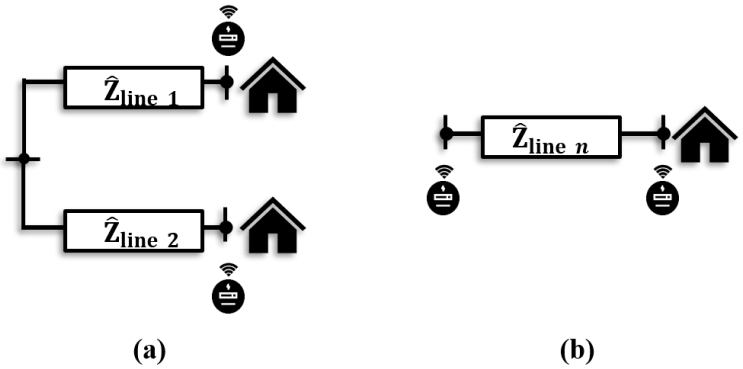

Figure 2-7. Connectivity of Customers: (a) Siblings; (b) Parent-Child

Works in [31, 32] assume having the full knowledge of LV networks. Both studies consider a single-phase LV feeder model (black lines in Figure 2-6), and the former [31] deals with the

feeder with branches (orange lines in Figure 2-6). Impedances in [79, 80] are estimated by solving non-linear voltage drop equations, involving the phase increments along the feeder, based on optimisation approaches. Iakovlev et al. [80] found that the non-linear optimisation approach needs at least thirty iterations in order to have significantly better accuracy than the results determined by the linearized approach. Thus, given that real LV networks can have dozens to hundreds of lines, a non-linear based approach is less scalable and requires larger computational effort.

Thus far, existing works in this category require that LV feeder models have full observability, which can be less practical in larger size of LV networks. Although linearised and non-linearised based approaches have been investigated to estimate impedances, with or without concerning the underlying network topology, they only determined the impedances for single-phase lines. Therefore, they cannot be applied in real unbalanced LV networks which have three-phase LV feeder models.

In the second category, all the works in [78, 81, 83, 84] that consider more realistic conditions limiting the number of meters. As shown in Figure 2-7, smart meters are only available at each household, and junction nodes are not metered. However, these works need the voltage at the head of the feeder. Besides, in contrast with the works in [83, 84], the approaches in [78, 81] need the full knowledge of the network topology.

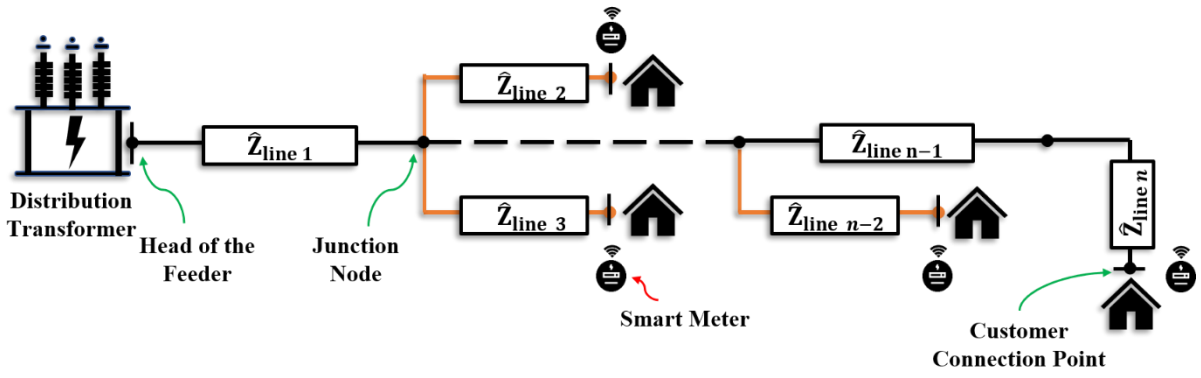

Figure 2-8. A more realistic LV feeder model with limited observability

In [78, 81], given the lack of the meter measurements at junction nodes, the voltage drop over multiple LV line models is used for impedance estimation. These two works implemented the linearised and non-linear optimisation approach, respectively. However, both studies

considered single-phase line models. Additionally, the approach in [78] only involves active power, and thus, it cannot be applied in networks that have non-negligible line reactance.

Methods in [83, 84] determines impedances without relying on the full knowledge of LV networks. In [83], measurements from the end-customers (i.e. active power, reactive power, and voltage magnitudes) are used to estimate the meter connectivity and single-phase line impedances in the LV network. Furthermore, the approach in [84] identifies the difference between service lines and the three-phase feeders in LV networks. Watson et al. [84] indicated that determining the impedance for each service line brings challenges; and thus, an average service line impedance was determined by using a voltage correlation approach. Furthermore, based on the known voltages at the head of the feeder, meter phases and connectivity were estimated using a correlation technique. However, for the impedance estimation, it only considers the active power and determines resistance using the ordinary least square technique. Although a three-phase feeder model is adopted, the phase couplings are not considered.

In summary, with limited meter measurements, the approaches in the second category can estimate impedances in more realistic LV networks, whether the full network knowledge exists or not. But the challenge is that they require that the underlying LV network only has single-phase or balanced three-phase lines.

2.3.2 Summary of Research Gaps

Based on state-of-the-art smart meter-driven impedance estimation methods discussed above, the major challenge in all the existing literature is that they have not considered full three-phase LV line models with phase couplings and single-phase service lines models. Therefore, all the existing approaches can only be used in single-phase or balanced three-phase LV networks, and they cannot cater for the needs of realistic unbalanced LV networks.

2.4 Voltage Calculation

Once LV line impedances are known, voltages due to DER are ready to be calculated for any demand/generation condition (i.e. what-if analysis). Although it can be achieved by using different methods, distribution companies need a tool to quickly and accurately determine voltages, particularly for the operational purposes. This section presents state-of-art voltage calculation approaches and outlines the research gaps.

2.4.1 State-of-the-Art

In the sinusoidal steady-state condition, several approaches have been used to calculate voltages in any demand/generation condition, which depends on the calculation accuracy and the implementation complexity [69, 86-91].

If the underlying network topology and parameters are correct, the most accurate method is to solve the non-linear algebraic equations by performing power flow analyses [86-88]. For a generic single-phase line l, as shown in Figure 2-9, power flow equations present the relationships between the voltage phasors (i.e. $\vec{V}_{l_x}^{\phi}$ and $\vec{V}_{l_y}^{\phi}$) and the nodal injections (i.e. $\vec{S}_{l_x}^{\phi} = P_{l_x}^{\phi} + jQ_{l_x}^{\phi}$ and $\vec{S}_{l_y}^{\phi} = P_{l_y}^{\phi} + jQ_{l_x}^{\phi}$), with the consideration of the single-phase line impedance $\hat{Z}_l^{\phi}$. Here, ϕ denotes the phase of the line; l_x and l_y represent the start and end node of the line, respectively. Power flow equations thorough a line can be expressed by $\vec{S}_{l_x}^{\phi} = \vec{V}_{l_x}^{\phi}\left(\frac{\vec{V}_{l_x}^{\phi} - \vec{V}_{l_y}^{\phi}}{\hat{Z}_l^{\phi}}\right)^*$. Similarly, if it is one of the three-phase line, equations are expressed by $\vec{S}_{l_x}^{\phi} = \vec{V}_{l_x}^{\phi}\left(\frac{\vec{V}_{l_x}^{\phi} - \vec{V}_{l_y}^{\phi}}{\sum_{\varphi \epsilon \Phi} \hat{Z}_l^{\phi,\varphi}}\right)^*$. Here, $\hat{Z}_l^{\phi,\varphi}$ is the impedance between phases ϕ and φ.

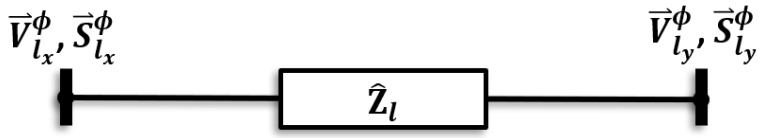

Figure 2-9. Single-phase line model

These non-linear power flow equations are solved by numerical iteration techniques, including fixed-point iteration, Gauss-Seidel, and Newton-based methods [88]. To converge to a solution, multiple iterations are needed. Also, given that LV networks may have hundreds and thousands of nodes, running power flow analyses is complex to implement for operational purposes (to assist the active management of DER).

To simplify the above voltage calculation, several approaches [69, 89-91] have been suggested, which are based on the single-phase voltage drop equation calculated by $\vec{V}_{l_x}^{\phi} - \vec{V}_{l_y}^{\phi} = \hat{Z}_l\left(\frac{\vec{S}_{l_x}^{\phi}}{\vec{V}_{l_x}^{\phi}}\right)^*$. Given that unbalances across phases are not considered, the 'unbalanced factor' has been developed in the literature to correct the above single-phase voltage drop equation [69, 89-91].

On the one hand, some distribution companies often calculate voltages using the linearised expression of the single-phase voltage drop equation, and it is eventually corrected by an empirically determined 'unbalanced factor' [89]. For example, in Australia, a series of distribution companies (i.e. Energex, Ergon, Essential Energy, and TasNetworks) have been using different 'unbalanced factors' [90, 91]. These empirical values cannot accurately cater for the needs of any demand/generation condition [69]. On the other hand, without relying on the local industry practice, Gupta et al. [69] have advised determining the 'unbalanced factor' via non-linear regression analyses and the machine-learning technique. However, this approach is also not practical enough. Firstly, a large number of smart meter measurements (i.e. half year or the whole year data) are needed to determine a relatively accurate trained 'unbalanced factor'. However, it cannot adequately describe the unbalanced nature in any demand/generation condition. Secondly, non-linear regression requires substantial effort to determine the best fit for the non-linear function of the problem. At the same time, it requires an appropriate start value to converge to a correct solution, but this searching process is not straightforward [105, 106]. Lastly, it is worth highlight that the 'unbalanced factor' can be appropriate for planning purposes, but it is not suitable for operational purposes.

2.4.2 Summary of Research Gaps

According to state-of-the-art voltage calculation approaches summarised above, the most accurate voltages can be determined by running conventional power flow analyses. However, it is complex to implement for operational purposes (to assist the active management of DER) The most recent and advanced works have simplified the voltage calculation by using single-phase line models and smart meter-driven 'unbalanced factors'. However, it cannot adequately capture the unbalanced nature in any demand/generation condition. At the same time, it is worth highlight that the 'unbalanced factor' can be appropriate for planning purposes, but it is not suitable for operational purposes. Thus far, no studies have proposed easily implementable methods to accurately and quickly calculate customer voltages for any demand/generation condition. Most importantly, no works have presented how to calculate customer voltages without assuming full knowledge of LV line impedances.

2.5 Summary

This chapter analysed the existing literature in terms of three aspects: LV line models, line impedance estimation, and voltage calculation. Research gaps regarding the last two points

were also summarised. To this end, it is necessary to answer some of the research questions based on the context of this chapter.

- What is the minimum requirement for the impedance of three-phase LV feeder lines to adequately capture the three-phase unbalanced characteristics of LV networks?

  Given that households are unevenly located at three phases of LV feeders, diverse demand/generation of customers make LV feeders unbalanced. To accurately analyse impacts of DER on voltages in inherently unbalanced three-phase LV networks, three-phase LV feeder line models must consider the phase couplings. The most simplified but adequate three-phase LV feeder line model has the same self-impedance and the same mutual impedance for all three phases, which is the minimum requirement for three-phase LV feeder lines. Although existing smart meter-driven impedance estimation approaches can estimate impedances, they do not consider phase couplings of three-phase LV feeder lines; and thus, they do not satisfy the minimum requirement. Therefore, this thesis will estimate the impedances of three-phase LV feeder lines with phase couplings and single-phase service lines.

- What smart meter data can be used for impedance estimation?

  Smart meters offer three types of data: active power, reactive power, and voltage magnitudes, which are available for impedance estimation. A few existing works did not use reactive power due to the lack of the corresponding data or its negligible impact on voltages, which is case-specific. In general, all the other works relied on all types of measurements. Thus, this thesis will exploit all three types of smart meter data to estimate impedances.

- Except for customer connection points, which point of three-phase LV feeders needs to be metered for impedance estimation?

  The most practical impedance estimation approach would not require any meter at three-phase LV feeders. Although some of the above-mentioned advanced impedance estimation approaches did not need meters along with three-phase LV feeders, they require voltages at the head of the feeder. Having only one three-phase meter at the head of the feeder can still be practical. Thus, this thesis will use meter data from

customer connection points and at the head of the feeder to estimate impedances, without relying on meter measurements along three-phase LV feeders.

- What is the minimum network knowledge required for impedance estimation?

  Both the customer connectivity and customer phase connection are needed for estimating impedances of LV feeder line and service line models. In the existing literature, approaches in [71, 72] can estimate the customer connectivity in unbalanced LV networks, and the method in [73] can identify the customer's phase connection. Therefore, the underlying network knowledge can be available, and thus, this thesis will estimate impedances of LV feeder line and service line models by assuming knowing the knowledge of the customer connectivity and the customer's phase connection.

- What methods can be used to exploit historical smart meter data?

  Both linearised and non-linearised optimisation approaches have been used for exploiting smart meter measurements. The linearised approach is preferable for a fast and simple calculation, but the accuracy is lower than that of the non-linearised method. However, given that some LV networks can be relatively large in terms of the number of lines and nodes, the non-linearised approach can be less scalable. Therefore, this thesis will exploit smart meter measurements by using a practical linearised based approach.

- Without using three-phase power flow analyses, how can we quickly and accurately determine customer voltages in any demand/generation condition (i.e. what-if analysis)?

  The most recent approach has used a single-phase non-linearised voltage drop equation with an 'unbalanced factor' to calculate customer voltages. The 'unbalanced factor' is trained by a large number of smart meter measurements (i.e. half year and one year) by using a machine learning technique. Although the method has tried to simplify the voltage calculation, it cannot adequately describe the 'unbalanced factor' at that moment in time. Thus, it can be appropriate for planning purposes, but it is not suitable for operational purposes. Most importantly, no works have presented how to calculate customer voltages without assuming full knowledge of LV line impedances. Thus, this

thesis will propose an easily implemented approach to quickly and accurately determine customer voltages based on estimated LV feeder line and service line model.

This page is intentionally left blank.

3 METHODOLOGY

3.1 Introduction

This chapter answers the main research question: *Can we assess the impacts of DER on customer voltages in what-if analyses using smart meter-driven LV line models (i.e. three-phase LV feeder lines and single-phase service lines)?*

The proposed methodology first presents how to estimate impedances of LV line models based on measurements from smart meters and at the head of the feeder. Once having the estimated impedances, it explains how to calculate customer voltages when performing what-if analyses for operational purposes. As such, Section 3.2 presents the overview and the assumptions of the proposed methodology. Then, Sections 3.3 and 3.4 explain the details of impedance estimation and voltage calculation. The pseudocodes are provided in each section. Lastly, Section 3.5 demonstrates the implementation of the proposed methodology on an example three-phase LV feeder (with single-phase service lines). This work aims to offer distribution companies a smart meter-driven tool to quickly and accurately calculate customer voltages in what-if analyses.

3.2 Overview and Assumptions

3.2.1 Overview

The proposed methodology has two parts. The first part aims to estimate the impedances of three-phase LV feeder lines and single-phase service lines, as shown on the left-hand side of Figure 3-1. Four inputs are needed in this process. The first two inputs are the historical measurements (i.e. active power, reactive power, and voltage magnitude) from smart meters and at the head of the feeder. It is worth highlight that the measurement device (transformer terminal unit) installed at the head of the feeder (the secondary side of pole or pad-mounted transformer) needs to capture the voltages and power flows. The last two inputs are the customer phase connection and location. These four inputs are sent to the linearised voltage drop equations and the multiple linear regression (MLR) technique to calculate the unknown

impedances. This process is a one-off calculation but can be used periodically to update impedances if conductors are changed. Then, once the impedances of LV lines are obtained, the second part calculates customer voltages in what-if analyses, as shown on the right-hand side of Figure 3-1. For any demand/generation conditions of households (with/without DER), the linearised voltage drop equations can be used to calculate the corresponding voltages.

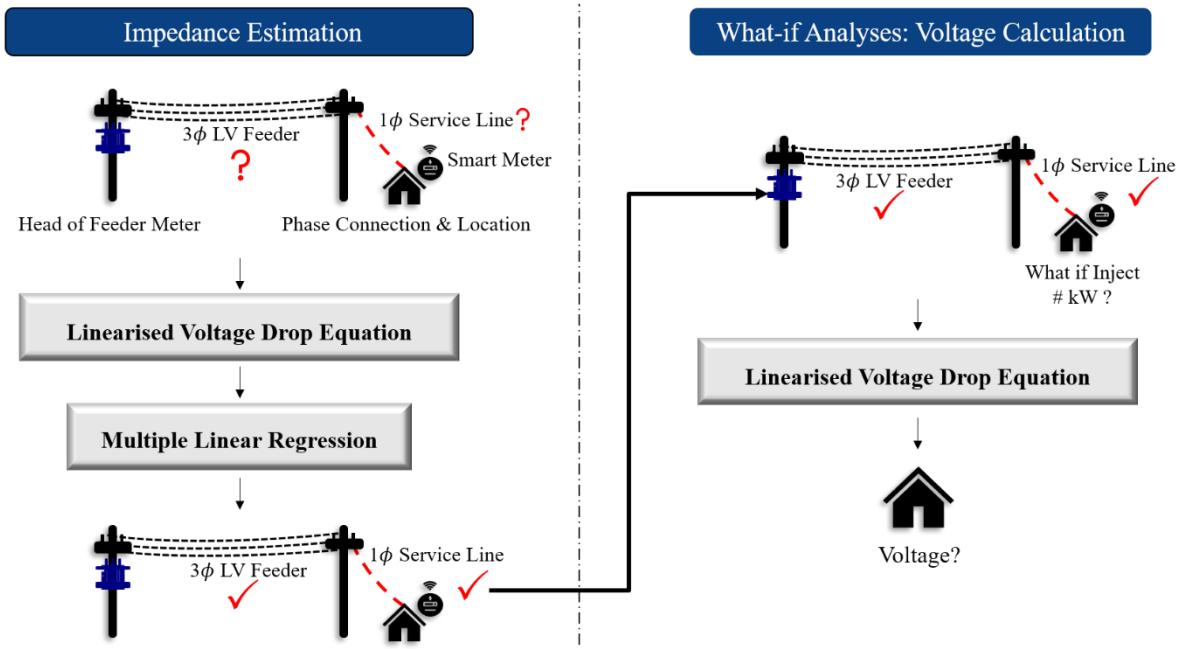

Figure 3-1. Illustration of the proposed approach

3.2.2 Assumptions

This section outlines the assumptions for each part of the proposed methodology. For ease of understanding, a general LV network (Figure 3-2) is used to explain the assumptions used in this study.

In Figure 3-2, the black line represents a three-phase LV feeder, which is divided into several lines $l \in L$. The start node and end node of three-phase line l are represented by $l_x \in N$ and $l_y \in N$, respectively. The three-phase line l is connected to a single-phase customer using a single-phase service line (the red line) s_l , $s \in S$. Similarly, $s_{l,x} \in N$ and $s_{l,y} \in N$ denote the start node and end node of service line s_l , respectively. The voltage with angle $\vartheta \in \Theta$ at the start node of the three-phase line l_x and phase $\phi \in \Phi = \{a, b, c\}$ is characterized by $V_{l_x}^{\phi} \angle \vartheta_{l_x}^{\phi}$; and the voltage with angle $\vartheta \in \Theta$ at the end node of the three-phase line l_y and phase $\phi \in \Phi = \{a, b, c\}$ is characterized by $V_{l_y}^{\phi} \angle \vartheta_{l_y}^{\phi}$. Similarly, the voltage with angle $\vartheta \in \Theta$ at the start node

of the single-phase line $s_{l,x}$ and phase $\phi \in \Phi = \{a, b, c\}$ is characterized by $v_{s_{l,x}}^{\phi} \angle \vartheta_{s_{l,x}}^{\phi}$; and the voltage with angle $\vartheta \in \Theta$ at the end node of the single-phase line $s_{l,y}$ and phase $\phi \in \Phi = \{a, b, c\}$ is characterized by $v_{s_{l,y}}^{\phi} \angle \vartheta_{s_{l,y}}^{\phi}$. Furthermore, for each part of the methodology, the corresponding known parameters are **bolded.** It should be noted that this work uses time-series data for voltage magnitudes, active power, and reactive power. For simplicity, the time indices $t \in T$ are not presented. The details about each of the assumptions for the impedance estimation and voltage calculations are summarised below.

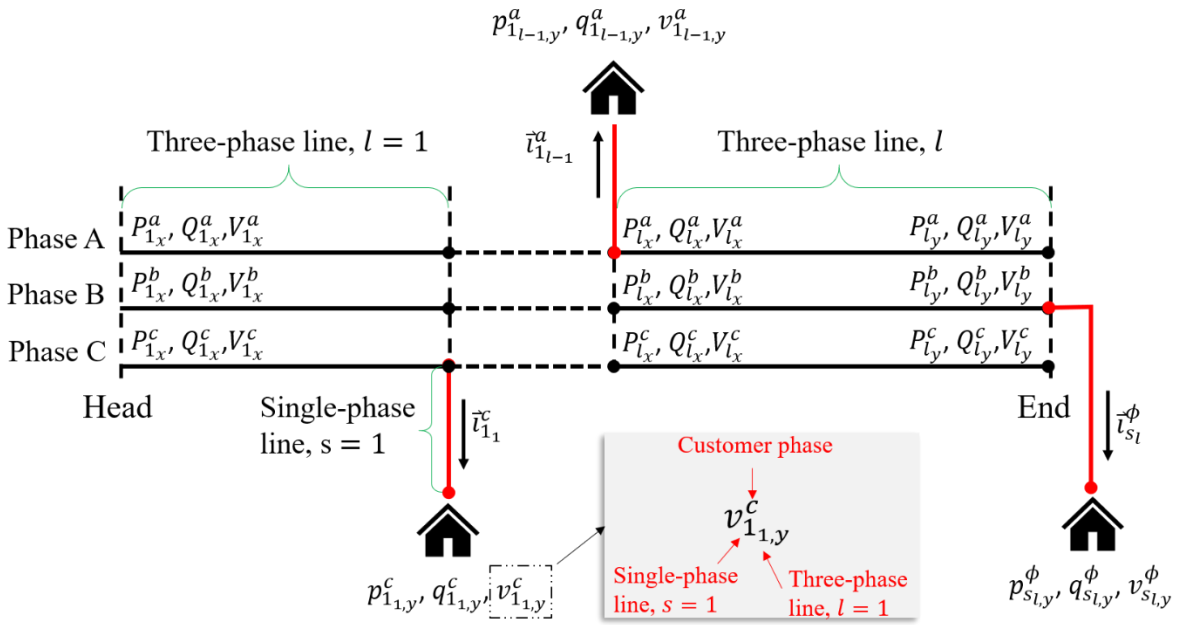

Figure 3-2. A general LV network

Impedance Estimation

1) The LV feeder is radial.

   As mentioned in Section 1.1.1, most LV feeders are radial in many countries [12]. For ease of understanding, the laterals are not included in the explanation. But it should be noted that the proposed approach can be used in an LV network that has feeders with laterals. Thus, this assumption is valid.

2) Single-phase customer location, $\sigma_h \in N$, customer connectivity, and customer phase connection, $\phi \in \Phi$, are known from the geographical information systems given by distribution companies.

As mentioned in Section 1.1.1, most residential households are single-phase [11]. Also, in real systems, the customer location is usually known [71, 72]. Furthermore, as mentioned in Section 1.2.1, given that most of the existing impedance estimation approaches have indicated knowing the customer connectivity and the customer phase connection, they can be available in practice. If not, the studies in [71-73] have been able to accurately identify them. Thus, this assumption is credible. At the same time, it should be noted that the distances are not needed.

3) Smart meter measurements of each customer are collected at the end node of the service line $s_{l,y}$ at phase ϕ, including active power, reactive power and voltage magnitude, denoted by $\boldsymbol{p}^{\boldsymbol{\phi}}_{\boldsymbol{s_{l,y}}}$, $\boldsymbol{q}^{\boldsymbol{\phi}}_{\boldsymbol{s_{l,y}}}$ and $\boldsymbol{v}^{\boldsymbol{\phi}}_{\boldsymbol{s_{l,y}}}$, respectively.

   It is worth mentioning that, in this work, all these smart meter parameters are defined in relation to the service lines. But they can also be defined with respect to customers.

4) Head of feeder meter measurements at the start node of the first three-phase line l_x ($l = 1$) at all three phases ϕ are known, including active power, reactive power and voltage magnitude, denoted by $\boldsymbol{P}^{\boldsymbol{\phi}}_{\boldsymbol{1_x}}$ (i.e. $\boldsymbol{P}^{\boldsymbol{a}}_{\boldsymbol{1_x}}$, $\boldsymbol{P}^{\boldsymbol{b}}_{\boldsymbol{1_x}}$, $\boldsymbol{P}^{\boldsymbol{c}}_{\boldsymbol{1_x}}$), $\boldsymbol{Q}^{\boldsymbol{\phi}}_{\boldsymbol{1_x}}$ (i.e. $\boldsymbol{Q}^{\boldsymbol{a}}_{\boldsymbol{1_x}}$, $\boldsymbol{Q}^{\boldsymbol{b}}_{\boldsymbol{1_x}}$, $\boldsymbol{Q}^{\boldsymbol{c}}_{\boldsymbol{1_x}}$) and $\boldsymbol{V}^{\boldsymbol{\phi}}_{\boldsymbol{1_x}}$(i.e. $\boldsymbol{V}^{\boldsymbol{a}}_{\boldsymbol{1_x}}, \boldsymbol{V}^{\boldsymbol{b}}_{\boldsymbol{1_x}}, \boldsymbol{V}^{\boldsymbol{c}}_{\boldsymbol{1_x}}$), respectively.

   Only one additional meter is required to record the three-phase data at the head of the LV feeder, which is feasible and not expensive. In addition, in this work, all these parameters are defined in relation to the lines. They can also be defined with respect to the head of the feeder.

5) The phase shift of three-phase lines is assumed as 120°.

   The study in [71] have assumed a 120° phase shift in an unbalanced three-phase LV network for topology estimation, and the results are highly accurate. Thus, it proves that the assumption is reasonable. Also, the findings of this thesis (in Figure 4-8), the phase shift is maintained at $120^{\circ} \pm 1^{\circ}$, show that this assumption is acceptable.

6) Negligible angle difference along the three-phase LV feeder.

At each phase of the three-phase LV feeder, voltage angle increments from the reference to the end of the feeder. However, as mentioned in [12], changes in these voltage angles are small and can be regarded as 0°.

7) Equation 2.8 is used as a three-phase line, and R_l^s, X_l^s, R_l^m, X_l^m are used to represent the self-resistance, self-reactance, mutual resistance, and mutual reactance of the three-phase line l.

   As mentioned in Section 2.5, this assumption satisfies the minimum requirement for LV feeders to run unbalanced three-phase power flow analyses. Hence, this assumption is reasonable. It is worth mentioning that ground impedances and neutral-wire impedances are not involved in this work. Thus, the impedance of a single-phase service line s_l at phase ϕ is accordingly presented by a complex value, which can be denoted by $r_{s_l}^{\phi} + jx_{s_l}^{\phi}$.

What-if analyses: Voltage Calculation

8) As in assumption 2, single-phase customer location, $\sigma_h \in N$, customer connectivity, and customer phase connection, $\phi \in \Phi$, are known.

9) Once the impedances are estimated, self-resistance, self-reactance, mutual-resistance and mutual-reactance of each three-phase line l are known, denoted by $\boldsymbol{R_l^s}$, $\boldsymbol{X_l^s}$, $\boldsymbol{R_l^m}$, and $\boldsymbol{X_l^m}$, respectively; resistance and reactance of each single-phase service line s_l at phase ϕ are known, which are denoted by $\boldsymbol{r_{s_l}^{\phi}}$, $\boldsymbol{x_{s_l}^{\phi}}$, respectively.

10) The active power and reactive power of demand/generation of each customer are known at the end of the service line $s_{l,y}$ at phase ϕ, which are denoted by $\boldsymbol{p_{s_{l,y}}^{\phi}}$, $\boldsymbol{q_{s_{l,y}}^{\phi}}$, respectively.

    It is worth mentioning that, in this work, all these parameters are defined in relation to the service lines. But they can also be defined with respect to customers.

11) As in assumption 4, the voltage magnitudes at the start node of the first three-phase line l_x ($l = 1$) at all three phases ϕ are known, denoted by $\boldsymbol{V_{1_x}^{\phi}}$ (i.e. $\boldsymbol{V_{1_x}^{a}}$, $\boldsymbol{V_{1_x}^{b}}$, $\boldsymbol{V_{1_x}^{c}}$).

12) Line losses of three-phase feeders and single-phase service lines are negligible.

13) As in assumption 5, the phase shift of three-phase lines is assumed as 120°.

14) As in assumption 6, negligible angle difference along the three-phase LV feeder [12].

3.3 Impedance Estimation

3.3.1 Linearised Voltage Drop Equation

This section mainly presents the linearised voltage drop equations for single-phase lines, three-phase lines and combo lines (i.e. combined three-phase lines l and single-phase service lines s_l). Although the classic single-phase linearised voltage drop equation has been used in many studies [12], as presented in Equation 2.8, the derivation is given here for ease of understanding.

3.3.1.1 Single-Phase Line

Voltage drop equation for single-phase service line s_l is shown in Equation 3.1. Here, $\hat{z}_{s_l}$ denotes the impedance of a service line s_l, and $\vec{\imath}_{s_l}^{\phi}$ represents the current on the service line s_l at phase ϕ. The current is determined by the power injection and voltage at the end node of the service line (i.e. $\boldsymbol{p}_{s_{l,y}}^{\boldsymbol{\phi}}$, $\boldsymbol{q}_{s_{l,y}}^{\boldsymbol{\phi}}$ and $\boldsymbol{v}_{s_{l,y}}^{\boldsymbol{\phi}}\angle\vartheta_{s_{l,y}}^{\phi}$).

$$v_{s_{l,x}}^{\phi}\angle\vartheta_{s_{l,x}}^{\phi} - \boldsymbol{v}_{s_{l,y}}^{\boldsymbol{\phi}}\angle\vartheta_{s_{l,y}}^{\phi} = \hat{z}_{s_l}\frac{\left(\boldsymbol{p}_{s_{l,y}}^{\boldsymbol{\phi}} + j\boldsymbol{q}_{s_{l,y}}^{\boldsymbol{\phi}}\right)^{*}}{\left(\boldsymbol{v}_{s_{l,y}}^{\boldsymbol{\phi}}\angle\vartheta_{s_{l,y}}^{\phi}\right)^{*}} = \hat{z}_{s_l}\vec{\imath}_{s_l}^{\phi}, \forall s \in S, \forall l \in L, \forall \phi \in \Phi \tag{3.1}$$

The simplified expression of Equation 3.1, as shown in Equation 3.2, is derived based on the assumption of negligible angle difference between two nodes of a service line s_l (i.e. $\vartheta_{s_{l,x}}^{\phi} \cong \vartheta_{s_{l,y}}^{\phi}$).

$$\begin{aligned}\left(v_{s_{l,x}}^{\phi} - \boldsymbol{v}_{s_{l,y}}^{\boldsymbol{\phi}}\right)\cos\vartheta_{s_{l,x}}^{\phi} + j\left(v_{s_{l,x}}^{\phi} - \boldsymbol{v}_{s_{l,y}}^{\boldsymbol{\phi}}\right)\sin\vartheta_{s_{l,x}}^{\phi} \cong r_{s_l}^{\phi}\Re\left[\vec{\imath}_{s_l}^{\phi}\right] - x_{s_l}^{\phi}\Im\left[\vec{\imath}_{s_l}^{\phi}\right] + \\ j\left(r_{s_l}^{\phi}\Im\left[\vec{\imath}_{s_l}^{\phi}\right] + x_{s_l}^{\phi}\Re\left[\vec{\imath}_{s_l}^{\phi}\right]\right), \forall s \in S, \forall l \in L, \forall \phi \in \Phi\end{aligned} \tag{3.2}$$

Given that $\vartheta_{s_{l,x}}^{\phi}$ is arbitrary, $\vartheta_{s_{l,x}}^{\phi}$ can be set to 0°. Then, the linearised expression of Equation 3.1 is shown in Equation 3.3, where $\vec{\imath}_{s_l}^{\phi}$ is given by $\left[\left(\boldsymbol{p}_{s_{l,y}}^{\boldsymbol{\phi}} + j\boldsymbol{q}_{s_{l,y}}^{\boldsymbol{\phi}}\right)/\boldsymbol{v}_{s_{l,y}}^{\boldsymbol{\phi}}\right]^{*}$.

$$v_{s_{l,x}}^{\phi} - \boldsymbol{v_{s_{l,y}}^{\phi}} = r_{s_l}^{\phi}\Re\left[\vec{\imath}_{s_l}^{\phi}\right] - x_{s_l}^{\phi}\Im\left[\vec{\imath}_{s_l}^{\phi}\right], \forall s \in S, \forall l \in L, \forall \phi \in \Phi \quad 3.3$$

3.3.1.2 Three-Phase Line

Taking phase $\psi \in \Phi$ as the reference, the other two phases of line l in clockwise order are denoted by $\varphi_1 \in \Phi\backslash\{\psi\}$ and $\varphi_2 \in \Phi\backslash\{\psi, \varphi_1\}$, respectively. The voltage drop equation for one three-phase line l at phase ψ of the feeder is expressed in Equation 3.4. This drop is not only caused by the self-impedance $\hat{Z}_l^s$ but also by the mutual impedance $\hat{Z}_l^m$. $\vec{I}_{\psi,l}^{\psi}$ is the current flowing through the line's self-impedance (i.e. $\hat{Z}_l^s$); and $\vec{I}_{\psi,l}^{\varphi 1}$ and $\vec{I}_{\psi,l}^{\varphi 2}$ are the current flowing through the line's mutual-impedance (i.e. $\hat{Z}_l^m$). These currents flowing through the three-phase line l are determined in Equation 3.5. It should be noted that, except for the head of the LV feeder, measurements on the other three-phase buses along the LV feeder are not considered available (as in practice is not possible to have multiple measurements throughout the three-phase feeder).

$$V_{l_x}^{\psi}\angle\vartheta_{l_x}^{\psi} - V_{l_y}^{\psi}\angle\vartheta_{l_y}^{\psi} = \hat{Z}_l^s\vec{I}_{\psi,l}^{\psi} + \hat{Z}_l^m\left(\vec{I}_{\psi,l}^{\varphi 1} + \vec{I}_{\psi,l}^{\varphi 2}\right), \forall l \in L, \forall \psi, \varphi 1, \varphi 2 \in \Phi \quad 3.4$$

$$\begin{cases} \vec{I}_{\psi,l}^{\psi} = \left[\left(P_{l_x}^{\psi} + jQ_{l_x}^{\psi}\right)/V_{l_x}^{\psi}\angle\vartheta_{l_x}^{\psi}\right]^* \\ \vec{I}_{\psi,l}^{\varphi 1} = \left[\left(P_{l_x}^{\varphi 1} + jQ_{l_x}^{\varphi 1}\right)/V_{l_x}^{\varphi 1}\angle\vartheta_{l_x}^{\varphi 1}\right]^*, \forall l \in L, \forall \psi, \varphi 1, \varphi 2 \in \Phi \\ \vec{I}_{\psi,l}^{\varphi 2} = \left[\left(P_{l_x}^{\varphi 2} + jQ_{l_x}^{\varphi 2}\right)/V_{l_x}^{\varphi 2}\angle\vartheta_{l_x}^{\varphi 2}\right]^* \end{cases} \quad 3.5$$

Assuming the negligible voltage angle difference for a three-phase line at any phase $\phi \in \Phi$ (i.e. $\vartheta_{l_x}^{\phi} \cong \vartheta_{l_y}^{\phi}$), the simplified expression of Equation 3.4 is shown in Equation 3.6 by separating the real and imaginary part. Furthermore, given that the phase shift of three-phase lines is assumed as 120°, the voltage angles in Equation 3.5 are expressed in Equation 3.7.

$$\left(V_{l_x}^{\psi}-V_{l_y}^{\psi}\right)\cos\vartheta_{l_x}^{\psi}+j\left(V_{l_x}^{\psi}-V_{l_y}^{\psi}\right)\sin\vartheta_{l_x}^{\psi}=R_l^s\Re\left[\vec{I}_{\psi,l}^{\psi}\right]-X_l^s\Im\left[\vec{I}_{\psi,l}^{\psi}\right]+R_l^m\left(\Re\left[\vec{I}_{\psi,l}^{\varphi 1}\right]+\Re\left[\vec{I}_{\psi,l}^{\varphi 2}\right]\right)-X_l^m\left(\Im\left[\vec{I}_{\psi,l}^{\varphi 1}\right]+\Im\left[\vec{I}_{\psi,l}^{\varphi 2}\right]\right)+j\langle R_l^s\Im\left[\vec{I}_{\psi,l}^{\psi}\right]+X_l^s\Re\left[\vec{I}_{\psi,l}^{\psi}\right]+R_l^m\left(\Im\left[\vec{I}_{\psi,l}^{\varphi 1}\right]+\Im\left[\vec{I}_{\psi,l}^{\varphi 2}\right]\right)+X_l^m\left(\Re\left[\vec{I}_{\psi,l}^{\varphi 1}\right]+\Re\left[\vec{I}_{\psi,l}^{\varphi 2}\right]\right)\rangle,\ \forall l\in L,\forall\psi,\varphi 1,\varphi 2\in\Phi \tag{3.6}$$

$$\left[\vartheta_{l_x}^{\psi}\quad\vartheta_{l_x}^{\varphi 1}\quad\vartheta_{l_x}^{\varphi 2}\right]=\left[\vartheta_{l_x}^{\psi}\quad\vartheta_{l_x}^{\psi}-120^{\circ}\quad\vartheta_{l_x}^{\psi}+120^{\circ}\right],\ \forall l\in L,\forall\psi,\varphi 1,\varphi 2\in\Phi \tag{3.7}$$

Similar to the single-phase voltage drop equation, $\vartheta_{l_x}^{\psi}$ is assumed as 0°, and thus, the set of the three-phase voltage angle is $[0^{\circ},-120^{\circ},120^{\circ}]$. This simplifies Equation 3.6 to Equation 3.8, which is the linearised expression of Equation 3.4. Here, the three-phase currents in Equation 3.8 are calculated by Equation 3.9.

$$V_{l_x}^{\psi}-V_{l_y}^{\psi}=R_l^s\Re\left[\vec{I}_{\psi,l}^{\psi}\right]-X_l^s\Im\left[\vec{I}_{\psi,l}^{\psi}\right]+R_l^m\left(\Re\left[\vec{I}_{\psi,l}^{\varphi 1}\right]+\Re\left[\vec{I}_{\psi,l}^{\varphi 2}\right]\right)-X_l^m\left(\Im\left[\vec{I}_{\psi,l}^{\varphi 1}\right]+\Im\left[\vec{I}_{\psi,l}^{\varphi 2}\right]\right),\ \forall l\in L,\forall\psi,\varphi 1,\varphi 2\in\Phi \tag{3.8}$$

$$\begin{cases}\vec{I}_{\psi,l}^{\psi}=\left[\left(P_{l_x}^{\psi}+jQ_{l_x}^{\psi}\right)/V_{l_x}^{\psi}\right]^{*}\\ \vec{I}_{\psi,l}^{\varphi 1}=\left[\left(P_{l_x}^{\varphi 1}+jQ_{l_x}^{\varphi 1}\right)/V_{l_x}^{\varphi 1}\angle-120^{\circ}\right]^{*}\\ \vec{I}_{\psi,l}^{\varphi 2}=\left[\left(P_{l_x}^{\varphi 2}+jQ_{l_x}^{\varphi 2}\right)/V_{l_x}^{\varphi 2}\angle 120^{\circ}\right]^{*}\end{cases},\ \forall\psi,\varphi 1,\varphi 2\in\Phi \tag{3.9}$$

Although another linearised expression of three-phase voltage drop has been derived in [71], the difference is that this work (this thesis) only uses the real part of voltage drop. Therefore, without considering the imaginary part of the voltage drop equation, the linearised voltage drop equation derived here is more efficient and practical.

3.3.1.3 Combo Line

To calculate the voltage drop of a combo line (i.e. the combined three-phase line l and single-phase service line s_l), Equation 3.3 and Equation 3.8 are aggregated (in Equation 3.10). Here, customers are located at phase $\psi\in\Phi$, and ϕ in Equation 3.3 is replaced by ψ, and thus, the voltage drop equation for the combo line is derived at phase ψ. Moreover, it cancels out the

unknown voltage at the start node of the service line $v_{s_{l,x}}^{\psi}$ in Equation 3.3, which is also the voltage at the end node of the three-phase line $V_{l_y}^{\psi}$ in Equation 3.8 at phase ψ.

$$V_{l_x}^{\psi} - \boldsymbol{v}_{\boldsymbol{s_{l,y}}}^{\psi} = R_l^s \Re\left[\vec{I}_{\psi,l}^{\psi}\right] - X_l^s \Im\left[\vec{I}_{\psi,l}^{\psi}\right] + R_l^m \left(\Re\left[\vec{I}_{\psi,l}^{\varphi 1}\right] + \Re\left[\vec{I}_{\psi,l}^{\varphi 2}\right]\right) - X_l^m \left(\Im\left[\vec{I}_{\psi,l}^{\varphi 1}\right] + \Im\left[\vec{I}_{\psi,l}^{\varphi 2}\right]\right) + r_{s_l}^{\psi} \Re\left[\vec{i}_{s_l}^{\psi}\right] - x_{s_l}^{\psi} \Im\left[\vec{i}_{s_l}^{\psi}\right], \forall s \in S, \forall l \in L, \forall \psi, \varphi 1, \varphi 2 \in \Phi \quad 3.10$$

3.3.2 Multiple Linear Regression

In order to estimate line impedances, the derived voltage drop equations need to be solved by multiple linear regression (MLR). This section firstly describes the principles of MLR. Then, it specifies the application of MLR in this work.

3.3.2.1 Definition

The MLR model, with T observations, is presented in Equation 3.11. For each observation, this model not only has one dependent variable Y_t and residual ϵ_t but has $I(I \geq 2)$ independent variables X_t^i and coefficients β^i [107, 108]. Furthermore, its compact expression is given by $y = \beta x + \epsilon$.

$$Y_t = \sum_{i=1}^{I} \beta^i X_t^i + \epsilon_t, \forall\, t \in T \quad 3.11$$

The goal of MLR is to find the "best" coefficients and determine the linear relationship between the independent variables and the dependent variable. To achieve this, ordinary least squares (OLS) regression is commonly used. The function of OLS is that it estimates parameters by minimizing the sum of squared residual using the relation $(y - \beta x)'(y - \beta x)$. If the sum of squared residual is zero, the expression for MLR will be $\hat{y} = x\hat{\beta}$, and the coefficients will be determined by $\hat{\beta} = (x^T x)^{-1} x^T y$ [108].

To avoid getting ill-defined coefficients, it is necessary to make sure that $(x^T x)$ is invertible. These non-invertible conditions are outlined as follows [109]:

1) If two (or more than two) of the independent variables are proportional to each other, the data are collinear.

   For example, in the context of this work, if $\Re\left[\vec{I}_{\psi,l}^{\psi}\right] = constant \times \Im\left[\vec{I}_{\psi,l}^{\psi}\right]$, the data are collinear.

2) If two (or more than two) of the independent variables are linearly related, the data are collinear.

   For example, in the context of this work, if $\Re\left[\vec{I}_{\psi,l}^{\psi}\right] = constant_1 \times \Im\left[\vec{I}_{\psi,l}^{\psi}\right] + constant_2$, the data are collinear.

3) If one (or more than one) of the independent variables is constant, the data are collinear.

   For example, in the context of this work, if $\Re\left[\vec{I}_{\psi,l}^{\psi}\right] = constant$, the data are collinear.

3.3.2.2 Application

The application of MLR in this work is to predict the multiple impedance variables in Equation 3.10, and the MLR at time t is given by Equation 3.12. Here, the left-hand side voltage drop represents the t^{th} observed dependent variable, and current variables on the right-hand side represent the t^{th} observed independent variables. The voltage drop and line currents are the inputs of MLR. Then, OLS is carried out to minimize the sum of the squared residual (i.e. $\sum_{t\in T} {\epsilon_t}^2$) to estimate the impedances (denoted by superscript ˜).

$$V_{l_x}^{\psi} - \boldsymbol{v}_{\boldsymbol{s_{l,y}}}^{\boldsymbol{\psi}} = \tilde{R}_l^s \Re\left[\vec{I}_{\psi,l}^{\psi}\right] - \tilde{X}_l^s \Im\left[\vec{I}_{\psi,l}^{\psi}\right] + \tilde{R}_l^m \left(\Re\left[\vec{I}_{\psi,l}^{\varphi 1}\right] + \Re\left[\vec{I}_{\psi,l}^{\varphi 2}\right]\right) - \tilde{X}_l^m \left(\Im\left[\vec{I}_{\psi,l}^{\varphi 1}\right] + \Im\left[\vec{I}_{\psi,l}^{\varphi 2}\right]\right) + \tilde{r}_{s_l}^{\psi} \Re[\vec{\imath}_{s_l}^{\psi}] - \tilde{x}_{s_l}^{\psi} \Im[\vec{\imath}_{s_l}^{\psi}] + \epsilon, \quad 3.12$$

$$\forall s \in S, \forall l \in L, \forall \psi, \varphi 1, \varphi 2 \in \Phi$$

In addition, if a single-phase service line s_l is connected to phase ψ of a three-phase line l at the end of the feeder, these two lines will share the same current. Thus, two pairs of current variables in Equation 3.12 are the same (i.e. $\Re\left[\vec{I}_{\psi,l}^{\psi}\right]$ & $\Re[\vec{\imath}_{s_l}^{\psi}]$, $\Im\left[\vec{I}_{\psi,l}^{\psi}\right]$ & $\Im[\vec{\imath}_{s_l}^{\psi}]$). Given that input variables are collinear, MLR is unable to correctly estimate each impedance variable in

Equation 3.12. To solve this issue, the mutual-impedance and the combined self-impedances (i.e. $\tilde{R}_l^s + \tilde{r}_{s_l}^{\psi}$, $\tilde{X}_l^s + \tilde{x}_{s_l}^{\psi}$) will be determined in Equation 3.13.

$$V_{l_x}^{\psi} - \boldsymbol{v}_{\boldsymbol{s_{l,y}}}^{\psi} = \left(\tilde{R}_l^s + \tilde{r}_{s_l}^{\psi}\right)\Re\left[\vec{I}_{\psi,l}^{\psi}\right] - \left(\tilde{X}_l^s + \tilde{x}_{s_l}^{\psi}\right)\Im\left[\vec{I}_{\psi,l}^{\psi}\right] + \tilde{R}_l^m\left(\Re\left[\vec{I}_{\psi,l}^{\varphi 1}\right] + \Re\left[\vec{I}_{\psi,l}^{\varphi 2}\right]\right) - \tilde{X}_l^m\left(\Im\left[\vec{I}_{\psi,l}^{\varphi 1}\right] + \Im\left[\vec{I}_{\psi,l}^{\varphi 2}\right]\right) + \epsilon, \forall s \in S, \forall l \in L, \forall \psi, \varphi 1, \varphi 2 \in \Phi \quad (3.13)$$

The impedance estimation process exploits historical time-series measurements from smart meters (i.e. $\boldsymbol{p}_{\boldsymbol{s_{l,y}}}^{\boldsymbol{\phi}}$, $\boldsymbol{q}_{\boldsymbol{s_{l,y}}}^{\boldsymbol{\phi}}$, $\boldsymbol{v}_{\boldsymbol{s_{l,y}}}^{\boldsymbol{\phi}}$) and at the head of the feeder (i.e. $\boldsymbol{P}_{\mathbf{1}_x}^{\boldsymbol{\phi}}$, $\boldsymbol{Q}_{\mathbf{1}_x}^{\boldsymbol{\phi}}$, $\boldsymbol{V}_{\mathbf{1}_x}^{\boldsymbol{\phi}}$). Current and voltage drop variables for all samples (historical time-series measurements) are needed to enable the estimation of impedances of three-phase and single-phase lines. The details of determining current and voltage drop variables for one sample are explained below.

Current

This section explains how to calculate the current on each single-phase service line and three-phase line. On the one hand, currents on service lines (i.e. $\vec{\imath}_{s_l}^{\psi}$) can be determined straightforwardly in $\left[\left(\boldsymbol{p}_{\boldsymbol{s_{l,y}}}^{\psi} + j\boldsymbol{q}_{\boldsymbol{s_{l,y}}}^{\psi}\right)/\boldsymbol{v}_{\boldsymbol{s_{l,y}}}^{\psi}\right]^*$. On the other hand, currents on each three-phase line (i.e. $\vec{I}_{\psi,l}^{\psi}$, $\vec{I}_{\psi,l}^{\varphi 1}$, $\vec{I}_{\psi,l}^{\varphi 2}$) are calculated in Equations 3.9 and 3.14 based on the meter measurements at the head of the feeder and Kirchhoff's current law.

$$\begin{cases} \vec{I}_{\psi,l+1}^{\psi} = \vec{I}_{\psi,l}^{\psi} - \sum_{s\in S}\left[\left(\boldsymbol{p}_{\boldsymbol{s_{l,y}}}^{\psi} + j\boldsymbol{q}_{\boldsymbol{s_{l,y}}}^{\psi}\right)/\boldsymbol{v}_{\boldsymbol{s_{l,y}}}^{\psi}\right]^* \\ \vec{I}_{\psi,l+1}^{\varphi 1} = \vec{I}_{\psi,l}^{\varphi 1} - \sum_{s\in S}\left[\left(\boldsymbol{p}_{\boldsymbol{s_{l,y}}}^{\boldsymbol{\varphi 1}} + j\boldsymbol{q}_{\boldsymbol{s_{l,y}}}^{\boldsymbol{\varphi 1}}\right)/\boldsymbol{v}_{\boldsymbol{s_{l,y}}}^{\boldsymbol{\varphi 1}}\angle -\mathbf{120}^{\circ}\right]^*, \\ \vec{I}_{\psi,l+1}^{\varphi 2} = \vec{I}_{\psi,l}^{\varphi 2} - \sum_{s\in S}\left[\left(\boldsymbol{p}_{\boldsymbol{s_{l,y}}}^{\boldsymbol{\varphi 2}} + j\boldsymbol{q}_{\boldsymbol{s_{l,y}}}^{\boldsymbol{\varphi 2}}\right)/\boldsymbol{v}_{\boldsymbol{s_{l,y}}}^{\boldsymbol{\varphi 2}}\angle \mathbf{120}^{\circ}\right]^* \end{cases} \quad (3.14)$$

$$\forall s \in S, \forall l \in L, \forall \psi, \varphi 1, \varphi 2 \in \Phi$$

Voltage Drop

The voltage drop of the combo line at phase ψ, as presented in Equations 3.12 or 3.13, relies on the voltages at the start node of the three-phase line (i.e. $V_{l_x}^{\psi}$, $V_{l_x}^{\varphi 1}$, $V_{l_x}^{\varphi 2}$). These voltages are

Algorithm I: Impedance Estimation

Input: $\boldsymbol{p}_{s_{l,y}}^{\boldsymbol{\phi}}$, $\boldsymbol{q}_{s_{l,y}}^{\boldsymbol{\phi}}$, $\boldsymbol{v}_{s_{l,y}}^{\boldsymbol{\phi}}$, $\boldsymbol{P}_{1_x}^{\boldsymbol{\phi}}$, $\boldsymbol{Q}_{1_x}^{\boldsymbol{\phi}}$, $\boldsymbol{V}_{1_x}^{\boldsymbol{\phi}}$

Output: $\tilde{R}_l^s$, $\tilde{X}_l^s$, $\tilde{R}_l^m$, $\tilde{X}_l^m$, $\tilde{r}_{s_l}^{\psi}$, $\tilde{x}_{s_l}^{\psi}$

For each $\boldsymbol{\psi}$ (reference), $\boldsymbol{\varphi 1}$, $\boldsymbol{\varphi 2}$, $\boldsymbol{l}$, $\boldsymbol{s}$:

For each $\boldsymbol{t}$:

1. Calculate three-phase line currents:

   if $l = 1$:
   $\vec{I}_{\psi,l}^{\psi}$, $\vec{I}_{\psi,l}^{\varphi 1}$, $\vec{I}_{\psi,l}^{\varphi 2}$ → Equation 3.9.
   else:
   $\vec{I}_{\psi,l}^{\psi}$, $\vec{I}_{\psi,l}^{\varphi 1}$, $\vec{I}_{\psi,l}^{\varphi 2}$ → Equation 3.14.

2. Calculate single-phase line currents $\vec{\imath}_{s_l}^{\psi}$ in $\left[\left(\boldsymbol{p}_{\boldsymbol{s_{l,y}}}^{\psi} + j\boldsymbol{q}_{\boldsymbol{s_{l,y}}}^{\psi}\right)/\boldsymbol{v}_{\boldsymbol{s_{l,y}}}^{\psi}\right]^*$.

3. Calculate voltage drop of a combo line in $V_{l_x}^{\psi} - \boldsymbol{v}_{\boldsymbol{s_{l,y}}}^{\psi}$:

   if $l = 1$:
   $V_{l_x}^{\psi} \rightarrow \boldsymbol{V}_{\boldsymbol{1_x}}^{\boldsymbol{\psi}}$
   else:
   $V_{l_x}^{\psi}$ → Equation 3.8.

End

4. Calculate impedances using MLR:

   if $\vec{I}_{\psi,l}^{\psi} \neq \vec{\imath}_{s_l}^{\psi}$:
   $\tilde{R}_l^s$, $\tilde{X}_l^s$, $\tilde{R}_l^m$, $\tilde{X}_l^m$, $\tilde{r}_{s_l}^{\psi}$, $\tilde{x}_{s_l}^{\psi}$ → Equation 3.12.
   else:
   $\tilde{R}_l^s + \tilde{r}_{s_l}^{\psi}$, $\tilde{X}_l^s + \tilde{x}_{s_l}^{\psi}$, $\tilde{R}_l^m$, $\tilde{X}_l^m$ → Equation 3.13.

End

obtained from Equation 3.8 and the measured voltages at the head of the feeder. Moreover, based on Equation 3.8, these voltages are determined using the impedances and the start node voltages of the last-connected three-phase line. Thus far, we should understand that the voltage drop and the impedances of the three-phase line rely on each other; and these two values are determined line by line from the head of the feeder. To illustrate the process, the pseudocode of the impedance estimation is summarised in Algorithm I.

3.3.2.3 Further Improvements

Given that current changes on three-phase lines (i.e. $\vec{I}_{\psi,l}^{\psi}$) are associated with the current varies on single-phase service line (i.e. $\vec{\imath}_{s_l}^{\psi}$), two pairs of current variables in Equation 3.12 are correlated. Due to multicollinearity, if those variables are highly correlated, the LV line impedances can be ill-estimated. Three poor estimation conditions are outlined as follows:

1) $\tilde{R}_l^s < 0, \tilde{X}_l^s < 0, \tilde{R}_l^m < 0, \tilde{X}_l^m < 0, \tilde{r}_{s_l}^{\psi} < 0$, and $\tilde{x}_{s_l}^{\psi} < 0$;

2) $\tilde{X}_l^s > \tilde{R}_l^s,\ \tilde{X}_l^m > \tilde{R}_l^m$, and $\tilde{x}_{s_l}^{\psi} > \tilde{r}_{s_l}^{\psi}$; and

3) $\tilde{R}_l^s < \tilde{R}_l^m$.

The first condition is because impedances must be positive values. The second condition is due to the fact that LV networks are mainly resistive [84]. Lastly, the third condition is because self-resistance is larger than the mutual resistance [110]. If the above three conditions are satisfied, then estimation issues will occur. The straightforward solution is to drop the current variables that contribute less to the corresponding voltage drop variable [109]. The details of how to reduce the variables are explained below.

In LV networks, the impact of reactance is smaller than that of resistance; and thus, reactance variables can be first removed from the MLR model when any of the above three conditions occur. Given that the impedance and the voltages of the three-phase lines rely on each other, neglecting feeder reactance introduces some errors in the determination of three-phase voltages. These errors can be accumulated along the feeder, which will make the problem even worse. Thus, to avoid the issues, service line reactance will be the first to be removed from the model (i.e. $\tilde{x}_{s_l}^{\psi} = 0$).

Moreover, the impact of each impedance variable on the corresponding three-phase line voltage drop is tested on an example feeder in the Appendix, which results in $\tilde{R}_l^s > \tilde{R}_l^m > \tilde{X}_l^s > \tilde{X}_l^m$. Thus far, whenever any of the above three conditions occur, the impedance variables will be removed from Equations 3.12 and 3.13 in an order of ($\tilde{x}_{s_l}^{\psi}, \tilde{X}_l^m, \tilde{X}_l^s, \tilde{r}_{s_l}^{\psi}, \tilde{R}_l^m, \tilde{R}_l^s$) and ($\tilde{X}_l^m, \tilde{x}_{s_l}^{\psi} + \tilde{X}_l^s, \tilde{R}_l^m, \tilde{r}_{s_l}^{\psi} + \tilde{R}_l^s$), respectively.

Algorithm II: What-if Analyses: Voltage Calculation

Input: $\boldsymbol{p_{s_{l,y}}^{\phi}, q_{s_{l,y}}^{\phi}, V_{1_x}^{\phi}, R_l^s, X_l^s, R_l^m, X_l^m, r_{s_l}^{\phi}, x_{s_l}^{\phi}}$

Output: $\boldsymbol{v_{s_{l,y}}^{\phi}}$

1. Calculate the aggregated active and reactive power at three phases at the start node of the first three-phase line $l_x(l = 1)$, denoted by $P_{1_x}^{\phi}$ (i.e. $P_{1_x}^{a}$, $P_{1_x}^{b}$, $P_{1_x}^{c}$), $Q_{1_x}^{\phi}$(i.e. $Q_{1_x}^{a}$, $Q_{1_x}^{b}$, $Q_{1_x}^{c}$).

For each $\boldsymbol{\psi}$ (reference), $\boldsymbol{\varphi 1}$, $\boldsymbol{\varphi 2}$, $\boldsymbol{l}$, $\boldsymbol{s}$:

2. Calculate three-phase line currents:

   if $l = 1$:
   $\vec{I}_{\psi,l}^{\psi}, \vec{I}_{\psi,l}^{\varphi 1}, \vec{I}_{\psi,l}^{\varphi 2}$ → Equation 3.9.
   else:
   $\vec{I}_{\psi,l}^{\psi}, \vec{I}_{\psi,l}^{\varphi 1}, \vec{I}_{\psi,l}^{\varphi 2}$ → Equation 3.15.
3. Calculate three-phase voltages at the end of each three-phase lines (i.e. $V_{l_y}^{\psi}$) in Equation 3.16.
4. Calculate single-phase service line currents and customer voltage:

   if customers connected with line l:
   $\vec{\imath}_{s_l}^{\psi}$ → Equation 3.17; $v_{s_{l,y}}^{\psi}$ → Equation 3.18
   else:
   $\vec{\imath}_{s_l}^{\psi} \rightarrow 0$; $v_{s_{l,y}}^{\psi} \rightarrow 0$

End

3.3.2.4 Extensions

In some cases, distribution companies may know the impedance of either the three-phase LV feeder line models or the single-phase service line models. They can be added to the MLR model, so only the unknown impedances are estimated.

3.4 What-if Analyses: Voltage Calculation

Once having the estimated LV line models (with estimated impedances of three-phase and single-phase lines), customer voltages can be determined at any demand/generation condition (i.e. what-if analysis). For example, for a given demand scenario, distribution companies could test different PV injections (e.g. 5kW) and determine the corresponding voltages. It is worth mentioning that these analyses are used for operational purposes, and thus, only real-time or near real-time data are needed. To conduct the voltage calculation (in what-if analysis) at time t, the known information is highlighted in **bold** and the assumptions are outlined in Section 3.2.2.

The customer voltages $v_{s_{l,y}}^{\psi}$ are assessed one by one from the head of the feeder using Equations 3.15-3.18. Here, the impedances are parameters (highlighted in **bold**), and the currents and voltages are variables. The details of the customer voltage calculation (in what-if analysis) are summarized in Algorithm II. It should be noted that, the three phases of the feeder are expressed in a clockwise order in $[\psi, \varphi_1, \varphi_2]$, where ψ is the reference phase.

$$\begin{cases} \vec{I}_{\psi,l}^{\psi} = \vec{I}_{\psi,l-1}^{\psi} - \sum_{s\in S}\left[\left(\boldsymbol{p}_{\boldsymbol{s_{l-1,y}}}^{\boldsymbol{\psi}} + j\boldsymbol{q}_{\boldsymbol{s_{l-1,y}}}^{\boldsymbol{\psi}}\right)/V_{l-1_y}^{\boldsymbol{\psi}}\right]^* \\ \vec{I}_{\psi,l}^{\varphi 1} = \vec{I}_{\psi,l-1}^{\varphi 1} - \sum_{s\in S}\left[\left(\boldsymbol{p}_{\boldsymbol{s_{l-1,y}}}^{\boldsymbol{\varphi 1}} + j\boldsymbol{q}_{\boldsymbol{s_{l-1,y}}}^{\boldsymbol{\varphi 1}}\right)/V_{l-1_y}^{\varphi 1}\angle -120^\circ\right]^*, \\ \vec{I}_{\psi,l}^{\varphi 2} = \vec{I}_{\psi,l-1}^{\varphi 2} - \sum_{s\in S}\left[\left(\boldsymbol{p}_{\boldsymbol{s_{l-1,y}}}^{\boldsymbol{\varphi 2}} + j\boldsymbol{q}_{\boldsymbol{s_{l-1,y}}}^{\boldsymbol{\varphi 2}}\right)/V_{l-1_y}^{\varphi 2}\angle 120^\circ\right]^* \end{cases} \quad 3.15$$

$$\forall s \in S, \forall l \in L, \forall \psi, \varphi 1, \varphi 2 \in \Phi$$

$$V_{l_x}^{\psi} - V_{l_y}^{\psi} = \boldsymbol{R}_{\boldsymbol{l}}^{\boldsymbol{s}}\Re\left[\vec{I}_{\psi,l}^{\psi}\right] - \boldsymbol{X}_{\boldsymbol{l}}^{\boldsymbol{s}}\Im\left[\vec{I}_{\psi,l}^{\psi}\right] + \boldsymbol{R}_{\boldsymbol{l}}^{\boldsymbol{m}}\left(\Re\left[\vec{I}_{\psi,l}^{\varphi 1}\right] + \Re\left[\vec{I}_{\psi,l}^{\varphi 2}\right]\right) - \boldsymbol{X}_{\boldsymbol{l}}^{\boldsymbol{m}}\left(\Im\left[\vec{I}_{\psi,l}^{\varphi 1}\right] + \Im\left[\vec{I}_{\psi,l}^{\varphi 2}\right]\right), \forall\, l \in L, \forall \psi, \varphi 1, \varphi 2 \in \Phi \quad 3.16$$

$$\vec{\imath}_{s_l}^{\psi} = (\boldsymbol{p}_{\boldsymbol{s_{l,y}}}^{\boldsymbol{\psi}} + j\boldsymbol{q}_{\boldsymbol{s_{l,y}}}^{\boldsymbol{\psi}})/\, V_{l_y}^{\psi}, \forall s \in S, \forall l \in L, \forall \psi \in \Phi \quad 3.17$$

$$V_{l_y}^{\psi} - v_{s_{l,y}}^{\psi} = \boldsymbol{r}_{\boldsymbol{s_l}}^{\boldsymbol{\phi}}\Re[\vec{\imath}_{s_l}^{\psi}] - \boldsymbol{x}_{\boldsymbol{s_l}}^{\boldsymbol{\phi}}\Im[\vec{\imath}_{s_l}^{\psi}], \forall s \in S, \forall l \in L, \forall \psi \in \Phi \quad 3.18$$

3.5 Implementation Using an Example LV Feeder (with Service Lines)

An example LV feeder (three-phase) with service lines (single-phase) is adopted in this section to demonstrate the implementation of the proposed methodology. The calculation processes for impedance estimation and voltage calculations are presented in Sections 3.5.1 and 3.5.2, and they correspond to the pseudocodes listed in Sections 3.3 and 3.4, respectively.

3.5.1 Impedance Estimation

This section presents the process for impedance estimation. An overview of the procedure is first outlined below. Then, the details of the impedance estimation are demonstrated on an example LV feeder (with service lines).

Overview of the Procedure

- **Step1:** Collect historical time-series measurements (from smart meters and at the head of the feeder) and identify modelling elements (three-phase LV feeder lines, single-phase service lines, and combo lines).
- **Step2:** Calculate the currents flowing and voltage drop for one combo line by using each sample within the historical data. This step aims to produce the corresponding voltage drop equation wherein impedances are the only variables. For one combo line, this step ends up having as many linearised voltage drop equations as the samples.
- **Step3:** Send all linearised voltage drop equations to the MLR technique to estimate the impedance variables of one combo line.
- **Step4:** Repeat the last two steps to cover all the combo lines from the head to the end of the LV feeder.

Example LV Feeder

Figure 3-3 presents that a three-phase LV feeder (solid black lines) is connected with multiple single-phase service lines (red lines). The known parameters are **bolded**, as shown in Figure 3-3 and are also listed below. It should be noted that these parameters are historical time-series data. For simplicity, the time indices $t \in T$ are not presented.

- Meter measurements are available at the head of the feeder which is the start node of, the first three-phase line $l_x (l = 1)$. It includes active power, $\boldsymbol{P}_{\boldsymbol{1_x}}^{\boldsymbol{\phi}}$ (i.e. $\boldsymbol{P}_{\boldsymbol{1_x}}^{\boldsymbol{a}}$, $\boldsymbol{P}_{\boldsymbol{1_x}}^{\boldsymbol{b}}$, $\boldsymbol{P}_{\boldsymbol{1_x}}^{\boldsymbol{c}}$), reactive power, $\boldsymbol{Q}_{\boldsymbol{1_x}}^{\boldsymbol{\phi}}$ (i.e. $\boldsymbol{Q}_{\boldsymbol{1_x}}^{\boldsymbol{a}}$, $\boldsymbol{Q}_{\boldsymbol{1_x}}^{\boldsymbol{b}}$, $\boldsymbol{Q}_{\boldsymbol{1_x}}^{\boldsymbol{c}}$), and voltage magnitude, $\boldsymbol{V}_{\boldsymbol{1_x}}^{\boldsymbol{\phi}}$ (i.e. $\boldsymbol{V}_{\boldsymbol{1_x}}^{\boldsymbol{a}}$, $\boldsymbol{V}_{\boldsymbol{1_x}}^{\boldsymbol{b}}$, $\boldsymbol{V}_{\boldsymbol{1_x}}^{\boldsymbol{c}}$).
- Measurements of each smart meter are available at the end node of the service line $s_{l,y}$ at phase ϕ. It includes active power, reactive power and voltage magnitude, which are denoted by $\boldsymbol{p}_{\boldsymbol{s_{l,y}}}^{\boldsymbol{\phi}}$, $\boldsymbol{q}_{\boldsymbol{s_{l,y}}}^{\boldsymbol{\phi}}$ and $\boldsymbol{v}_{\boldsymbol{s_{l,y}}}^{\boldsymbol{\phi}}$, respectively.

For example, Customer 1 is connected to the first three-phase line ($l = 1$) at phase C ($\phi = c$) through the first service line ($s = 1$). The active power, reactive power and voltage magnitude of Customer1 are collected at the end node of the first service line, $s_{l,y}$, denoted by $\boldsymbol{p^c_{1_{1,y}}}$, $\boldsymbol{q^c_{1_{1,y}}}$, and $\boldsymbol{v^c_{1_{1,y}}}$, respectively.

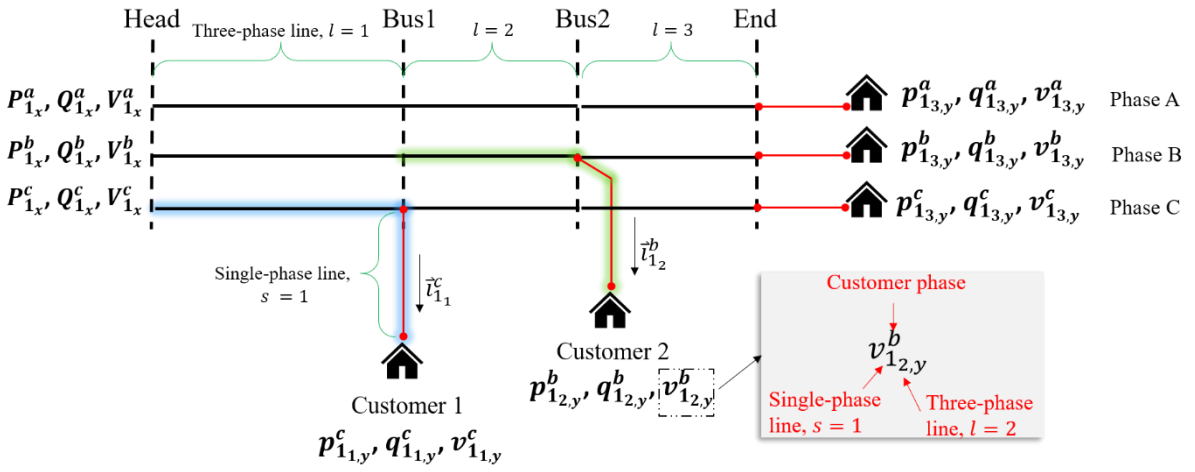

Figure 3-3. Example three-phase LV feeder with single-phase service lines (with the bolded parameters required by the impedance estimation approach)

The impedance estimation corresponds to the pseudocodes described in Section 3.3. The following shows the process of estimating the impedances on two combo lines. The description of these two combo lines are listed as follows:

- First Combo Line (blue glow)

  The first three-phase line at phase C (Head → Bus 1, $l = 1$, $\phi = c$) & The first single-phase service line that is connected to the first three-phase line at phase C (Bus 1 → Customer 1, $s = 1$, $l = 1$, $\phi = c$).

- Second Combo Line (green glow)

  The second three-phase line at phase B (Bus 1 → Bus 2, $l = 2$, $\phi = b$) & The first single-phase service line that is connected to the second three-phase line at phase B (Bus 2 → Customer 2, $s = 1$, $l = 2$, $\phi = b$).

Impedance of the First Combo Line

- **Step1:** Calculate three-phase line currents for all the samples (historical data).

Based on Equation 3.9, currents on the three-phase line l are expressed in $\left[\vec{I}_{\psi,l}^{\psi} \quad \vec{I}_{\psi,l}^{\varphi 1} \quad \vec{I}_{\psi,l}^{\varphi 2}\right]$. Here, phase $\psi \in \Phi$ is the reference, the other two phases of the line l in clockwise order are denoted by $\varphi_1 \in \Phi \backslash \{\psi\}$ and $\varphi_2 \in \Phi \backslash \{\psi, \varphi_1\}$, respectively. $\vec{I}_{\psi,l}^{\psi}$ is the current flowing through the line's self-impedance (i.e. $\hat{Z}_l^s$); and $\vec{I}_{\psi,l}^{\varphi 1}$ and $\vec{I}_{\psi,l}^{\varphi 2}$ are the current flowing through the line's mutual-impedance (i.e. $\hat{Z}_l^m$).

For the first three-phase line at phase C (Head → Bus 1, $l = 1$), phase C is regarded as the reference phase ψ. In a clockwise order, phase A and phase B are denoted by phase $\varphi 1$ and $\varphi 2$, respectively. Therefore, the currents on the first three-phase line can be presented as $\left[\vec{I}_{c,1}^{c} \quad \vec{I}_{c,1}^{a} \quad \vec{I}_{c,1}^{b}\right]$ and calculated by Equation 3.19.

$$\begin{cases} \vec{I}_{c,1}^{c} = \left[\left(\boldsymbol{P}_{1_x}^{c} + j\boldsymbol{Q}_{1_x}^{c}\right)/\boldsymbol{V}_{1_x}^{c}\right]^* \\ \vec{I}_{c,1}^{a} = \left[\left(\boldsymbol{P}_{1_x}^{a} + j\boldsymbol{Q}_{1_x}^{a}\right)/\boldsymbol{V}_{1_x}^{a} \angle -120^\circ\right]^* \\ \vec{I}_{c,1}^{b} = \left[\left(\boldsymbol{P}_{1_x}^{b} + j\boldsymbol{Q}_{1_x}^{b}\right)/\boldsymbol{V}_{1_x}^{b} \angle 120^\circ\right]^* \end{cases} \quad 3.19$$

It should be noted that, given multiple customers located along the feeder at different phases, phase A and phase B can also be regarded as the reference phase ψ. For example, phase B can be the reference phase ψ. In clockwise order, phase C and phase A are denoted by phase $\varphi 1$ and $\varphi 2$, respectively. Therefore, the currents on the first three-phase line can be presented as $\left[\vec{I}_{b,1}^{b} \quad \vec{I}_{b,1}^{c} \quad \vec{I}_{b,1}^{a}\right]$ and calculated by Equation 3.20. However, to calculate the impedance of the first combo line, only Equation 3.19 is needed.

$$\begin{cases} \vec{I}_{b,1}^{b} = \left[\left(\boldsymbol{P}_{1_x}^{b} + j\boldsymbol{Q}_{1_x}^{b}\right)/\boldsymbol{V}_{1_x}^{b}\right]^* \\ \vec{I}_{b,1}^{c} = \left[\left(\boldsymbol{P}_{1_x}^{c} + j\boldsymbol{Q}_{1_x}^{c}\right)/\boldsymbol{V}_{1_x}^{c} \angle -\mathbf{120}^\circ\right]^* \\ \vec{I}_{b,1}^{a} = \left[\left(\boldsymbol{P}_{1_x}^{a} + j\boldsymbol{Q}_{1_x}^{a}\right)/\boldsymbol{V}_{1_x}^{a} \angle \mathbf{120}^\circ\right]^* \end{cases} \quad 3.20$$

- **Step2:** Calculate single-phase line currents for all the samples (historical data).

The currents on the single-phase service line s_l at phase ψ can be calculated using the single-phase linearized voltage drop equation in $\vec{i}_{s_l}^{\psi} = \left[\left(\boldsymbol{p}_{s_{l,y}}^{\psi} + j\boldsymbol{q}_{s_{l,y}}^{\psi}\right)/\boldsymbol{v}_{s_{l,y}}^{\psi}\right]^*$.

Given that Customer 1 is located at phase C, phase C is regarded as the reference phase ψ. At the same time, Customer 1 is located at the end node of the first service line ($s = 1$) that is connected to the first three-phase line ($l = 1$). Thus, the current on the first single-phase service line at phase C (Bus 1 → Customer 1) is determined in $\vec{\imath}_{1_1}^{c} = \left[\left(\boldsymbol{p}_{\mathbf{1}_{1,y}}^{c} + j\boldsymbol{q}_{\mathbf{1}_{1,y}}^{c}\right)/\boldsymbol{v}_{\mathbf{1}_{1,y}}^{c}\right]^{*}$.

- **Step3:** Produce the voltage drop equations for all the samples (historical data).

The produced voltage drop equations of the combo line are expressed by $[V_{l_x}^{\psi} - \boldsymbol{v}_{\boldsymbol{s_{l,y}}}^{\boldsymbol{\psi}}]$. Here, $V_{l_x}^{\psi}$ is the voltage at the start node of the three-phase line l_x at customer's phase ψ. And $\boldsymbol{v}_{\boldsymbol{s_{l,y}}}^{\boldsymbol{\psi}}$ is the voltage at the end node of the sing-phase service line $s_{l,y}$ at customer's phase ψ.

Customer 1 is located at the end node of the first service line ($s = 1$) that is connected to the first three-phase line ($l = 1$) at phase C ($\psi = c$). Thus, voltage drop equations are expressed by $[\boldsymbol{V}_{\mathbf{1}_x}^{\boldsymbol{c}} - \boldsymbol{v}_{\mathbf{1}_{1,y}}^{\boldsymbol{c}}]$, and these two voltages are the known parameters from the head of the feeder and the smart meter. Thus, based on Equation 3.12, the voltage drop across the first combo line can be expressed in Equation 3.21. Here, the voltage drop (left-hand side of Equation 3.21) and the currents (right-hand side of Equation 3.21) are known, and impedances are the only variables.

$$\begin{aligned} V_{1_x}^{c} - \boldsymbol{v}_{\mathbf{1}_{1,y}}^{\boldsymbol{c}} = {} & \tilde{R}_1^{s}\Re\left[\vec{I}_{c,1}^{c}\right] - \tilde{X}_1^{s}\Im\left[\vec{I}_{c,1}^{c}\right] + \tilde{R}_1^{m}\left(\Re\left[\vec{I}_{c,1}^{a}\right] + \Re\left[\vec{I}_{c,1}^{b}\right]\right) \\ & - \tilde{X}_1^{m}\left(\Im\left[\vec{I}_{c,1}^{a}\right] + \Im\left[\vec{I}_{c,1}^{b}\right]\right) + \tilde{r}_{1_1}^{c}\Re\left[\vec{\imath}_{1_1}^{c}\right] - \tilde{x}_{1_1}^{c}\Im\left[\vec{\imath}_{1_1}^{c}\right] \end{aligned} \qquad 3.21$$

- **Step4:** Calculate impedances using MLR.

Using the produced voltage drop equations in Equation 3.21 and MLR, the impedance variables in Equation 3.21 can be calculated by using the ordinary least squares technique. The self-resistance, self-reactance, mutual-resistance and mutual-reactance of the first three-phase line l ($l = 1$) are presented as $\tilde{R}_1^{s}$, $\tilde{X}_1^{s}$, $\tilde{R}_1^{m}$ and $\tilde{X}_1^{m}$, respectively. At the same, the resistance and reactance of the first single-phase service line $s_l (s = 1, l = 1)$ at phase C are presented as $\tilde{r}_{1_1}^{c}$ and $\tilde{x}_{1_1}^{c}$.

Impedance of the Second Combo Line

- **Step1:** Calculate three-phase line currents for all the samples (historical data).

  Based on Equation 3.14, currents on the three-phase line l are expressed in $\left[\vec{I}_{\psi,l}^{\psi} \quad \vec{I}_{\psi,l}^{\varphi 1} \quad \vec{I}_{\psi,l}^{\varphi 2}\right]$. Here, phase $\psi \in \Phi$ is the reference, the other two phases of line l in clockwise order are denoted by $\varphi_1 \in \Phi \backslash \{\psi\}$ and $\varphi_2 \in \Phi \backslash \{\psi, \varphi_1\}$, respectively. $\vec{I}_{\psi,l}^{\psi}$ is the current flowing through the line's self-impedance (i.e. $\hat{Z}_l^s$); and $\vec{I}_{\psi,l}^{\varphi 1}$ and $\vec{I}_{\psi,l}^{\varphi 2}$ are the current flowing through the line's s mutual-impedance (i.e. $\hat{Z}_l^m$).

  For the second three-phase line at phase B (Bus 1 → Bus 2, $l = 2$), phase B is regarded as the reference phase ψ. In a clockwise order, phase C and phase A are denoted by phase $\varphi 1$ and $\varphi 2$, respectively. Therefore, the currents on the second three-phase line can be presented as $\left[\vec{I}_{b,2}^{b} \quad \vec{I}_{b,2}^{c} \quad \vec{I}_{b,2}^{a}\right]$ and calculated by Equation 3.22.

$$\begin{cases} \vec{I}_{b,2}^{b} = \left[\left(\boldsymbol{P}_{\mathbf{1}_x}^{\boldsymbol{b}} + j\boldsymbol{Q}_{\mathbf{1}_x}^{\boldsymbol{b}}\right)/\boldsymbol{V}_{\mathbf{1}_x}^{\boldsymbol{b}}\right]^* \\ \vec{I}_{b,2}^{c} = \left[\left(\boldsymbol{P}_{\mathbf{1}_x}^{\boldsymbol{c}} + j\boldsymbol{Q}_{\mathbf{1}_x}^{\boldsymbol{c}}\right)/\boldsymbol{V}_{\mathbf{1}_x}^{\boldsymbol{c}} \angle -\mathbf{120}^\circ\right]^* - \left[\left(\boldsymbol{p}_{\mathbf{1}_{1,y}}^{\boldsymbol{c}} + j\boldsymbol{q}_{\mathbf{1}_{1,y}}^{\boldsymbol{c}}\right)/\boldsymbol{v}_{\mathbf{1}_{1,y}}^{\boldsymbol{c}} \angle -\mathbf{120}^\circ\right]^* \\ \vec{I}_{b,2}^{a} = \left[\left(\boldsymbol{P}_{\mathbf{1}_x}^{\boldsymbol{a}} + j\boldsymbol{Q}_{\mathbf{1}_x}^{\boldsymbol{a}}\right)/\boldsymbol{V}_{\mathbf{1}_x}^{\boldsymbol{a}} \angle \mathbf{120}^\circ\right]^* \end{cases} \quad 3.22$$

- **Step2:** Calculate single-phase line currents for all the samples (historical data).

  The currents on the single-phase service line s_l at phase ψ can be calculated using the single-phase linearized voltage drop equation in $\vec{i}_{s_l}^{\psi} = \left[\left(\boldsymbol{p}_{\boldsymbol{s}_{l,y}}^{\psi} + j\boldsymbol{q}_{\boldsymbol{s}_{l,y}}^{\psi}\right)/\boldsymbol{v}_{\boldsymbol{s}_{l,y}}^{\psi}\right]^*$.

  Given that Customer 2 is located at phase B, phase B is regarded as the reference phase ψ. At the same time, Customer 2 is located at the end node of the first service line ($s = 1$) that is connected to the second three-phase line ($l = 2$). Thus, the current on the first single-phase service line at phase B (Bus 2 → Customer 2) is determined in $\vec{i}_{1_2}^{b} = \left[\left(\boldsymbol{p}_{\mathbf{1}_{2,y}}^{\boldsymbol{b}} + j\boldsymbol{q}_{\mathbf{1}_{2,y}}^{\boldsymbol{b}}\right)/\boldsymbol{v}_{\mathbf{1}_{2,y}}^{\boldsymbol{b}}\right]^*$.

- **Step3:** Produce the voltage drop equations for all the samples (historical data).

The produced voltage drop equations of the combo line are expressed by $[V_{l_x}^{\psi} - \boldsymbol{v}_{\boldsymbol{s_{l,y}}}^{\boldsymbol{\psi}}]$, where $V_{l_x}^{\psi}$ is the voltage at the start node of the three-phase line l_x at customer's phase ψ, and $\boldsymbol{v}_{\boldsymbol{s_{l,y}}}^{\boldsymbol{\psi}}$ is the voltage at the end node of the sing-phase service line $s_{l,y}$ at customer's phase ψ.

Customer 2 is located at the end node of the first service line ($s = 1$) that is connected to the second three-phase line ($l = 2$) at phase B ($\psi = b$). Thus, the voltage drop equations are expressed by $[V_{2_x}^{b} - \boldsymbol{v}_{\boldsymbol{1_{2,y}}}^{\boldsymbol{b}}]$, where $\boldsymbol{v}_{\boldsymbol{1_{2,y}}}^{\boldsymbol{b}}$ is known from the smart meter. But the voltage at the start node of the second three-phase line ($l_x,\ l = 2$) at phase B ($\psi = b$), $V_{2_x}^{b}$, is unknown. Given that $V_{2_x}^{b}$ is the same as the voltage at the end node of the first three-phase line ($l_y, l = 1$) at phase B ($\psi = b$), $V_{1_y}^{b}$, it can be calculated in Equations 3.20 and 3.23. This calculation uses the estimated impedances and the corresponding currents of the first three-phase line. Lastly, once having $V_{2_x}^{b}$ (or $V_{1_y}^{b}$), the voltage drop across the second combo line can be expressed in Equation 3.24.

$$\begin{aligned}\boldsymbol{V}_{\boldsymbol{1_x}}^{\boldsymbol{b}} - V_{1_y}^{b} = \tilde{R}_1^s \Re\left[\vec{I}_{b,1}^{b}\right] - \tilde{X}_1^s \Im\left[\vec{I}_{b,1}^{b}\right] + \\ \tilde{R}_1^m\left(\Re\left[\vec{I}_{b,1}^{a}\right] + \Re\left[\vec{I}_{b,1}^{c}\right]\right) - \tilde{X}_1^m\left(\Im\left[\vec{I}_{b,1}^{a}\right] + \Im\left[\vec{I}_{b,1}^{c}\right]\right)\end{aligned} \quad 3.23$$

$$\begin{aligned}V_{2_x}^{b} - \boldsymbol{v}_{\boldsymbol{1_{2,y}}}^{\boldsymbol{b}} = \tilde{R}_2^s \Re\left[\vec{I}_{b,2}^{b}\right] - \tilde{X}_2^s \Im\left[\vec{I}_{b,1}^{b}\right] + \tilde{R}_2^m\left(\Re\left[\vec{I}_{b,1}^{c}\right] + \Re\left[\vec{I}_{b,1}^{a}\right]\right) \\ -\tilde{X}_2^m\left(\Im\left[\vec{I}_{b,1}^{c}\right] + \Im\left[\vec{I}_{b,1}^{a}\right]\right) + \tilde{r}_{1_2}^{b} \Re\left[\vec{\imath}_{1_2}^{b}\right] - \tilde{x}_{1_2}^{b} \Im\left[\vec{\imath}_{1_2}^{b}\right]\end{aligned} \quad 3.24$$

- **Step4:** Calculate impedances using MLR.

Using the produced voltage drop equations in Equation 3.24 and MLR, the impedance variables in Equation 3.24 can be calculated by using the ordinary least squares technique. The self-resistance, self-reactance, mutual-resistance and mutual-reactance of the second three-phase line l ($l = 2$) are presented as $\tilde{R}_2^s$, $\tilde{X}_2^s$, $\tilde{R}_2^m$ and $\tilde{X}_2^m$, respectively. And the resistance and reactance of the connected first single-phase service line $s_l (s = 1, l = 2)$ at phase B ($\psi = b$) are presented as $\tilde{r}_{1_2}^{b}$ and $\tilde{x}_{1_2}^{b}$, respectively.

3.5.2 What-if Analyses: Voltage Calculation

This section presents the process for customer voltage calculation (in what-if analyses). An overview of the procedure is first outlined below. Then, the details of the customer voltage calculation are demonstrated on an example LV feeder (with service lines).

Overview of the Procedure

- Step1: Get real-time or near real-time time-series data (from customers and at the head of the feeder), identify modelling elements (three-phase LV feeder lines, single-phase service lines, and combo lines), and know their corresponding estimated impedances.

- Step2: Use each real-time or near real-time time-series data to calculate currents flowing and voltage drop of one combo line and to determine customer voltages (most important).

- Step3: Repeat the second step to cover all the combo lines and customers from the head to the end node of the LV feeder.

Example LV Feeder

Figure 3-4 presents that a three-phase LV feeder (solid black lines) is connected with multiple single-phase service lines (red lines). The known parameters are **bolded,** as shown in Figure 3-4, and are also listed below. It should be noted that these parameters are time-series data. For simplicity, the time indices $t \in T$ are not presented.

- The real-time or near real time active power and reactive power of demand/generation of each customer are known, denoted by $\boldsymbol{p}_{s_{l,y}}^{\boldsymbol{\phi}}$, $\boldsymbol{q}_{s_{l,y}}^{\boldsymbol{\phi}}$, respectively.

  For example, Customer 1 is located at the end node of the first service line ($s = 1$) that is connected to the first three-phase line ($l = 1$) at phase C ($\phi = c$). The active and reactive power of Customer 1 can be denoted by $\boldsymbol{p}_{1_{1,y}}^{\boldsymbol{c}}$, $\boldsymbol{q}_{1_{1,y}}^{\boldsymbol{c}}$, respectively.

- The head of feeder voltage magnitudes at three phases are known, denoted by $\boldsymbol{V}_{1_x}^{\boldsymbol{\phi}}$(i.e. $\boldsymbol{V}_{1_x}^{\boldsymbol{a}}$, $\boldsymbol{V}_{1_x}^{\boldsymbol{b}}$, $\boldsymbol{V}_{1_x}^{\boldsymbol{c}}$).

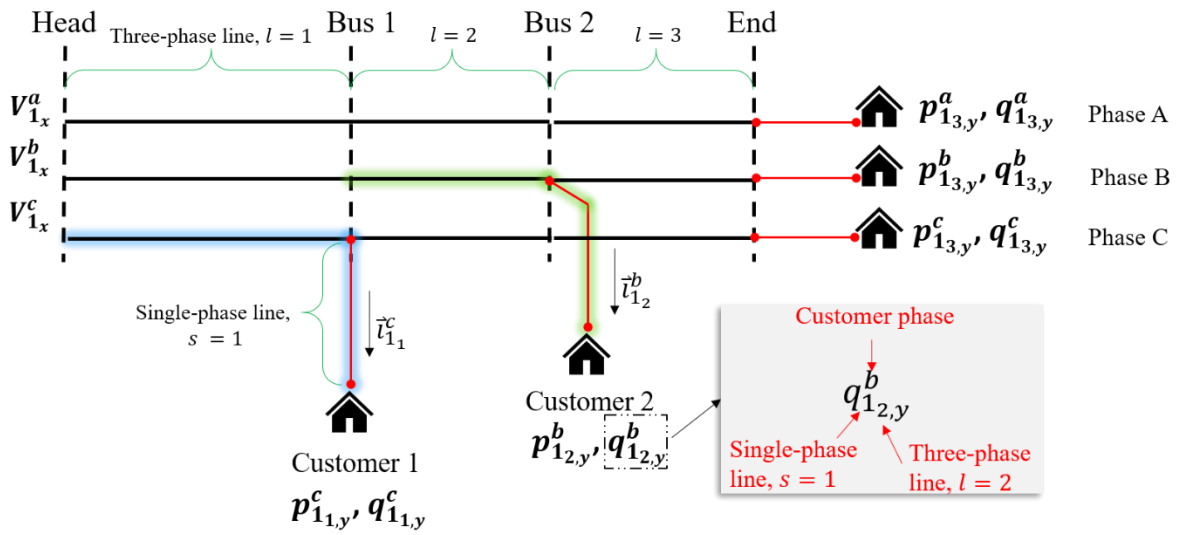

Figure 3-4. An example three-phase LV feeder with single-phase service lines (with the bolded parameters required by the voltage calculation approach)

The voltage calculation corresponds to the pseudocodes described in Section 3.4, and the following shows the process of calculating voltages of Customer 1 and Customer 2. These two customers are connected with the first combo line and the second combo line, respectively. The description of these two combo lines are listed as follows:

- First Combo Line (blue glow)

  The first three-phase line at phase C (Head → Bus 1, $l = 1, \phi = c$) & The first single-phase service line that is connected to the first three-phase line at phase C (Bus 1 → Customer 1, $s = 1, l = 1, \phi = c$).

- Second Combo Line (yellow glow)

  The second three-phase line at phase B (Bus 1 → Bus 2, $l = 2, \phi = b$) & The first single-phase service line that is connected to the second three-phase line at phase B (Bus 2 → Customer 2, $s = 1, l = 2, \phi = b$).

To start the calculation, the aggregated active and reactivate power at the head of the feeder are first calculated, and the line losses of the three-phase feeder and single-phase service lines are not considered. The aggregated active power at the head of the feeder (i.e. the start node of the first three-phase line l_x, $l = 1$) at three phases are denoted by $P^a_{1_x}$, $P^b_{1_x}$ and $P^c_{1_x}$. They are determined by $\boldsymbol{p^a_{1_{3,y}}}$, $(\boldsymbol{p^b_{1_{2,y}}} + \boldsymbol{p^b_{1_{3,y}}})$, and $(\boldsymbol{p^c_{1_{1,y}}} + \boldsymbol{p^c_{1_{3,y}}})$, respectively. Similarly, the

aggregated reactive power at the head of the feeder at three phases are denoted by $Q_{1_x}^a$, $Q_{1_x}^b$ and $Q_{1_x}^c$. They are calculated by $\boldsymbol{q_{1_{3,y}}^a}$, $(\boldsymbol{q_{1_{2,y}}^b} + \boldsymbol{q_{1_{3,y}}^b})$, and $(\boldsymbol{q_{1_{1,y}}^c} + \boldsymbol{q_{1_{3,y}}^c})$, respectively.

Voltage of Customer 1

- **Step1:** Calculate three-phase line currents.

  Based on Equation 3.9, currents on the three-phase line l are expressed in $\left[\vec{I}_{\psi,l}^{\psi} \quad \vec{I}_{\psi,l}^{\varphi 1} \quad \vec{I}_{\psi,l}^{\varphi 2}\right]$. Here, phase $\psi \in \Phi$ is the reference, the other two phases of line l in clockwise order are denoted by $\varphi_1 \in \Phi \backslash \{\psi\}$ and $\varphi_2 \in \Phi \backslash \{\psi, \varphi_1\}$, respectively. $\vec{I}_{\psi,l}^{\psi}$ is the current flowing through the line's self-impedance (i.e. $\hat{Z}_l^s$); and $\vec{I}_{\psi,l}^{\varphi 1}$ and $\vec{I}_{\psi,l}^{\varphi 2}$ are the current flowing through the line's mutual-impedance (i.e. $\hat{Z}_l^m$).

  For the first three-phase line at phase C (Head → Bus 1, $l = 1$), phase C is regarded as the reference phase ψ. In a clockwise order, phase A and phase B are denoted by phase $\varphi 1$ and $\varphi 2$, respectively. Therefore, the currents on the first three-phase line can be presented as $\left[\vec{I}_{c,1}^{c} \quad \vec{I}_{c,1}^{a} \quad \vec{I}_{c,1}^{b}\right]$ and calculated by Equation 3.25.

$$\begin{cases} \vec{I}_{c,1}^{c} = \left[\left(P_{1_x}^c + jQ_{1_x}^c\right)/\boldsymbol{V_{1_x}^c}\right]^* \\ \vec{I}_{c,1}^{a} = \left[\left(P_{1_x}^a + jQ_{1_x}^a\right)/\boldsymbol{V_{1_x}^a} \angle -120^\circ\right]^* \\ \vec{I}_{c,1}^{b} = \left[\left(P_{1_x}^b + jQ_{1_x}^b\right)/\boldsymbol{V_{1_x}^b} \angle 120^\circ\right]^* \end{cases} \quad 3.25$$

  It should be noted that, given multiple customers located along the feeder at different phases, phase A and phase B can also be regarded as the reference phase ψ. For example, phase B can be the reference phase ψ. In clockwise order, phase C and phase A are denoted by phase $\varphi 1$ and $\varphi 2$, respectively. Therefore, the currents on the first three-phase line can be presented as $\left[\vec{I}_{b,1}^{b} \quad \vec{I}_{b,1}^{c} \quad \vec{I}_{b,1}^{a}\right]$ and calculated by Equation 3.26. However, to calculate voltages of Customer 1, only Equation 3.25 is needed.

$$\begin{cases} \vec{I}_{b,1}^{b} = \left[\left(P_{1_x}^b + jQ_{1_x}^b\right)/\boldsymbol{V_{1_x}^b}\right]^* \\ \vec{I}_{b,1}^{c} = \left[\left(P_{1_x}^c + jQ_{1_x}^c\right)/\boldsymbol{V_{1_x}^c} \angle -120^\circ\right]^* \\ \vec{I}_{b,1}^{a} = \left[\left(P_{1_x}^a + jQ_{1_x}^a\right)/\boldsymbol{V_{1_x}^a} \angle 120^\circ\right]^* \end{cases} \quad 3.26$$

- **Step2:** Calculate three-phase voltages at the end node of each three-phase line.

  Based on Equation 3.16, once having the first three-phase currents, $\begin{bmatrix}\vec{I}^{c}_{c,1} & \vec{I}^{a}_{c,1} & \vec{I}^{b}_{c,1}\end{bmatrix}$, voltages at the end node of the first three-phase line at phase C ($V^{c}_{l_y}, l = 1$) can be calculated by Equation 3.27.

$$\boldsymbol{V^{c}_{1_x}} - V^{c}_{1_y} = \boldsymbol{R^{s}_{1}}\Re\left[\vec{I}^{c}_{c,1}\right] - \boldsymbol{X^{s}_{1}}\Im\left[\vec{I}^{c}_{c,1}\right] + \boldsymbol{R^{m}_{1}}\left(\Re\left[\vec{I}^{a}_{c,1}\right] + \Re\left[\vec{I}^{b}_{c,1}\right]\right) - \boldsymbol{X^{m}_{1}}\left(\Im\left[\vec{I}^{a}_{c,1}\right] + \Im\left[\vec{I}^{b}_{c,1}\right]\right) \quad 3.27$$

  Furthermore, it should be noted that the voltages at the end node of the first three-phase line at phase A ($V^{a}_{l_y}, l = 1$) and at phase B ($V^{b}_{l_y}, l = 1$) can be calculated. For example, $V^{b}_{1_y}$ can be calculated in Equations 3.26 and 3.28. However, to calculate the voltages of Customer1, only Equation 3.27 is needed.

$$\boldsymbol{V^{b}_{1_x}} - V^{b}_{1_y} = \boldsymbol{R^{s}_{1}}\Re\left[\vec{I}^{b}_{b,1}\right] - \boldsymbol{X^{s}_{1}}\Im\left[\vec{I}^{b}_{b,1}\right] + \boldsymbol{R^{m}_{1}}\left(\Re\left[\vec{I}^{a}_{b,1}\right] + \Re\left[\vec{I}^{c}_{b,1}\right]\right) - \boldsymbol{X^{m}_{1}}\left(\Im\left[\vec{I}^{a}_{b,1}\right] + \Im\left[\vec{I}^{c}_{b,1}\right]\right) \quad 3.28$$

- **Step3:** Calculate single-phase service line currents and customer voltages.

  Once having voltages at the end node of the three-phase line l_y at phase ψ, $V^{\psi}_{l_y}$, the currents on the connected single-phase service line s_l at phase ψ can be calculated by using $\vec{\imath}^{\psi}_{s_l} = \left[\left(\boldsymbol{p^{\psi}_{s_{l,y}}} + j\boldsymbol{q^{\psi}_{s_{l,y}}}\right)/V^{\psi}_{l_y}\right]^{*}$. Here, Customer 1 is connected at the end node of the first service line ($s = 1$) that is connected to the first three-phase line ($l = 1$) at phase C ($\psi = c$). Thus, the single-phase service line currents from Customer 1 is expressed in $\vec{\imath}^{c}_{1_1} = (\boldsymbol{p^{c}_{1_{1,y}}} + j\boldsymbol{q^{c}_{1_{1,y}}})/\, V^{c}_{1_y}$. Here, the losses of the service line are not considered.

  Lastly, based on Equation 3.18, Customer 1 voltage, $v^{c}_{1_{1,y}}$, can be calculated in Equation 3.29. It uses the known impedances, the calculated service line currents (i.e. $\vec{\imath}^{c}_{1_1}$) and the voltage at the end node of the first three-phase line at phase C (i.e. $V^{c}_{1_y}$).

$$V_{1_y}^{c} - v_{1_{1,y}}^{c} = \boldsymbol{r}_{\mathbf{1_1}}^{\boldsymbol{c}} \Re\left[\vec{\imath}_{1_1}^{c}\right] - \boldsymbol{x}_{\mathbf{1_1}}^{\boldsymbol{c}} \Im\left[\vec{\imath}_{1_1}^{c}\right] \quad 3.29$$

Voltage of Customer 2

- **Step 1**: Calculate three-phase line currents.

  Based on Equation 3.14, currents on the three-phase line l are expressed in $\left[\vec{I}_{\psi,l}^{\psi} \quad \vec{I}_{\psi,l}^{\varphi 1} \quad \vec{I}_{\psi,l}^{\varphi 2}\right]$. Here, phase $\psi \in \Phi$ is the reference, the other two phases of line l in clockwise order are denoted by $\varphi_1 \in \Phi \backslash \{\psi\}$ and $\varphi_2 \in \Phi \backslash \{\psi, \varphi_1\}$, respectively. $\vec{I}_{\psi,l}^{\psi}$ is the current flowing through the line's self-impedance (i.e. $\hat{Z}_l^s$); and $\vec{I}_{\psi,l}^{\varphi 1}$ and $\vec{I}_{\psi,l}^{\varphi 2}$ are the currents flowing through the line's mutual-impedance (i.e. $\hat{Z}_l^m$).

  For the second three-phase line at phase B (Bus 1 → Bus 2, $l = 2$), phase B is regarded as the reference phase ψ. In a clockwise order, phase C and phase A are denoted by phase $\varphi 1$ and $\varphi 2$, respectively. Therefore, the currents on the second three-phase line can be presented as $\left[\vec{I}_{b,2}^{b} \quad \vec{I}_{b,2}^{c} \quad \vec{I}_{b,2}^{a}\right]$ and calculated by Equation 3.30.

$$\begin{cases} \vec{I}_{b,2}^{b} = \left[\left(P_{1_x}^{b} + jQ_{1_x}^{b}\right)/\boldsymbol{V}_{\mathbf{1}_x}^{\boldsymbol{b}}\right] \\ \vec{I}_{b,2}^{c} = \left[\left(P_{1_x}^{c} + jQ_{1_x}^{c}\right)/\boldsymbol{V}_{\mathbf{1}_x}^{\boldsymbol{c}} \angle -\mathbf{120}^{\circ}\right]^{*} - \left[\left(\boldsymbol{p}_{\mathbf{1}_{1,y}}^{\boldsymbol{c}} + j\boldsymbol{q}_{\mathbf{1}_{1,y}}^{\boldsymbol{c}}\right)/\boldsymbol{v}_{\mathbf{1}_{1,y}}^{\boldsymbol{c}} \angle -\mathbf{120}^{\circ}\right]^{*} \\ \vec{I}_{b,2}^{a} = \left[\left(\boldsymbol{p}_{\mathbf{1}_{3,y}}^{\boldsymbol{a}} + \boldsymbol{j}\boldsymbol{q}_{\mathbf{1}_{3,y}}^{\boldsymbol{a}}\right)/\boldsymbol{V}_{\mathbf{1}_x}^{\boldsymbol{a}} \angle 120^{\circ}\right]^{*} \end{cases} \quad 3.30$$

- **Step2:** Calculate three-phase voltages at the end node of each three-phase line.

  Based on Equation 3.16, once having currents on the second three-phase line, $\left[\vec{I}_{b,2}^{b} \quad \vec{I}_{b,2}^{c} \quad \vec{I}_{b,2}^{a}\right]$, voltages at the end node of the second three-phase line at phase B ($V_{l_y}^{b}, l = 2$) can be calculated by Equation 3.31. Here, the voltage at the start of the second three-phase line at phase B ($V_{l_x}^{b}, l = 2$) equals to the voltages at the end node of the first three-phase line at phase B ($V_{l_y}^{b}, l = 1$), which is calculated in Equations 3.26 and 3.28.

$$V_{2_x}^b - V_{2_y}^b = \boldsymbol{R_2^s}\Re\left[\vec{I}_{b,2}^b\right] - \boldsymbol{X_2^s}\Im\left[\vec{I}_{b,2}^b\right] + \boldsymbol{R_2^m}\left(\Re\left[\vec{I}_{b,2}^c\right] + \Re\left[\vec{I}_{b,2}^a\right]\right) - \boldsymbol{X_2^m}\left(\Im\left[\vec{I}_{b,2}^c\right] + \Im\left[\vec{I}_{b,2}^a\right]\right) \quad 3.31$$

- **Step3:** Calculate single-phase service line currents and customer voltages.

  Once having the voltage at the end node of the three-phase line l_y at phase ψ, $V_{l_y}^{\psi}$, the currents on the connected single-phase service line s_l at phase ψ can be calculated by using $\vec{\imath}_{s_l}^{\psi} = \left[\left(\boldsymbol{p}_{\boldsymbol{s_{l,y}}}^{\psi} + j\boldsymbol{q}_{\boldsymbol{s_{l,y}}}^{\psi}\right)/V_{l_y}^{\psi}\right]^*$. Here, Customer 2 is connected at the end node of the first service line ($s = 1$) that is connected to the second three-phase line ($l = 2$) at phase B ($\psi = b$). Thus, the single-phase service line currents from Customer 2 is expressed in $\vec{\imath}_{1_2}^b = (\boldsymbol{p}_{\boldsymbol{1_{2,y}}}^{\boldsymbol{b}} + j\boldsymbol{q}_{\boldsymbol{1_{2,y}}}^{\boldsymbol{b}})/\, V_{2_y}^b$. Here, losses of the service line are not considered.

  Lastly, based on Equation 3.18, voltages of Customer 2, $v_{1_{2,y}}^b$, can be determined in 3.32. Here, it uses the known impedances, the currents of the service line (i.e. $\vec{\imath}_{1_2}^b$) , and the voltage at the end node of the second three-phase line at phase B (i.e. $V_{2_y}^b$).

$$V_{2_y}^b - v_{1_{2,y}}^b = \boldsymbol{r}_{\boldsymbol{1_2}}^{\boldsymbol{b}}\Re\left[\vec{\imath}_{1_2}^b\right] - \boldsymbol{x}_{\boldsymbol{1_2}}^{\boldsymbol{b}}\Im\left[\vec{\imath}_{1_2}^b\right] \quad 3.32$$

3.6 Summary

This chapter introduced the proposed methodology of this work, which aims to determine customer voltages (in what-if analyses) using smart meter-driven LV line models (i.e. adequate three-phase LV feeder lines and single-phase service lines). The proposed methodology has two parts. The first part, a one-off calculation, uses linearised voltage drop equations and the MLR technique to estimate impedances of LV line models (i.e. adequate three-phase LV feeder lines and single-phase service lines). Particularly, this process exploits historical time-series measurements (from smart meters and at the head of the feeder) and assumes that the customer connectivity and customer phase connection are known. Then, the second part, an operational calculation, calculates customer voltages (in what-if analyses). For any demand/generation conditions of households (with/without DER), linearised voltage drop equations and the

estimated LV line models can be used to calculate the corresponding voltages. In particular, this process uses real-time or near real-time data (from households and at the head of the feeder).

4 CASE STUDIES

4.1 Introduction

This chapter presents the application and the performance of the proposed methodology. Two cases using realistic Australian and UK LV networks are discussed in Sections 4.2 and 4.3, respectively. This assessment considers the accuracy of the estimated impedances, as well as the accuracy and the speed of the voltage calculation. Comparisons are carried out with a full three-phase power flow calculation. Lastly, the performance of the proposed methodology is analysed and summarised in Sections 4.4 and 4.5.

In both cases, impedances are estimated considering values that mimic realistic weekly historical meter measurements (i.e. active power, reactive power and voltage magnitudes), with a 15-minute resolution (672 time steps). Here, the realistic time-series active and reactive power profiles for residential customers are used to run three-phase power flows and extract the corresponding voltage magnitudes. Thus, these voltages may be different from the actual values that would be recorded by meters. The estimated impedances are then compared with their actual values and assessed by calculating the absolute percent error (APE). As for the voltage calculations in what-if analyses, weekly demand and generation profiles with a 1-minute resolution (10,080 time steps) are used. The accuracy and the speed of voltage calculations are compared with those determined by running power flow analyses.

The impedance estimation and the voltage calculation processes are coded in Python [111]. Furthermore, all time-series three-phase power flow simulations are performed using the distribution system analysis tool, OpenDSS [112], which was driven by Python.

4.2 Australian Low Voltage Network

4.2.1 Low Voltage Network Modelling

A realistic 400V (line to line) LV feeder from Victoria, Australia is used. Its topology is shown in Figure 4-1. In total, there are 23 single-phase customers (blue boxes), which divide the three-phase feeder (solid black lines) into 16 lines (or segments). The length of the first feeder line is 205m, and the others are 9.7m each. Each customer connects to the three-phase LV feeder via a 10m single-phase service line (solid red line, i.e. with a nominal voltage of 230V line to neutral). The actual self and mutual impedances of the first feeder line are 40.6646+j15.8974mΩ, 14.6693+j1.1599mΩ, respectively. Further, for the rest of the three-phase LV feeder lines, they are 1.92458+j0.752396mΩ and 0.694271+j5.49E-02mΩ, respectively. In addition, the actual impedance of each service line is 11.5+j0.83mΩ. The actual impedances are used to assess the performance of the proposed methodology in estimating impedances.

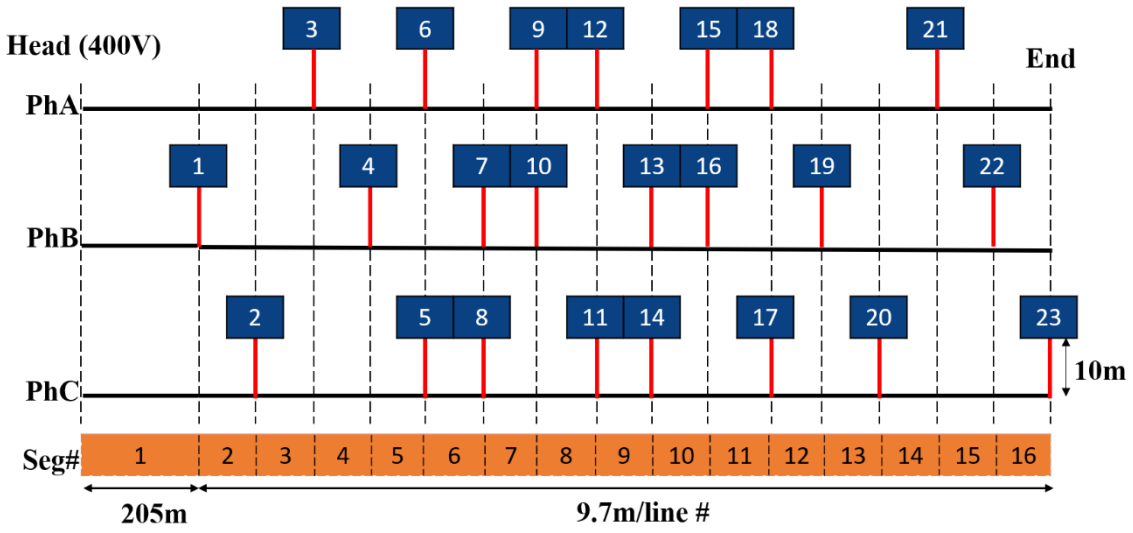

Figure 4-1. Schemematic of realistic Australian LV Feeder

4.2.2 Meter Data

4.2.2.1 Realistic Historical Meter Measurements – Impedance Estimation

A pool of anonymised 15-min resolution smart meter measurements (active power only) from 2014 provided by AusNet Services were used in this case study. More specifically, a week-long set of data (i.e. 672 time steps) from October (spring) is selected. Each of the 23 customers

in Figure 4-1 is assigned a demand profile (i.e. active power) from the pool of anonymized smart meter data, as shown in Figure 4-2(a). For each customer, their active power profiles and randomly selected power factors [1] (between 0.85 and 1.00, inductive) determine the corresponding reactive power profiles. Furthermore, given that customers may or may not adopt PV systems, two scenarios are developed to estimate impedances: with 0% (Scenario 1) and 50% (Scenario 2, half of the customers with a PV installation of 5.5kW) PV penetration, respectively. Given the small geographical area under study, customers with PV systems (same size, 5.5kW) are assigned the same weekly PV generation profile with 15-min resolution, as shown in Figure 4-2(b). Finally, to illustrate the differences between the two scenarios, the aggregated active power at the head of the feeder (per phase) are compared in Figure 4-3. In general, Scenario 2 has a relatively larger aggregated power than that in Scenario 1, which is due to a great number of injections of PV systems during midday.

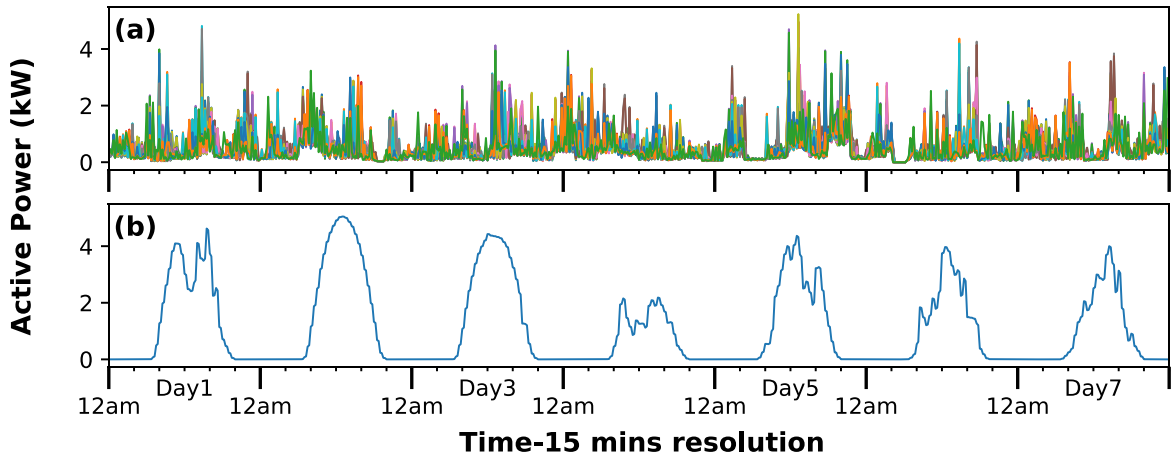

Figure 4-2. Historical meter measurements with 15-minute resolution for each of the 23 customers (a)demand profiles (b)generation profiles

[1] It is important to use random power factors to avoid collinearity between active and reactive power.

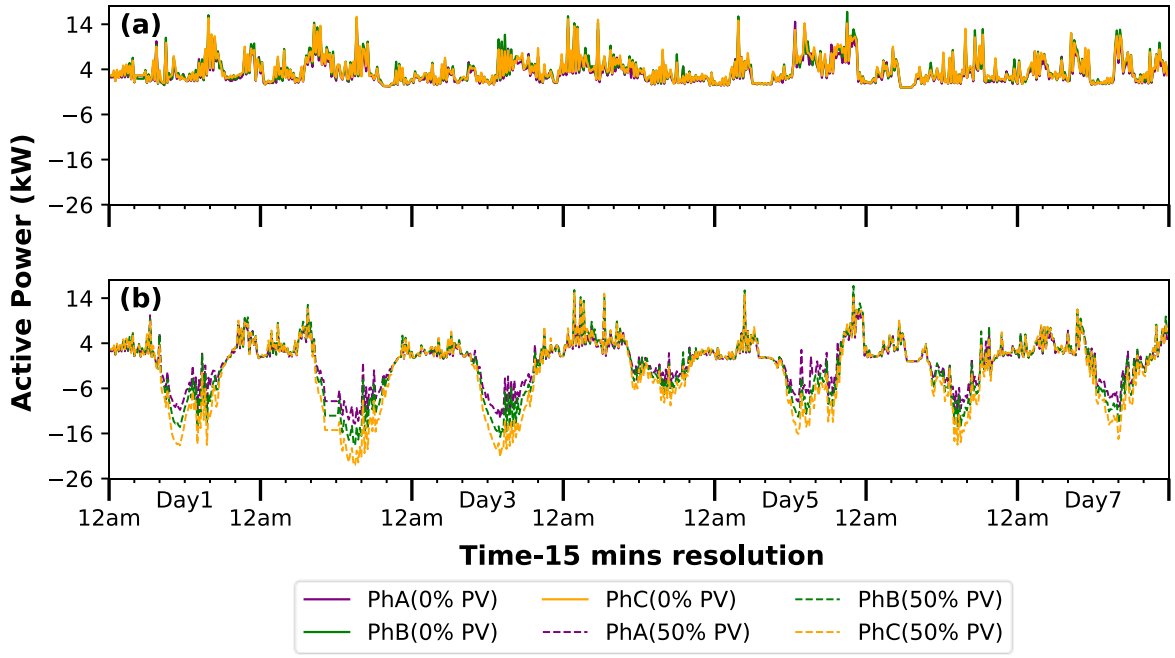

Figure 4-3. Aggregated active power at the head of the feeder with 15-minute resolution (a) 0% PV penetration (b) 50% PV penetration

4.2.2.2 Near Real-Time Operational Data – Voltage Calculations

Values that mimic near real-time operational data are used to assess customer voltages in what-if analyses (once the impedances have been estimated). In this study, the what-if scenario refers to a 100% PV penetration condition (all customers with a PV installation of 5.5kW). The demand and generation profiles with one-minute resolution are shown in Figures 4-4(a) and 4-4(b), respectively. The aggregated active power at the head of the feeder is shown in Figure 4-5. Due to 1-min resolution data has been used, data points are overlapped in Figures 4-4 and 4-5. In fact, demand profiles in Figure 4-4(a) are similar to that shown in Figure 4-2(a). Furthermore, under 100% PV penetration condition, all customers adopt the same size of PV systems (5.5kW). It causes that differences between phases (in Figure 4-5) are relatively smaller than those determined under the 50% PV penetration (in Figure 4-4).

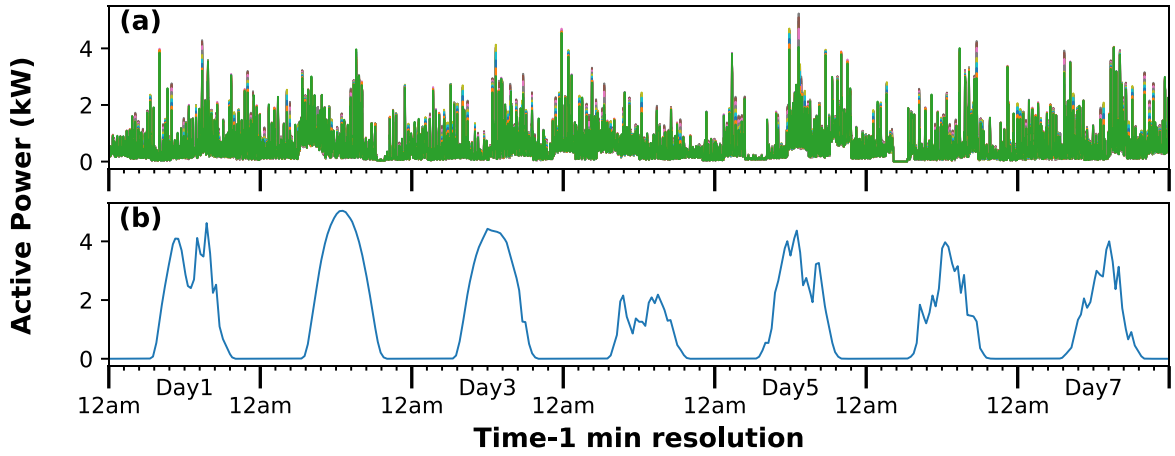

Figure 4-4. Near real-time operational data with 1-minute resolution for each customer (a)demand profiles (b)generation profiles

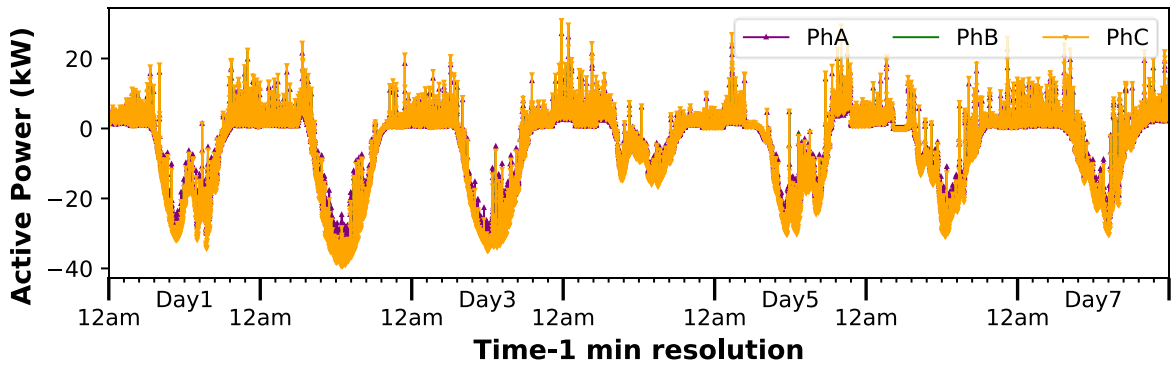

Figure 4-5. Aggregated active power (per phase) at the head of the feeder with 1-minute resolution

4.2.3 Results - Impedance Estimation

This section presents the estimated impedances for the three-phase LV feeder lines and single-phase service lines under two PV penetration conditions (Scenarios 1 and 2). It should be noted that, at each phase, the current on the last service line is the same as that in the connected three-phase LV feeder line. Thus, their impedances are combined in the impedance estimation process. The three aggregated lines are as below (using the structure in Figure 4-1).

- 1st aggregated line: line 14 and the last service line at phase A.
- 2nd aggregated line: lines 14, 15 and the last service line at phase B.
- 3rd aggregated line: lines 14, 15, 16 and the last service line at phase C.

Linearised voltage drop equations resulting from using historical meter measurements (672 time steps) are sent to the MLR to estimate the impedance of each line of the LV feeder and each service line. In the end, $23 \times 672 = 15{,}456$ equations are produced. The resulting impedances estimated for the three-phase feeder lines and single-phase service lines in both scenarios are compared with their actual values, as shown in Figure 4-6. The proposed approach determines the impedances of 16 three-phase feeder lines and 20 service lines. The last three service lines are merged into the three aggregated lines mentioned above (i.e. 1st aggregated line, 2nd aggregated line, and 3rd aggregated line) The red line represents the actual impedance. The green and orange lines represent the impedances determined under the 0% and 50% PV penetration conditions, respectively. Overall, the accuracy of the last few three-phase feeder lines impedances is lower than those for the head and the middle of the LV feeder. However, in general, there is an insignificant mismatch between the estimated and actual values.

To understand the impedance estimation accuracy in two scenarios, the absolute percent error (APE) for each three-phase line and single-phase service line is determined using Equation 4.1, as shown in Figure 4-7.

$$APE(\%) = [|Estimated\ Impedance\ of\ Line\ \# - Actual\ Impedance\ of\ Line\ \#|/Actual\ Impedance\ of\ Line\ \#] \times 100 \quad 4.1$$

The green and orange lines in Figure 4-7 represent the accuracy of the impedances determined under the 0% and 50% PV penetration conditions, respectively. In general, the 50% PV penetration condition has relatively worse results. Based on the MLR model in Equations 3.12 and 3.13, the accuracy of the impedances depends on two factors: the current and the three-phase voltage magnitude.

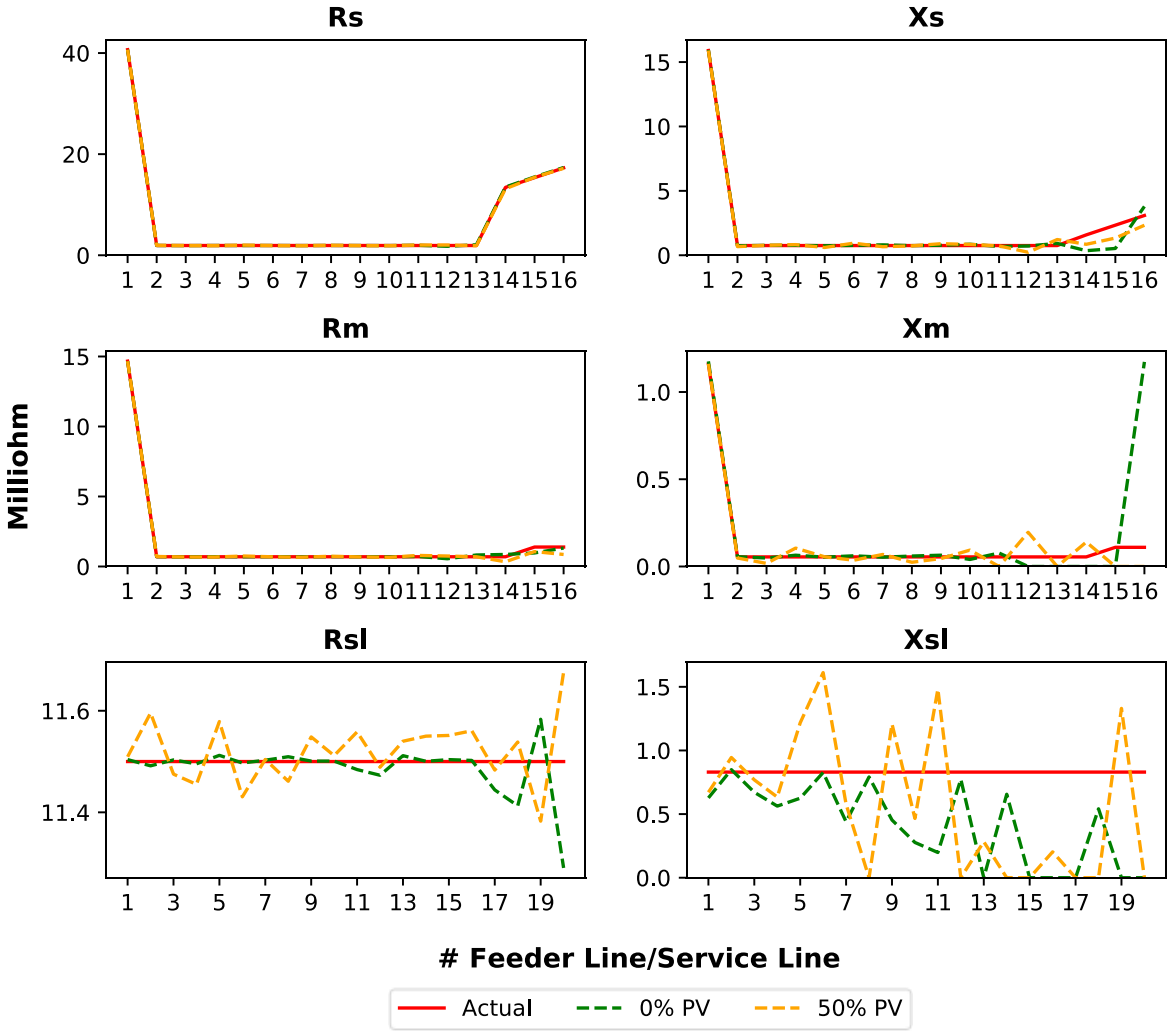

Figure 4-6. Comparison between the actual impedance and two estimated impedances determined under the 0% and 50% PV penetration conditions

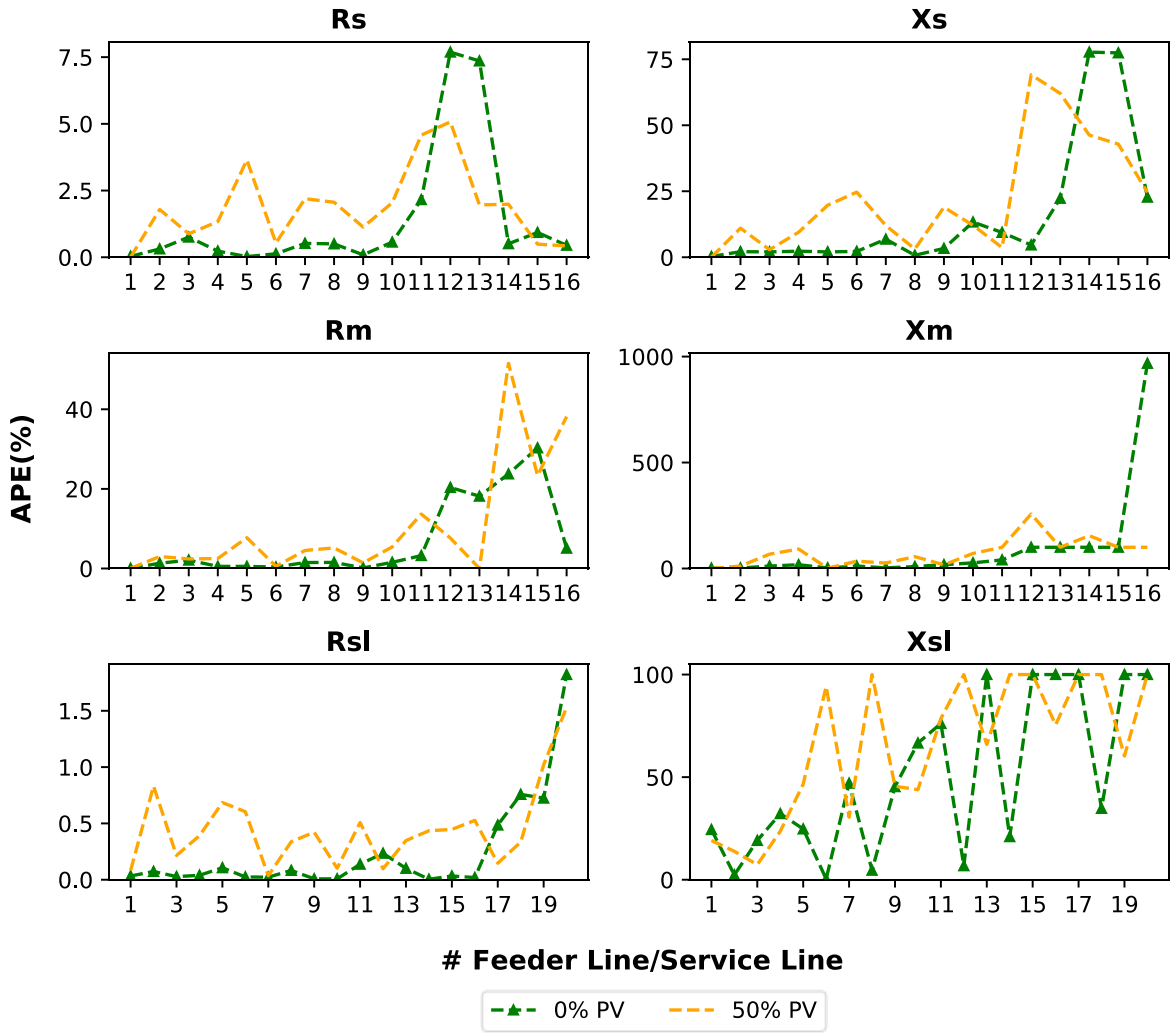

Figure 4-7. APE of the estimated impedances determined under the 0% and 50% PV penetration conditions

For the accuracy of the current, it depends on the voltage angle according to Equation 3.9. In theory, voltage angles increase from the head (reference) to the end of the feeder. However, the proposed approach assumes three fixed voltage angles along the three-phase feeder, which are 0°, -120° and 120°. Therefore, the mismatch between the actual and the estimated voltage angles increases along the LV feeder. Furthermore, the mismatch can be even larger under unbalanced conditions. In this case, in comparison to the 0% PV penetration condition, the allocation of demand or generation is relatively more unbalanced under the 50% PV condition at midday, as shown in Figure 4-5(b). Thus, the impedances determined under the 50% PV penetration condition are less accurate. At the same time, the actual voltage angles on the three-phase buses along the feeder under the 0% and 50% PV penetration conditions are shown in Figure 4-8. The figure indicates that the voltage angles determined under the 50% PV

penetration condition are generally larger than those determined under the 0% PV penetration condition. Thus, the mismatch between the actual and estimated voltage angle is relatively significant under the 50% PV penetration condition. Therefore, it causes larger errors when calculating three-phase line currents, which eventually reduces the accuracy of determining impedances.

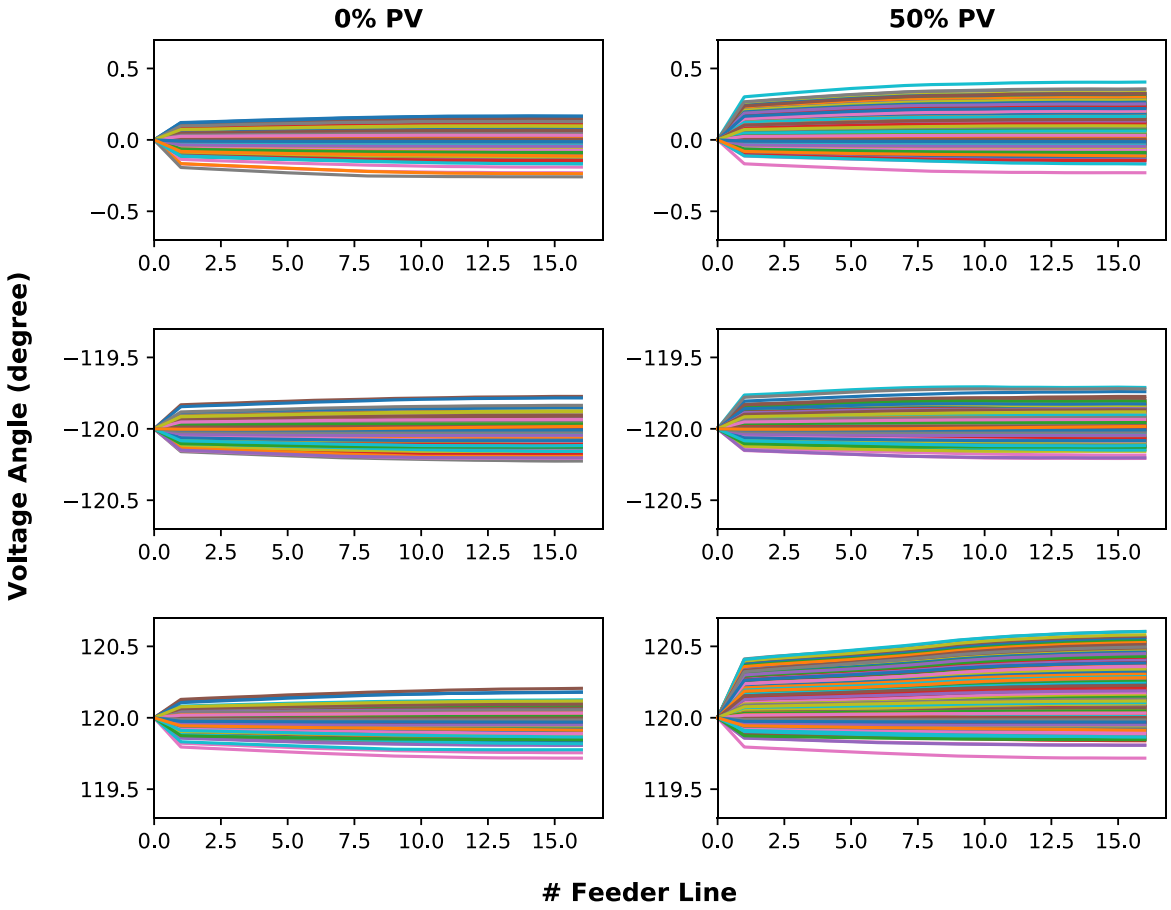

Figure 4-8. Voltage angles along the three-phase LV feeder under the 0% and 50% PV penetration conditions

As for the accuracy due to the three-phase voltage magnitudes, it depends on the level of demand or generation as shown in Equations 3.8 and 3.9. For instance, with a fixed impedance error, the larger the demand or generation, the worse the three-phase voltages in Equations 3.8 and 3.9. In this case study, given that the generation is relatively larger under the 50% PV penetration condition (Figure 4-3), voltage errors are bigger, and thus, the accuracy of determining impedances is reduced.

Nonetheless, the first half of the feeder lines and service lines have much more accurately estimated impedances, particularly for the 0% PV penetration scenario. Under this condition, except for the reactance of service lines, other impedance variables have almost 0% error. In contrast, the last half of the three-phase feeder lines and service lines have relatively worse impedances, which are likely due to the voltage errors accumulating along the feeder. However, it is important to highlight that, from the perspective of voltage calculations for what-if analyses, given that the currents at the end of the feeder are relatively small (only a few customers), the errors in impedances cannot cause significant voltage error. This will be presented in the next section.

4.2.4 Results - Voltage Calculations for What-if Analyses

This section aims to calculate customer voltages by using the previously estimated impedances. The near real-time demand and generation profiles presented in Section 4.3.2.2 are used here, considering a 100% PV penetration condition (all customers with a PV installation of 5.5kW). The performance of the proposed methodology is assessed by determining the total voltage mismatch. It is computed by subtracting the actual voltage (calculated using the actual impedances and a three-phase power flow engine) from the estimated voltage. Table 4-1 presents the considerations to produce these two voltages.

The results of the total voltage mismatches are shown in Figure 4-9. The top half and the bottom half of Figure 4-9 represent the results determined by using the impedances determined under the 0% and 50% PV penetration condition, respectively. It should be noted that there are no significant differences between the two scenarios. Therefore, the accuracy of the impedances does not significantly affect the accuracy of the calculated voltages.

Additionally, given that these two scenarios have similar results, let us focus on the 0% PV penetration condition. As shown in Figure 4-9(a), the median voltage mismatches for all the customers are around zero. Furthermore, what stands out is that the maximum voltage mismatch is less than 0.25V at the end of the feeder. These results demonstrate that the proposed approach is a promising for alternation.

Table 4-1. Considerations for the voltage comparision

	Impedance		Method	
	Actual	**Estimated**	**Simplified Voltage Equations**	**Power Flow Engine**
Actual Voltage	✓			✓
Calculated Voltage		✓	✓	

Moreover, given that voltage errors are accumulated along the feeder, there is a slightly increasing trend of voltage mismatch in all three phases, as presented in Figure 4-9. At the same time, this proposed voltage calculation approach has assumed that losses in the three-phase lines and single-phase service lines are negligible. Thus, the farther the customers from the head of the feeder, the higher the neglected line losses. Therefore, customer voltages are less accurate at the end of the feeder. More interestingly, the maximum and the minimum voltage mismatch occur at phase C and phase A, respectively. This is because the accuracy of the voltage calculation is affected by the level of the demand/generation, based on Equations 3.15-3.18. As shown in Figure 4-5, there is a slightly higher level of generation at phase C. Thus, customers at phase C experience more significant voltage errors.

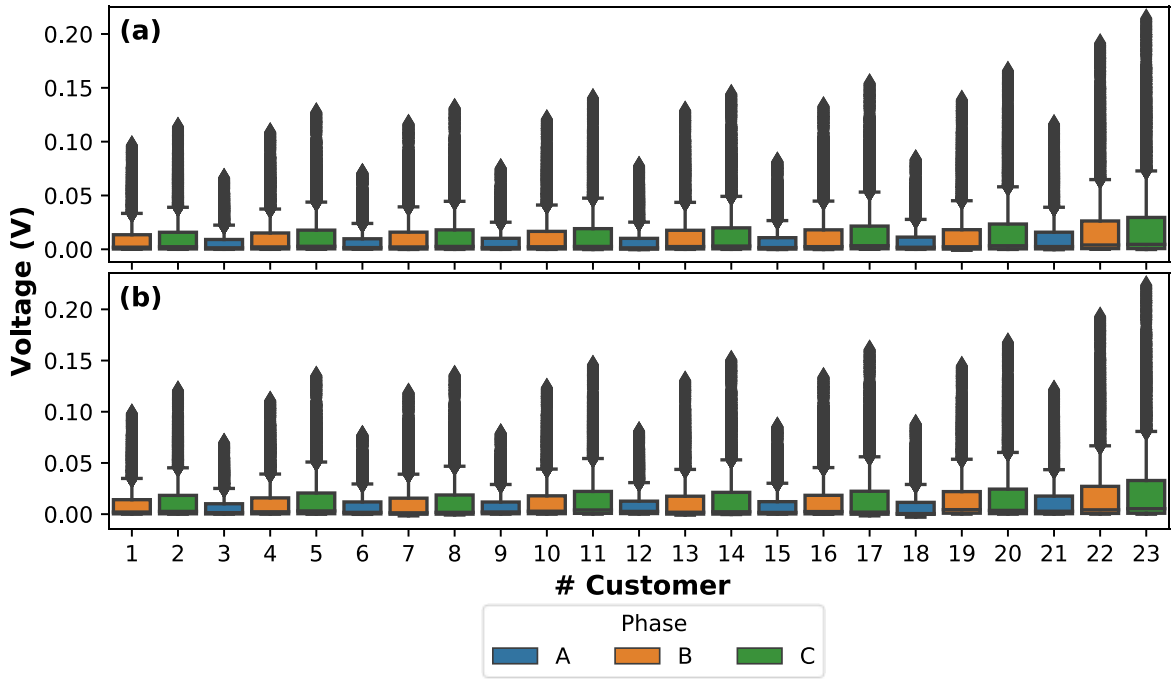

Figure 4-9. Total voltage mismatch caused by the proposed approach (a) 0% PV penetration condition (b) 50% PV penetration condition

Finally, to clearly illustrate the accuracy of the proposed method, the voltages for the following cases are computed, and then compared to the 'Actual Voltage' (as in Table 4-1).

- Case 1: estimated impedance and the power flow engine.
- Case 2: actual impedance and the simplified voltage calculations

Figure 4-10 presents the voltage mismatch caused by the impedances. Although impedances determined under the 50% PV penetration condition cause relatively larger voltage errors, the overall impact of the impedance errors on the accuracy of the voltages is small. As shown in Figure 4-10, the maximum voltage mismatch is only about 0.01V. Finally, the voltage mismatch caused by the linearised voltage drop equations is shown in Figure 4-11. Interestingly, the results are similar to those for the total voltage mismatch (Figure 4-9). Thus far, the accuracy of the impedance estimation does not have a substantial impact on voltages, and the proposed voltage drop equation is the main reason for the voltage mismatch.

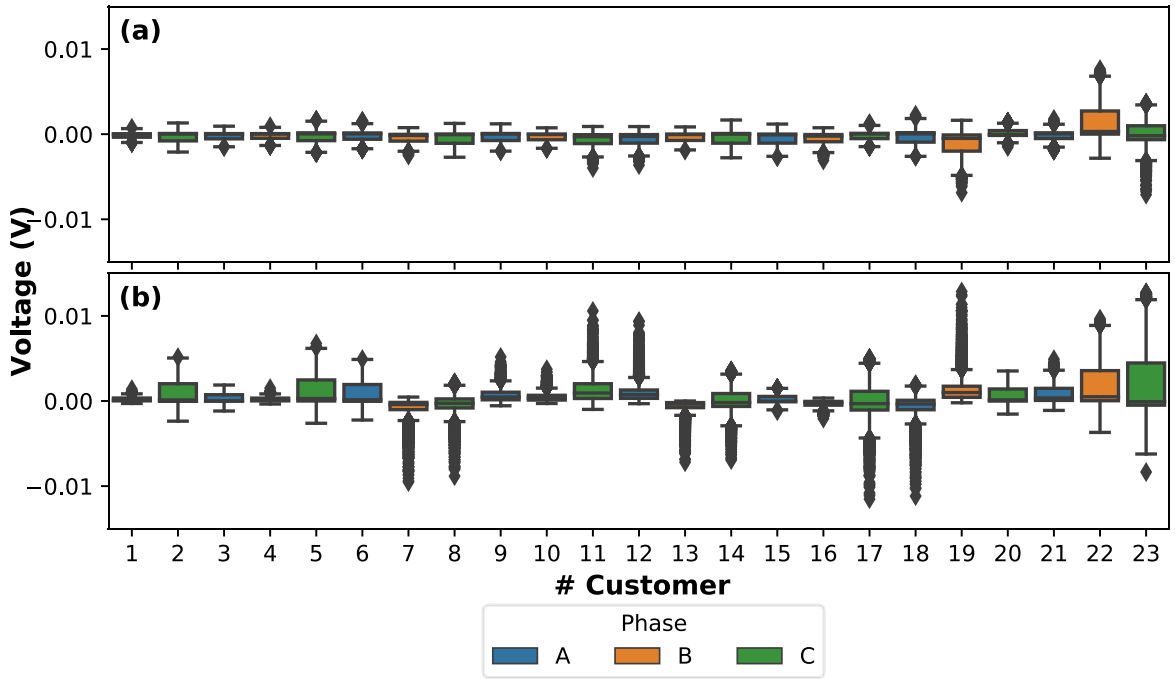

Figure 4-10. Case 1 vs Actual Voltage: Voltage mismatch caused by the impedances errors (a) 0% PV penetration condition (b) 50% PV penetration condition

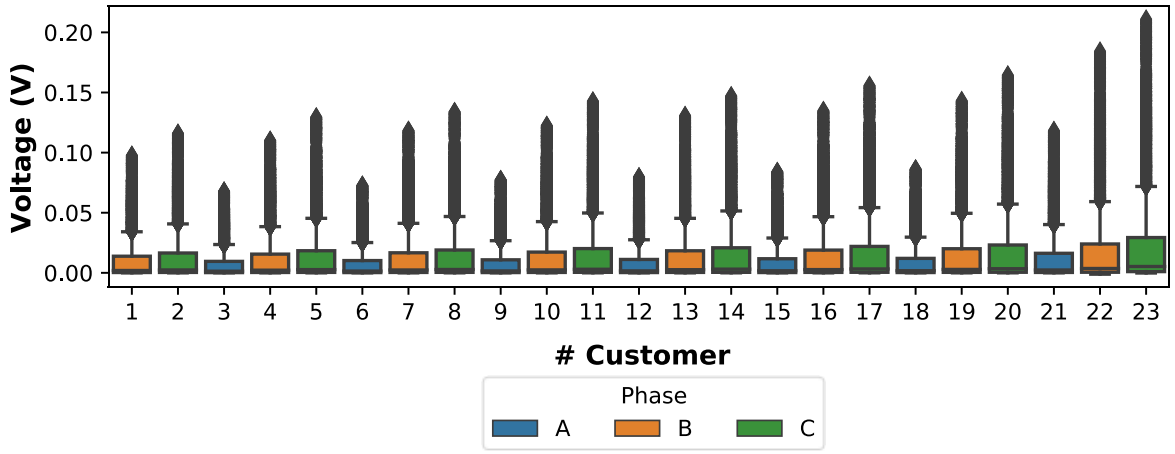

Figure 4-11.Case 2 vs Actual Voltage: Voltage mismatch caused by the linearised voltage drop equations

However, it is unclear why the notable impedance errors of the last few feeder lines (i.e. from feeder line 12) have such a small impact on the final voltage estimation. Thus, it is worth understanding the effects of the impedances of the last few feeder lines and service lines on the

customer voltages. To achieve this, a new case (Case 3) is presented, and the details of impedances are listed as follows:

- Before customer 18, both feeder lines and service lines use actual impedances; and
- After customer 18, both feeder lines and service lines use the estimated impedances (determined under the 0% PV penetration condition).

Under this condition, customer voltages are calculated using the proposed linearised voltage drop equations, and the voltage mismatch is shown in Figure 4-12. It shows that the errors in the impedances at the end of the feeder lines and service lines have little impact on the voltages of the last five customers. This is primarily because most LV lines have almost correct impedances. The total length of the LV lines is about 360m, and the actual LV lines (before customer 18) are around 310m. Customer voltages depend on the impedances from the head of the feeder to the customers' location. Given that impedances are correct for the first 310 m, they are the dominant factor affecting the accuracy of customers' voltages. The fact that there are notable impedance errors in the last few lines but a small amount of current flowing in those short lines, results in a slight voltage mismatch.

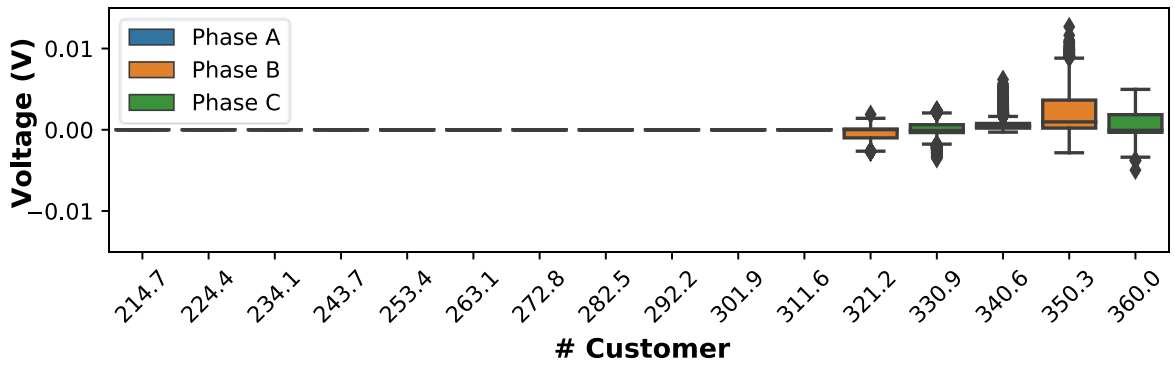

Figure 4-12. Case 3 vs Case 2:Voltage mismatch of the last five customers

Finally, compared to using the power flow engine, using the linearized voltage drop equations significantly speeds up the calculation from 69.5s to 0.22s (three hundred times faster), which makes it much scalable for for the simultaneous near real-time calculations of hundreds of LV feeders.

4.3 UK Low Voltage Network

4.3.1 Low Voltage Network Modelling

A real underground, residential UK LV network from the North West of England (Feeder 1, Network 5) is studied here [113]. The selected network has 130 nodes and 129 lines. Lines that share the same currents are combined, which results in nine nodes and eight lines in the modified LV network (in Figure 4-13). The black line represents the three-phase LV feeder, which feeds four customers through single-phase service lines (i.e. red lines). The first two customers (i.e. customers 1 and 2) connected to phase A, and the others to phase C. The characteristics of the LV lines are listed in Table 4-2. This network differs from the Australian network in that more than one customer is connected to the same node of the three-phase feeder, i.e, part of the service line is shared (which is a relatively common situation around the world).

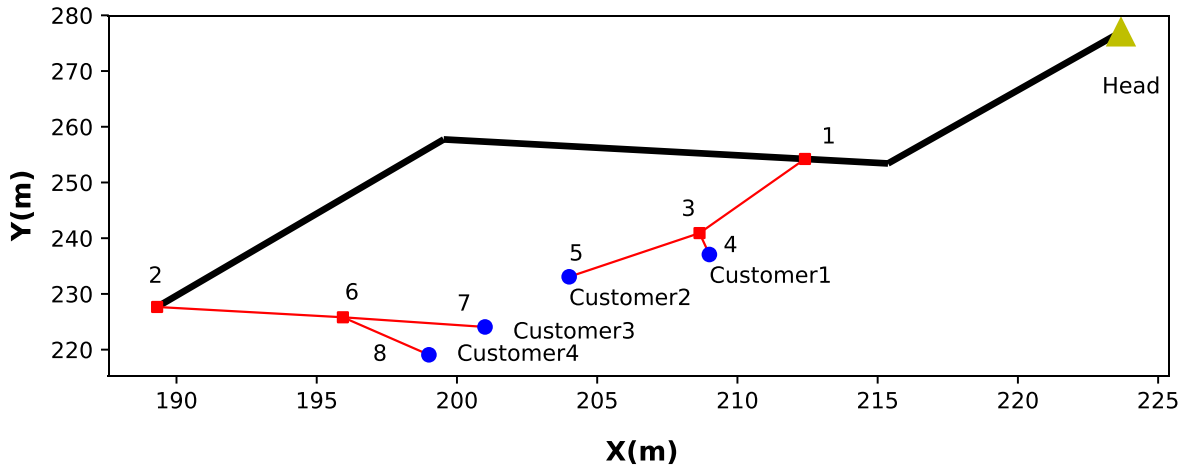

Figure 4-13. Topology of the UK LV feeder

Table 4-2. Characteristics of equivalent LV lines

Line	Node x	Node y	Length (m)	Rs + jXs (mΩ)	Rm + jXm (mΩ)
1	Head	1	29.9	24.1 + j2.4	10.7+j0.15
2	1	2	45.5	47 + j3.7	20.0+j0.18
3	1	3	14.41	27.4 + j1.3	0
4	3	4	3.86	7.35 + j0.35	0
5	3	5	11.44	21.77 + j1.03	0
6	2	6	6.88	13.09 + j0.62	0
7	6	7	5.36	10.19 + j0.48	0
8	6	8	7.71	14.68 + j0.69	0

4.3.2 Meter Data

4.3.2.1 Realistic Historical Meter Measurements – Impedance Estimation

In this case, demand and PV generation profiles, with one-minute resolution, are produced using the tool developed by the Centre for Renewable Energy Systems Technology (CREST) [114]. Demand profiles consider the number of residents, type of day (weekday or weekend), seasonality, and the electrical consumption of the appliances. At the same time, PV generation profiles depend on the system configurations (i.e. panel and inverter efficiencies; slope, azimuth, and area of the array) and the geographical location (i.e. irradiance and clearness index). In this case study, the demand and PV generation profiles (assuming 5.5kW systems) for each customer during a summer week in June (Summer) are determined, as shown in Figures 4-14(a) and 4-14(b), respectively. For each customer, the demand (active power) profiles and randomly selected power factors (between 0.85 and 1.00, inductive) determine the corresponding reactive power profiles.

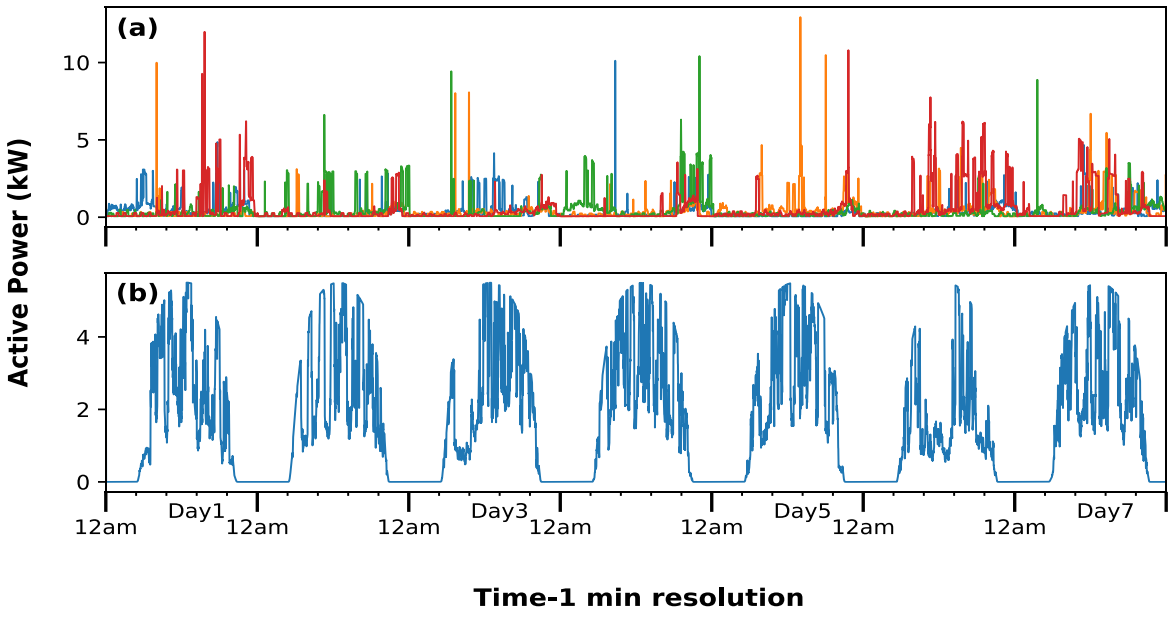

Figure 4-14. Realistic Historical meter measurements with 1-minute resolution for each customer (a)demand profiles (b)generation profiles

To estimate the impedances of the LV lines, the 1-min resolution profiles have been modified to have a resolution of 15 minutes, as in the case of the Australian LV feeder. This modification considers that, in practice, some smart meters may not have high-resolution data. Further, the

aggregated power at the head of the feeder is shown in Figure 4-15, where the upper part and the lower part represent the 0% and 50% PV penetration (half of the customers with PV systems) conditions, respectively. In general, during midday, the 50% PV penetration condition has a slightly larger aggregated power than that in the 100% PV penetration condition.

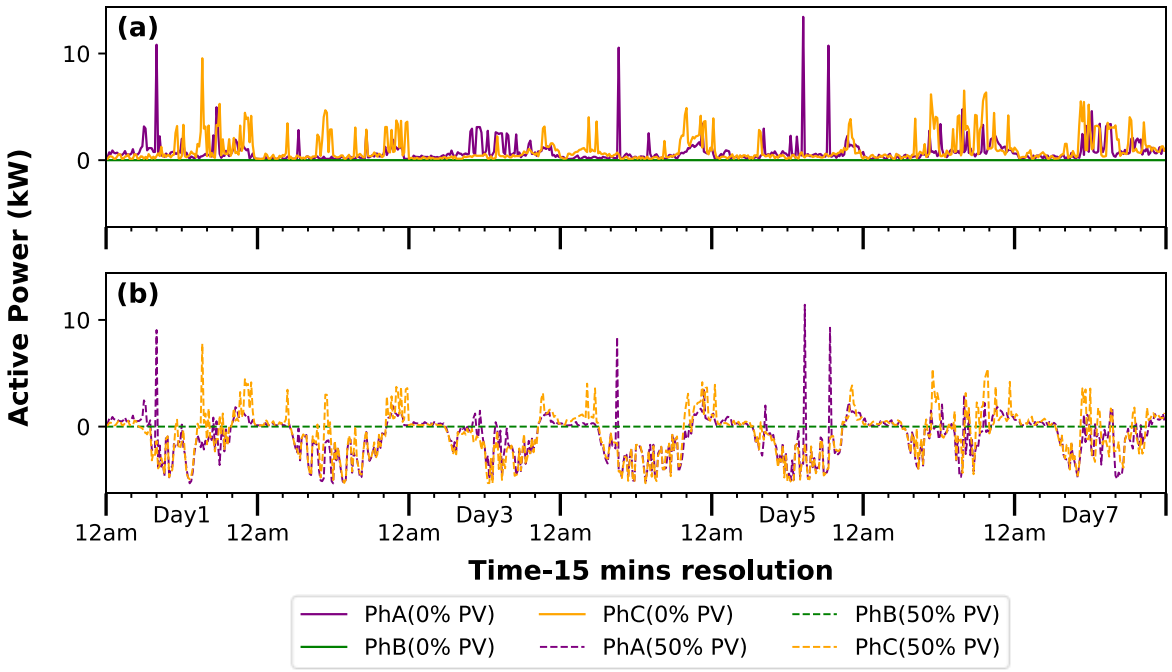

Figure 4-15. Aggregated active power at the head of the feeder with 15-minute resolution (a) 0% PV penetration (b) 50% PV penetration

4.3.2.2 Near Real-Time Operational Data – Voltage Calculations

Near real-time operational data is used to assess customer voltages in what-if analyses. In this study, the what-if scenario refers to a 100% PV penetration condition (all customers with a PV installation of 5.5kW). The demand and generation profiles of each customer, with one-minute resolution, are presented in Figure 4-14. The aggregated active power at the head of the feeder is shown in Figure 4-16, which presents a higher level of reverse power flow during midday.

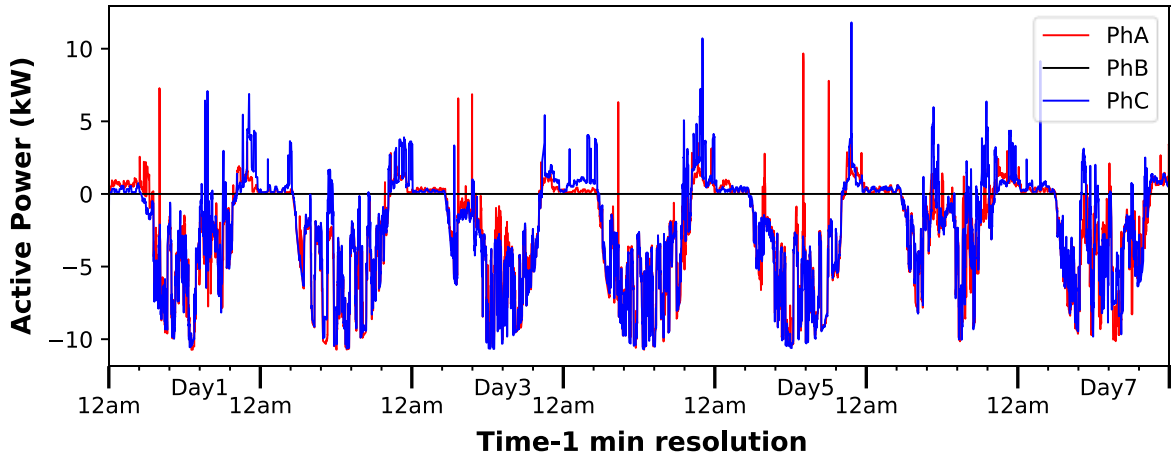

Figure 4-16. Aggregated active power at the head of the feeder (1-minute resolution)

4.3.3 Results - Impedance Estimation

To facilitate understanding, the single-line diagram in Figure 4-13 is represented by the three-phase LV feeder lines and single-phase service lines in Figure 4-17. Looking at phase A, lines 1 and 3 share the same current. Similarly, the same current flows through lines 1, 2, and 6. Given that these lines carry the same amount of current, the impedances are combined per phase. This results in two combined lines (three-phase) and four service lines (single-phase), as listed in Tables 4-3 and 4-4.

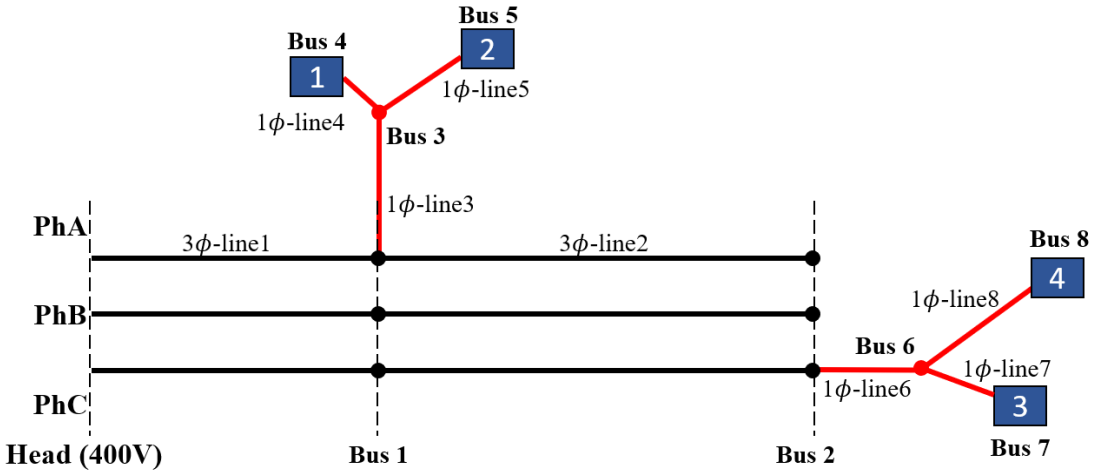

Figure 4-17. Schematics of the UK three-phase LV feeder and single-phase service lines

Table 4-3. Impedances of combined lines

Combined Line	Node x (start)	Node y (end)	Length (m)	Rs + jXs (mΩ)	Rm + jXm (mΩ)
1	Head	Bus 3	44.3	51.5+ j3.69	10.66 +j 0.15
2	Head	Bus 6	82.3	83.98+j6.702	10.66 +j 0.15

Table 4-4. Impedances of individual service lines

Service Line	Node x (start)	Node y (end)	Length (m)	Rs + jXs (mΩ)	Rm + jXm (mΩ)
1	Bus 3	Bus 4	3.86	7.3 + j0.3	0
2	Bus 3	Bus 5	11.44	21.8 + j1.02	0
3	Bus 6	Bus 7	5.36	10.2 + j0.48	0
4	Bus 6	Bus 8	7.71	14.68 + j0.69	0

Based on Equations 3.12 and 3.13, the impedances of combined lines (three-phase) and service lines (single-phase) can be calculated. Take Combined Line 1 ($cl1$) and Service Line 1 ($sl1$) as an example, as shown in Figure 4-18, impedances are calculated in Equation 4.2. Here, $\boldsymbol{V_{head}^{phA}}$ represents the voltage at the head of the feeder at phase A, and $\boldsymbol{v_{bus4}^{phA}}$ is the Customer 1 voltage at Bus 4 at phase A. The currents on the three-phase Combined Line 1 ($cl1$) are expressed in $[\vec{I}_{phA,cl1}^{phA}, \vec{I}_{phA,cl1}^{phB}, \vec{I}_{phA,cl1}^{phC}]$, and the current on Service Line 1 ($sl1$) at phase A is denoted by $\vec{\imath}_{sl1}^{phA}$. The self-resistance (Rs), self-reactance (Xs), mutual-resistance (Rm) and mutual-reactance (Xm) of Combined Line 1 ($cl1$) are denoted by $\tilde{R}_{cl1}^{s}$, $\tilde{X}_{cl1}^{s}$, $\tilde{R}_{cl1}^{m}$ and $\tilde{X}_{cl1}^{m}$, respectively. The resistance (Rsl) and reactance (Xsl) of Service Line 1 ($sl1$) are denoted by $\tilde{r}_{sl1}^{phA}$ and $\tilde{x}_{sl1}^{phA}$, respectively. Similarly, Equation 4.3 can be used to calculate the impedances of Combined Line 1 ($cl1$) and Service Line 2 ($sl2$). Given that impedances of Combined Line 1 are calculated twice in Equations 4.2 and 4.3, an average value is determined.

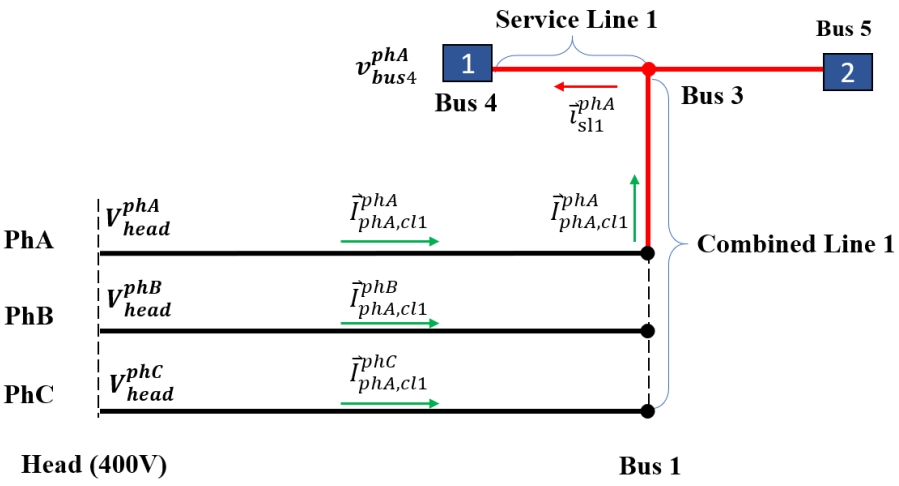

Figure 4-18. Schematics of the part of the UK three-phase LV feeder and single-phase service lines

$$\boldsymbol{V_{head}^{phA} - v_{bus4}^{phA}} = \tilde{R}_{cl1}^{s}\Re\left[\vec{I}_{phA,cl1}^{phA}\right] - \tilde{X}_{cl1}^{s}\Im\left[\vec{I}_{phA,cl1}^{phA}\right] + \tilde{R}_{cl1}^{m}\left(\Re\left[\vec{I}_{phA,cl1}^{phB}\right] + \Re\left[\vec{I}_{phA,cl1}^{phC}\right]\right) - \tilde{X}_{cl1}^{m}\left(\Im\left[\vec{I}_{phA,cl1}^{phB}\right] + \Im\left[\vec{I}_{phA,cl1}^{phC}\right]\right) + \tilde{r}_{sl1}^{phA}\Re\left[\vec{i}_{sl1}^{phA}\right] - \tilde{x}_{sl1}^{phA}\Im\left[\vec{i}_{sl1}^{phA}\right] \quad 4.2$$

$$\boldsymbol{V_{head}^{phA} - v_{bus5}^{phA}} = \tilde{R}_{cl1}^{s}\Re\left[\vec{I}_{phA,cl1}^{phA}\right] - \tilde{X}_{cl1}^{s}\Im\left[\vec{I}_{phA,cl1}^{phA}\right] + \tilde{R}_{cl1}^{m}\left(\Re\left[\vec{I}_{phA,cl1}^{phB}\right] + \Re\left[\vec{I}_{phA,cl1}^{phC}\right]\right) - \tilde{X}_{cl1}^{m}\left(\Im\left[\vec{I}_{phA,cl1}^{phB}\right] + \Im\left[\vec{I}_{phA,cl1}^{phC}\right]\right) + \tilde{r}_{sl2}^{phA}\Re\left[\vec{i}_{sl2}^{phA}\right] - \tilde{x}_{sl2}^{phA}\Im\left[\vec{i}_{sl2}^{phA}\right] \quad 4.3$$

To assess the accuracy of the estimation, the resulting impedances are compared with their actual values (Tables 4-3 and 4-4) using absolute percent error (APE), as presented in Figure 4-19. Here, the first two rows present the APE for the combined lines, and the last row shows the APE for the service lines. Except for the service line reactance, all other estimated impedance variables are considerably accurate. Interestingly, here does not have the errors shown in the Australian network. This is because, in the UK network, customers per phase are connected to the same three-phase bus.

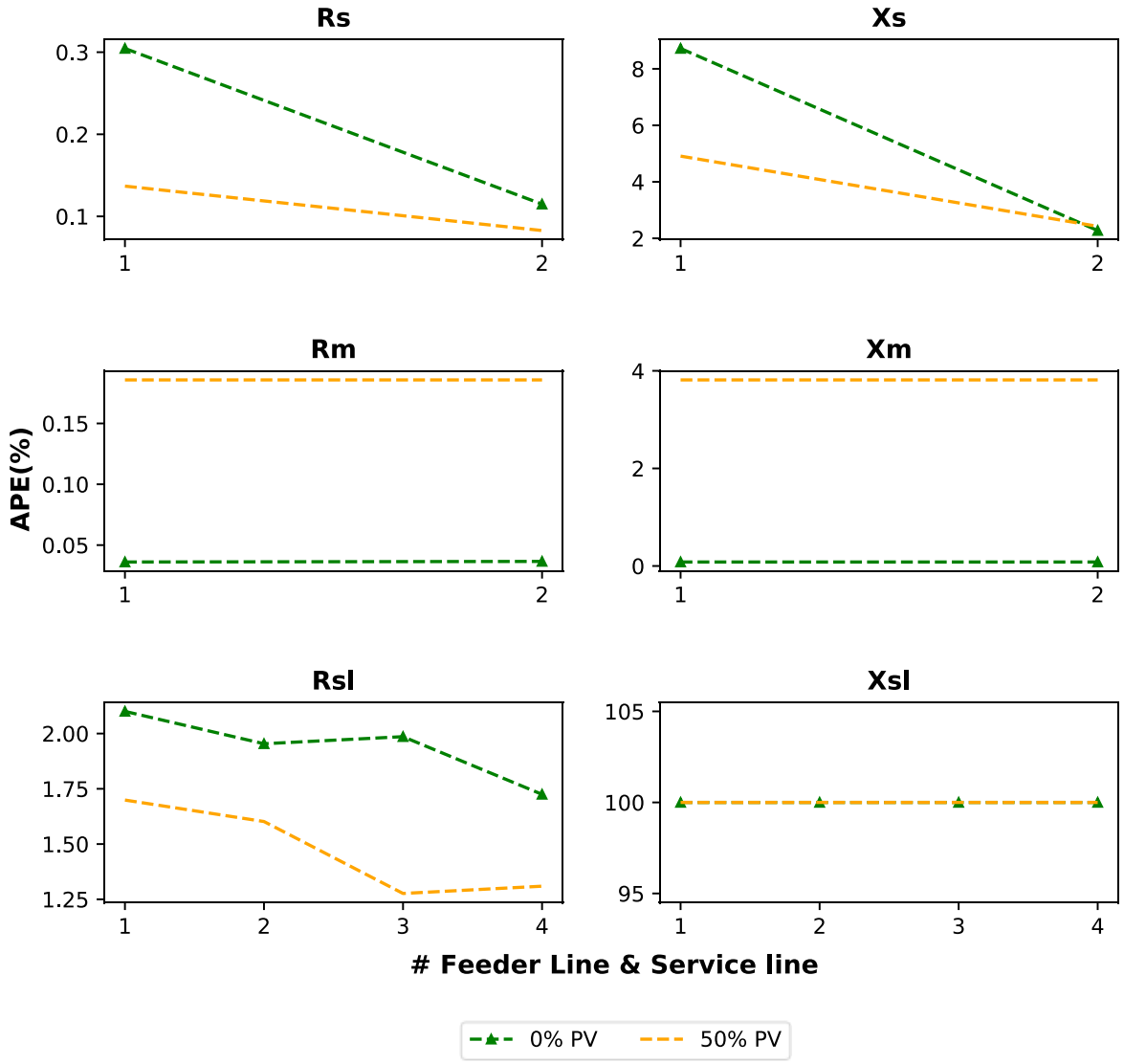

Figure 4-19. APE of the estimated impedances determined under the 0% and 50% PV penetration conditions

4.3.4 Results - Voltage Calculations for What-if Analyses

This section covers the results for the customer voltages through what-if analyses using the previously estimated impedances. In a similar manner as in the Australian LV feeder, the total voltage mismatch is determined here, as shown in Figure 4-20. The results are compared to the voltages obtained using the actual impedances and a three-phase power flow engine. First, it can be seen that impedances estimated under different PV penetration conditions do not lead to significantly different calculated voltages. Furthermore, the last two customers have greater voltage mismatches (i.e. 0.1V) because the proposed voltage assessment approach assumes that losses in the three-phase lines and single-phase service lines are negligible. However, given

that the last two customers are farthest from the head of the feeder, these neglected line losses are higher. Thus, their voltages are less accurate. Finally, in comparison to using the power flow engine, using the linearized voltage drop equations makes the calculation much faster (a reduction from 2.85s to 0.005s).

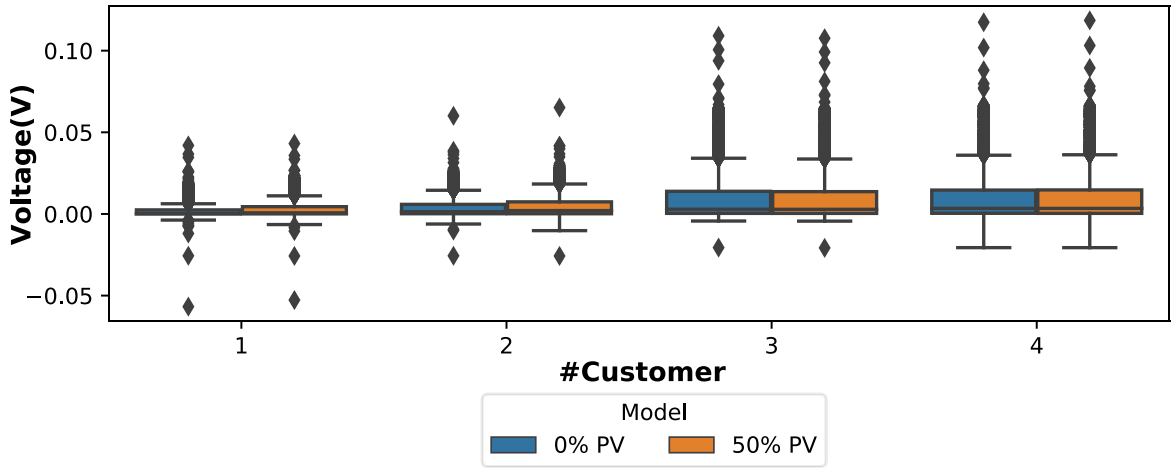

Figure 4-20. Total voltage mismatch caused by the proposed approach

4.4 Impedance Estimation Errors

In comparison to the Australian LV network, the UK LV network has fewer three-phase LV feeder lines and customers. In the UK LV network, customers per phase are connected to the same three-phase bus. In contrast, the Australian LV network has customers per phase connected to different three-phase buses. There is a cumulative error in the three-phase voltage estimation, and the mismatch between the actual and estimated voltage angles are also increased along the feeder. Thus, it is necessary to understand how the three-phase voltages and the current affect the accuracy of impedances. Therefore, the following two scenarios are conducted to estimate the impedances of LV feeder lines and service lines based on having the knowledge of:

- The actual current (from the three-phase power flow); and
- The actual current and three-phase voltage (also from the three-phase power flow).

The absolute percent error (APE) of each impedance variable is determined for the two scenarios considering the Australian LV network. Then, they are compared with the original

results determined by the proposed approach under the 0% and 50% PV penetration condition. The results are as shown in Figures 4-21 and 4-22, respectively.

In both figures, the red line represents the APE determined using the proposed approach under the 0% and 50% PV penetration conditions. After using the actual current in the MLR model, the determined impedances are slightly more accurate, as shown by the green lines. However, errors are not significantly reduced because of the small changes in voltage angles along the feeder, as shown in Figure 4-8.

After using the accurate three-phase voltages, the overall accuracy is greatly improved, demonstrated by the yellow lines shown in both figures. Under the 0% PV penetration condition, except for lines 12 and 19, all lines have the most accurate estimated impedances. Thus, the three-phase voltages have a significant impact on the accuracy of the impedances. Furthermore, under the 50% PV penetration condition, these effects are even more noticeable. In particular, the estimation errors for the Rs and Rsl of all the lines are less than 1% and 0.5%, respectively.

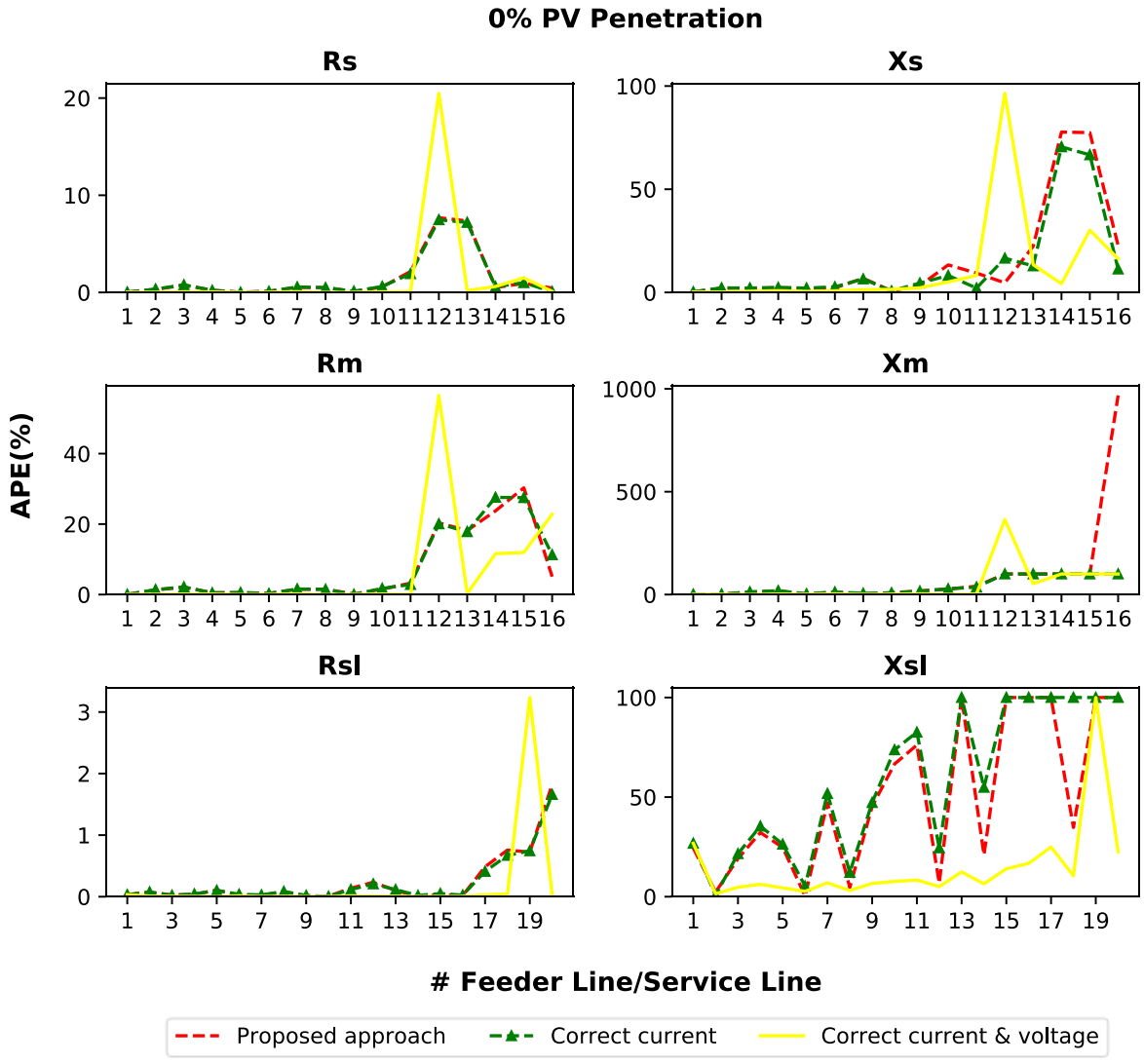

Figure 4-21. APE of impedances determined by the proposed approach, the proposed approach with the correct current, and the proposed approach with the correct current and three-phase voltages (0% PV penetration condition)

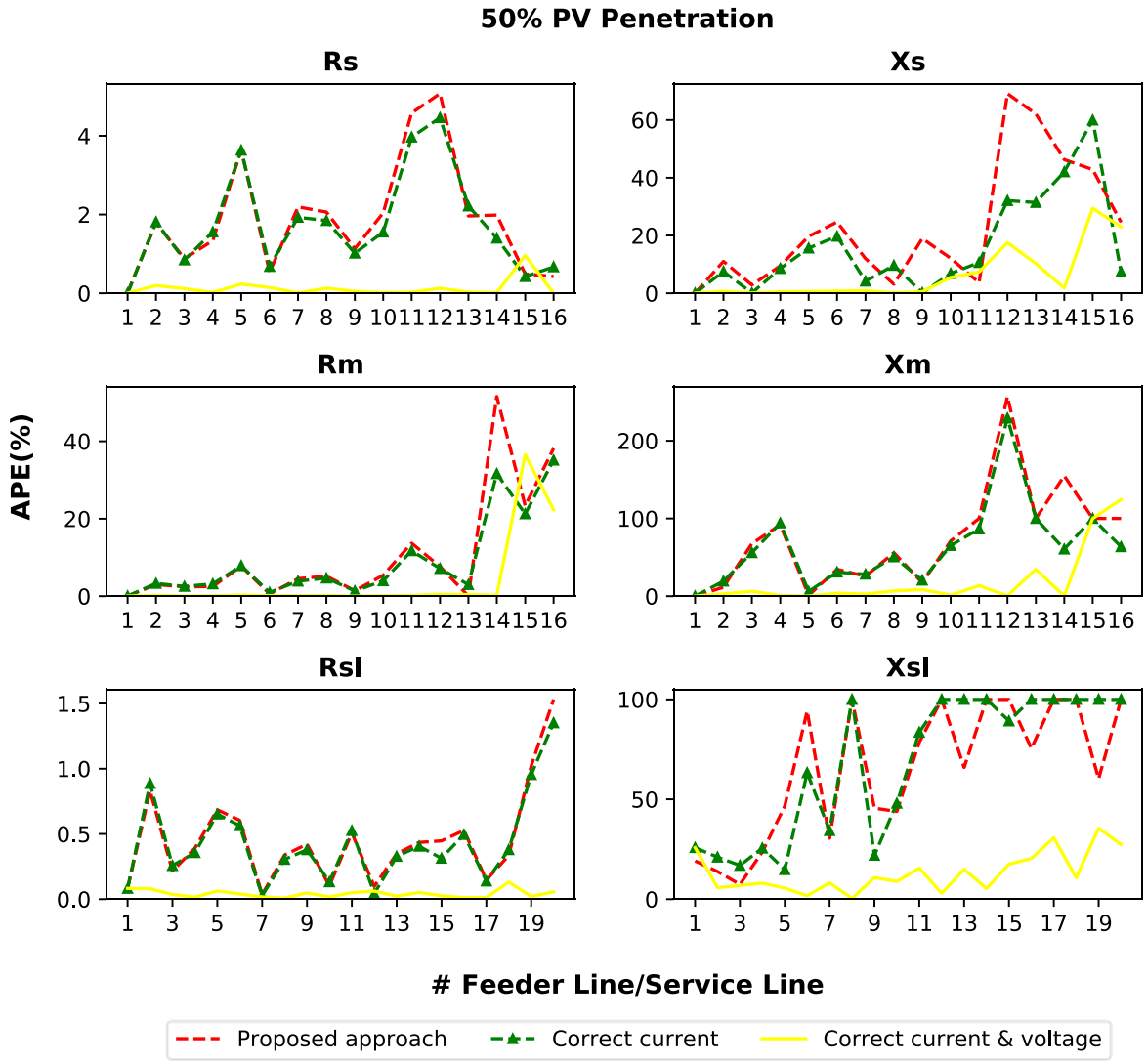

Figure 4-22. APE of impedances determined by the proposed approach, the proposed approach with the correct current, and the proposed approach with the correct current and three-phase voltages (50% PV penetration condition)

4.5 Summary

In this chapter, the performance of the proposed approach was evaluated using realistic Australian and UK LV networks. To assess the accuracy of the impedances, APE was determined based on the actual impedances of the LV lines. Then, for the estimated voltages, both calculation accuracy and computing speed were assessed by comparing the estimations with actual results from a power flow engine.

The results show that the accuracy of voltage calculations depends on the impedances of the LV lines. Furthermore, the accuracy of the impedances depends on the corresponding line's voltage drop and current. These two variables, in turn, depend on the accuracy of the three-

phase bus voltages and the voltage angle, respectively. Based on the above discussion, it is clear that the three-phase voltages have dominated the accuracy of the proposed approach. The lower the cumulated error of the three-phase voltages, the better the estimated impedances of the LV lines. Thus, more accurate customer voltages can be determined. Furthermore, using voltage drop equations can significantly reduce the computing time. Thus, the proposed approach can effectively help distribution companies to quickly and accurately assess the impacts of DER on voltages before taking any action to manage DER.

5 CONCLUSIONS AND FUTURE WORK

This final chapter first presents a summary of the research challenges investigated in this thesis, the research gaps in existing literature, and the main contributions. This is followed by the conclusions of the thesis regarding the performance of the proposed approach for LV line impedance estimation and voltage calculations (for what-if analyses). Lastly, the thesis ends with discussion of potential future research.

5.1 Research Challenges, Research Gaps, and Main Contributions

Driven by the decreasing costs of advanced technologies and high electricity bills, there has been an exponential growth in the installation of residential solar PV systems in LV networks. This encourages the increasing adoption of residential BES systems and EVs to store the surplus solar energy for later use. Along with the rapid adoption of DER, voltage rise/drop issues during periods of excessive DER injections/absorptions are becoming a significant issue for distribution companies. Thus, these companies increasingly need a tool to understand the extent of the impacts of DER on customer voltages (what-if analyses), particularly for operational purposes so as to determine the most adequate operation (settings, injections, etc.) for these technologies.

Extensive research has been carried out in the literature about three-phase power flow analyses to assess the impacts of DER on customer voltages in any demand/generation condition (also known as what-if analyses). However, running conventional three-phase power flow analyses has two main challenges. The first one is the limited knowledge of the underlying LV network model: impedance of LV line models (i.e. three-phase LV feeder lines and single-phase service lines), customer connectivity, and customer phase connection. The second challenge is that, if such studies are needed for operational purposes (calculations in near real time), then implementing power flows to be run for hundreds of LV feeders can be a complex task for distribution companies. Several studies have been reported in the literature to tackle these two challenges, the gaps still exist which are discussed below.

- Limited knowledge of LV networks. Studies in the recent literature can accurately estimate the customer connectivity and the customer phase connection in inherently unbalanced LV networks using smart meter measurements. However, no existing smart meter-driven approaches can determine adequate impedances of three-phase LV feeders with phase couplings. Therefore, estimating impedances for different types of LV line models (i.e. three-phase LV feeder line and single-phase service line models) has become the most difficult part, which needs to be tackled.

- Simplified Voltage Calculations (for Operational Purposes). existing simplified methods are based on the single-phase voltage drop equations and an additional 'unbalanced factor'. Given that the 'unbalanced factor' is determined either empirically or using data-driven techniques that require large amounts of data, such methods cannot are not precise or practical enough for their actual implementation by distribution companies scenarios.

Given the gaps in the existing literature, this thesis proposes a practical approach to calculate customer voltages (in what-if analyses) using smart meter-driven LV line that adequately capture the effects among the three phases. The contributions of this thesis are summarised below.

1) A novel impedance estimation approach

   It uses historical time-series measurements (i.e. the voltage magnitude, active power, and reactive power) from smart meters and at the head of the to estimate the impedances of LV line models (i.e, the three-phase LV feeder line and the single-phase service line models). Crucially, the phase couplings are considered in three-phase LV feeder line models.

2) A novel accurate, fast and practical simplified three-phase voltage calculation algorithms

   This process uses the estimated impedances and the linearised voltage drop equations to directly calculate the impacts of DER on customer voltages in what-if analyses.

3) Realistic case studies

Realistic Australian and UK LV networks have been used for both impedance estimation and voltage calculations. It is worth highlighting that realistic demand/generation data are used to emulate smart meter measurements.

5.2 Key Findings

This section covers the conclusions regarding the performance of the proposed approach for impedance estimation and voltage calculation.

5.2.1 Impedance Estimation

The performance of the proposed approach was evaluated in realistic Australian and UK LV networks. The impedances of LV line models (i.e. three-phase LV feeder line and single-phase service line models) are estimated by using weekly historical meter measurements (active power, reactive power, and voltage magnitudes) with a 15-minute resolution (672 time steps). Then, the estimated impedances are compared with their actual values and assessed using the absolute percent error.

For the impedance estimation, there is an accumulation of errors along the LV feeder. Results show adequate accuracy for the estimated impedances in both Australian and UK LV networks. In the Australian network, customers at the same phase are connected to different three-phase buses, and the accuracy of the last few three-phase feeder lines impedances is lower than those for the head and the middle of the LV feeder. However, similar errors are not seen in the UK LV network, and this is due to customers at the same phase are connected to the same three-phase bus, and there are no accumulated errors along the feeder. However, it is important to highlight that, from the perspective of voltage calculations for what-if analyses, given that the currents at the end of the feeder are relatively small (only a few customers), the errors in impedances cannot cause significant voltage error.

5.2.2 Voltage Calculations for What-if Analyses

For the customer voltage calculations (for what-if analyses), there is an accumulation of errors along the LV feeder. At the same time, the proposed voltage calculation approach has assumed that losses in the three-phase lines and single-phase service lines are negligible. Thus, the farther the customers from the head of the feeder, the higher the neglected line losses, and thus, the less accurate calculated voltages. Nonetheless, results show that all calculated customer

voltages are highly accurate in both Australian and UK LV networks. Furthermore, the computing speed is much faster than with a power flow engine, which makes it much scalable for the simultaneous near real-time calculations of hundreds of LV feeders. Consequently, the findings suggest that the proposed approach is accurate and practical enough for its use by distribution companies.

5.3 Future Work

5.3.1 Improvement of the Impedance Estimation Approach

For LV line impedance estimation, the biggest assumption of the proposed approach is that it requires an extra three-phase meter at the head of the feeder. Thus, future works should consider how to estimate impedances of three-phase LV feeder lines and single-phase service lines without using the measurements at the head of the feeder.

5.3.2 Other Application of the Proposed Approach

For operational purposes, the voltage calculation tool proposed in this thesis can be used to determine the maximum time-varying export or import limits (called ‘operating envelopes’) of each household based on the network voltage and thermal constraints. This could help avoiding network issues when aggregators manage a large number of DER to provide services upstream the LV networks (e.g., injecting or absorbing power). Once the operating envelopes are obtained, aggregators managing DER can decide how to operate the DER in each household according to their objective (e.g. increase profit from services) but respecting the operating envelope per household.

References

[1] Center for Disaster Philanthropy. "2019-2020 Australian Bushfires." Center for Disaster Disaster Philanthropy. https://disasterphilanthropy.org/disaster/2019-australian-wildfires/ (Accessed Jun. 20, 2020).

[2] Climate Council. "11 countries leading the charge on renewable energy | Climate Council." Climate Council. https://www.climatecouncil.org.au/11-countries-leading-the-charge-on-renewable-energy/ (Accessed Jun. 20, 2020).

[3] International Energy Agency. " Tracking Power 2020." IEA. https://www.iea.org/reports/tracking-power-2020/solar-pv#abstract (Accessed Jun. 20, 2020).

[4] SolarPower Europe, "Global Market Outlook: For Solar Power / 2018 – 2022," SolarPower Europe, Brussels, Belgium, 2018. [Online]. Available: https://www.solarpowereurope.org/wp-content/uploads/2018/09/Global-Market-Outlook-2018-2022.pdf

[5] Australian Renewable Energy Agency. "What are distributed energy resources and how do they work? – ARENAWIRE." ARENA. https://arena.gov.au/blog/what-are-distributed-energy-resources/ (Accessed Jun. 20, 2020).

[6] T. Haggis, "Network Design Manual - E.ON UK", 2006. [Online]. Available: https://www.yumpu.com/en/document/read/8953808/network-design-manual-eon-uk

[7] Australian Energy Market Commission. "Electricity supply chain." AEMC. https://www.aemc.gov.au/energy-system/electricity/electricity-system/electricity-supply-chain (Accessed Jun. 20, 2020).

[8] Electrical Installation. "Low-voltage consumers - Electrical Installation Guide." Electrical Installation. https://www.electrical-installation.org/enwiki/Low-voltage_consumers#:~:text=Contents&text=The%20most%2Dcommon%20LV%20supplies,LV%20networks%20are%20marginally%20adequate (Accessed Jun. 21, 2020).

[9] J. Hall, "Distribution Network Standard: Standard for Electrical Design and Construction Requirements for Chamber Substations," Ergon Energy, Queensland, Australia, n.d. [Online]. Available: https://www.ergon.com.au/__data/assets/pdf_file/0008/326339/STNW3389.pdf

[10] Australian Rectifiers. "AC Supply voltage ratings in Australia have been lowered – Australian Rectifiers." Australian Rectifiers. https://www.australianrectifiers.com.au/regulatory/ac-supply-voltage-ratings-in-australia-have-been-lowered/ (Accessed Jun. 21, 2020).

[11] F. Shahnia, P. J. Wolfs and A. Ghosh, "Voltage Unbalance Reduction in Low Voltage Feeders by Dynamic Switching of Residential Customers Among Three Phases," *IEEE Transactions on Smart Grid*, vol. 5, no. 3, pp. 1318-1327, May 2014, doi: 10.1109/TSG.2014.2305752.

[12] E. Lakervi and E. Holmes, *Electricity distribution network design*, Stevenage: Peter Peregrins Ltd. on behalf of The Institution of Engineering and Technology, 1995.

[13] Z. Hilson, A. Cunsolo and B. McKenzie. "Electricity regulation in Australia: overview." Thomson Reuters Practical Law. https://uk.practicallaw.thomsonreuters.com/w-010-

9549?transitionType=Default&contextData=(sc.Default)&firstPage=true&bhcp=1 (Accessed Mar. 17, 2020).

[14] C. Noel and A. Bletchly, "Standard for Distribution Line Design Underground", Ergon Energy, Queensland, Australia, 2019. [Online]. Available: https://www.ergon.com.au/__data/assets/pdf_file/0005/326633/STNW3369-Distribution-Line-Design-UG.pdf

[15] Ausgrid, "NS110 DESIGN AND CONSTRUCTION STANDARD FOR URDS", Ausgrid, New South Wales, Australia, 2018. [Online]. Available: https://www.ausgrid.com.au/-/media/Documents/Technical-Documentation/NS/NS110.pdf

[16] D. H. O. McQueen, P. R. Hyland and S. J. Watson, "Monte Carlo simulation of residential electricity demand for forecasting maximum demand on distribution networks," *IEEE Transactions on Power Systems*, vol. 19, no. 3, pp. 1685-1689, Aug. 2004.

[17] C. Barteczko-Hibbert, "After Diversity Maximum Demand (ADMD) Report," 2015. [Online]. Available: http://www.networkrevolution.co.uk/wp-content/uploads/2015/02/After-Diversity-Maximum-Demand-Insight-Report.pdf

[18] A. Baitch, "VOLTAGE CONTROL FOR DISTRIBUTION NETWORKS and the 230V/400V Standard", in *Conference of the Electric Energy Society of Australia*, Canberra, 2000.

[19] Australian Energy Regulator. 'Smart meters.' AER. https://www.aer.gov.au/consumers/my-energy-service/smart-meters (Accessed Apr. 1, 2020).

[20] Victoria State Government. 'Smart meters.' Victoria State Government. https://www.energy.vic.gov.au/electricity/smart-meters (Accessed Apr. 1, 2020).

[21] Jemena. ‘My smart meter – Jemena.’ Jemena. https://jemena.com.au/electricity/monitor-my-electricity-usage/my-smart-meter (Accessed Apr. 1, 2020).

[22] FRONIUS, “FRONIUS SMART METER – APPLICATION GUIDE,” FRONIUS, Australia, Version 5, 2019.

[23] H. SELJESETH, H. KIRKEBY and H. TAXT, "BENEFITS OF VOLTAGE MEASUREMENTS WITH SMART METERS" in *23rd International Conference on Electricity Distribution*, 2015.

[24] P. Scully. "Smart Meter Market 2019: Global penetration reached 14%", Iot Analytics, 2019. https://iot-analytics.com/smart-meter-market-2019-global-penetration-reached-14-percent/ (Accessed: Jul. 27, 2020).

[25] EnergyAustralia. ‘Smart meters.’ EnergyAustralia https://www.energyaustralia.com.au/business/help-and-support/faqs/smart-meters (Accessed Apr. 1, 2020).

[26] Research and Markets. "Insights Into the World's $2.9B+ Smart Grid Data Analytics Market, 2025." GlobeNewswire News Room. https://www.globenewswire.com/news-release/2020/03/18/2002567/0/en/Insights-Into-the-World-s-2-9B-Smart-Grid-Data-Analytics-Market-2025.html (Accessed Jun. 21, 2020).

[27] Y. Wang, Q. Chen, T. Hong and C. Kang, "Review of Smart Meter Data Analytics: Applications, Methodologies, and Challenges" *IEEE Transactions on Smart Grid*, vol. 10, no. 3, pp. 3125-3148, May 2019, doi: 10.1109/TSG.2018.2818167.

[28] D. Gielen, F. Boshell, D. Saygin, M. Bazilian, N. Wagner and R. Gorini, "The role of renewable energy in the global energy transformation", *Energy Strategy Reviews*, vol. 24, pp. 38-50, 2019. Available: 10.1016/j.esr.2019.01.006.

[29] Australian Government Clean Energy Regulator, "Postcode data for small-scale installations", Clean Energy Regulator. http://www.cleanenergyregulator.gov.au/RET/Forms-and-resources/Postcode-data-for-small-scale-installations (Accessed Jun. 21, 2020).

[30] Australian Photovoltaic Institute, "Mapping Australian Photovoltaic installations." API https://pv-map.apvi.org.au/historical (Accessed Jul. 27, 2020).

[31] Australian Government. "Solar PV and batteries." Australian Government. https://www.energy.gov.au/households/solar-pv-and-batteries (Accessed Apr. 1, 2020).

[32] Energy Matters. "How a grid connected solar power system works." Energy Matters. https://www.energymatters.com.au/residential-solar/how-solar-power-works/ (Accessed Apr. 1, 2020).

[33] Energy Education. "Photovoltaic system." Energy Education. https://energyeducation.ca/encyclopedia/Photovoltaic_system (Accessed Apr. 1, 2020).

[34] EnergyMatters. "How Much Rooftop Solar Power Can You Install? – A State by State Guide.", EnergyMatters. https://www.energymatters.com.au/residential-solar/rooftop-solar-power-panels-install-state/ (Accessed Jun. 21, 2020).

[35] J. Martin II. "Solar system size limits explained by state | Solar Choice." Solar Choice. https://www.solarchoice.net.au/blog/solar-system-size-limits-by-network (Accessed Jun. 21, 2020).

[36] SolarQuotes. "Determining The Best Sized Solar Power System To Maximise Returns." SolarQuotes. https://www.solarquotes.com.au/good-solar-guide/system-sizing/ (Accessed Jun. 21, 2020).

[37] Solar Choice. "Solar power and single-phase vs 3-phase power connections | Solar Choice." Solar Choice. https://www.solarchoice.net.au/blog/solar-power-single-phase-vs-3-phase-connections (Accessed Jun. 21, 2020).

[38] ENERGEIA, "Distributed Energy Resources and Electric Vehicle Forecasts," ENERGEIA, 2019. [Online]. Available: https://www.aemo.com.au/-/media/Files/Electricity/NEM/Planning_and_Forecasting/Inputs-Assumptions-Methodologies/2019/Distributed-Energy-Resources-and-Electric-Vehicle-Forecasts---Report-by-Energeia.pdf

[39] Queensland Government. "How battery energy storage works." Queensland Government. https://www.qld.gov.au/housing/buying-owning-home/energy-water-home/solar/battery-energy-storage/how-battery-energy-storage-works (Accessed Apr. 1, 2020).

[40] K. Thoubboron. "DOD Battery: What Does Depth of Discharge Mean? | EnergySage." Solar News. https://news.energysage.com/depth-discharge-dod-mean-battery-important/#:~:text=A%20battery's%20depth%20of%20discharge,DoD%20is%20approximately%2096%20percent (Accessed Jun. 21, 2020).

[41] International Energy Agency. "Global EV Outlook 2019 – Analysis – IEA." IEA. https://www.iea.org/reports/global-ev-outlook-2019 (Accessed Jun. 21, 2020).

[42] Australian Energy Market Commission. "2020 RETAIL ENERGY COMPETITION REVIEW: ELECTRIC VEHICLES." AEMC, https://www.aemc.gov.au/sites/default/files/documents/rpr0012_-

_2020_retail_energy_competition_review_-_electric_vehicles_-_issues_paper.pdf. (Accessed Jun. 21, 2020).

[43] BloombergNEF. “Australia to Be Largest Residential Storage Market in 2019.” BloombergNEF. https://about.bnef.com/blog/australia-largest-residential-storage-market-2019/ (Accessed Mar. 17, 2020).

[44] S. Vorrath. "Labor battery subsidy could deliver 80% cut to household electricity bills.", RenewEconomy. https://reneweconomy.com.au/labor-battery-subsidy-could-deliver-80-cut-to-household-electricity-bills-93697/ (Accessed Jun. 21, 2020).

[45] B. SCHMIDT. "Tesla's switch on vehicle-to-grid technology is big news for clean energy shift | The Driven." The Driven. https://thedriven.io/2020/05/20/teslas-switch-on-vehicle-to-grid-technology-is-big-news-for-clean-energy-shift/ (Accessed Jun. 21, 2020).

[46] G. Parkinson. "Why electric vehicles could kill the market for household batteries." RenewEconomy. https://reneweconomy.com.au/why-electric-vehicles-could-kill-the-market-for-household-batteries-72526/ (Accessed Jun. 21, 2020).

[47] Mozo. “Home Battery Guide.” Mozo. https://mozo.com.au/energy/guides/home-battery-storage (Accessed Apr. 01, 2020).

[48] Clean Energy Council, "GUIDE TO INSTALLING A HOUSEHOLD BATTERY STORAGE SYSTEM," Beyondsolar, 2018. [Online]. Available: https://www.beyondsolar.com.au/wp-content/uploads/2018/11/guide-to-installing-a-household-battery-storage-system.pdf

[49] Solar Choice. "kW vs kWh in solar & battery storage | Solar Choice." Solar Choice https://www.solarchoice.net.au/blog/kW-vs-kWh-solar-battery-power-energy-capacity (Accessed Jun. 21, 2020).

[50] B. Gaton. "Is a 3-phase electric vehicle charger at home really necessary? | The Driven." The Driven. https://thedriven.io/2019/08/18/is-a-3-phase-electric-vehicle-charger-at-home-really-necessary/ (Accessed Jun. 21, 2020).

[51] M. Thomson and D. Infield, "Network Power-Flow Analysis for a High Penetration of Distributed Generation", *IEEE Transactions on Power Systems*, vol. 22, no. 3, pp. 1157-1162, 2007. Available: 10.1109/tpwrs.2007.901290.

[52] A. Navarro-Espinosa and L. F. Ochoa, "Probabilistic Impact Assessment of Low Carbon Technologies in LV Distribution Systems," *IEEE Transactions on Power Systems*, vol. 31, no. 3, pp. 2192-2203, May 2016, doi: 10.1109/TPWRS.2015.2448663.

[53] K. Alboaouh and S. Mohagheghi, "Impact of Rooftop Photovoltaics on the Distribution System", *Journal of Renewable Energy*, vol. 2020, pp. 1-23, 2020. Available: 10.1155/2020/4831434.

[54] H. Jain, B. Palmintier, I. Krad and D. Krishnamurthy, "Studying the Impact of Distributed Solar PV on Power Systems using Integrated Transmission and Distribution Models," in *IEEE PES T&D Conference and Exposition*, Denver, Colorado, April 16–19, 2018.

[55] A. T. Procopiou, K. Petrou, L. F. Ochoa, T. Langstaff and J. Theunissen, "Adaptive Decentralized Control of Residential Storage in PV-Rich MV–LV Networks," *IEEE Transactions on Power Systems*, vol. 34, no. 3, pp. 2378-2389, May 2019, doi: 10.1109/TPWRS.2018.2889843.

[56] C. Long and L. F. Ochoa, "Voltage Control of PV-Rich LV Networks: OLTC-Fitted Transformer and Capacitor Banks," *IEEE Transactions on Power Systems*, vol. 31, no. 5, pp. 4016-4025, Sept. 2016, doi: 10.1109/TPWRS.2015.2494627.

[57] International Energy Agency, "High Penetration of PV in Local Distribution Grids: Subtask 2: Case-Study Collection," IEA, 2014. [Online]. Available: https://iea-pvps.org/wp-content/uploads/2014/11/High_penetration_of_PV_in_local_distribution_grids_REPORT_PVPS_T14_02_2014-1.pdf

[58] R. Tonkoski, D. Turcotte and T. H. M. ELFouly, "Impact of High PV Penetration on Voltage Profiles in Residential Neighborhoods," *IEEE Transactions on Sustainable Energy*, vol. 3, no. 3, pp. 518-527, July 2012, doi: 10.1109/TSTE.2012.2191425.

[59] C. Gonzalez et al., "LV distribution network feeders in Belgium and power quality issues due to increasing PV penetration levels," in *IEEE PES Innovative Smart Grid Technologies Europe (ISGT Europe)*, Berlin, 2012, pp. 1-8, doi: 10.1109/ISGTEurope.2012.6465624.

[60] J. Quiros-Tortos, G. Valverde, A. Arguello and L. N. Ochoa, "Geo-Information Is Power: Using Geographical Information Systems to Assess Rooftop Photovoltaics in Costa Rica," in *IEEE Power and Energy Magazine*, vol. 15, no. 2, pp. 48-56, March-April 2017, doi: 10.1109/MPE.2016.2637158.

[61] K. Petrou, A. T. Procopiou, L. Gutierrez-Lagos, L. F. Ochoa, T. Langstaff and J. Theunissen, " Ensuring Distribution Network Integrity Using Dynamic Operating Limits for Prosumers," submitted for publication.

[62] J. F. Franco, A. T. Procopiou, J. Quirós-Tortós and L. F. Ochoa, "Advanced control of OLTC-enabled LV networks with PV systems and EVs," in *IET Generation, Transmission & Distribution*, vol. 13, no. 14, pp. 2967-2975, 23 7 2019, doi: 10.1049/iet-gtd.2019.0208.

[63] Tesla. “Powerwall”. Tesla. https://www.tesla.com/en_AU/powerwall. (Accessed Mar. 17, 2020).

[64] K. Petrou et al., "Limitations of Residential Storage in PV-Rich Distribution Networks: An Australian Case Study," *2018 IEEE Power & Energy Society General Meeting (PESGM)*, Portland, OR, 2018, pp. 1-5, doi: 10.1109/PESGM.2018.8585998.

[65] K. Petrou, A. T. Procopiou, L. F. Ochoa, T. Langstaff and J. Theunissen, "Impacts of Price-led Operation of Residential Storage on Distribution Networks: An Australian Case Study," *2019 IEEE Milan PowerTech*, Milan, Italy, 2019, pp. 1-6, doi: 10.1109/PTC.2019.8810955.

[66] K. Petrou and L. F. Ochoa, "Customer-Led Operation of Residential Storage for the Provision of Energy Services," *2019 IEEE PES Innovative Smart Grid Technologies Conference - Latin America (ISGT Latin America)*, Gramado, Brazil, 2019, pp. 1-6, doi: 10.1109/ISGT-LA.2019.8895319.

[67] A. T. Procopiou, J. Quirós-Tortós and L. F. Ochoa, "HPC-Based Probabilistic Analysis of LV Networks With EVs: Impacts and Control," *IEEE Transactions on Smart Grid*, vol. 8, no. 3, pp. 1479-1487, May 2017, doi: 10.1109/TSG.2016.2604245.

[68] J. A. P. Lopes, F. J. Soares, and P. M. R. Almeida, "Integration of Electric Vehicles in the Electric Power System," Proceedings of the IEEE, vol. 99, pp. 16-183, 2011.

[69] A. B. Gupta, T. Alpcan and A. B. Morton, "Predicting Voltage Variations in Low Voltage Networks with Prosumers," *2018 IEEE PES Asia-Pacific Power and Energy Engineering Conference (APPEEC)*, Kota Kinabalu, 2018, pp. 183-188, doi: 10.1109/APPEEC.2018.8566480.

[70] M. J. E. Alam, K. M. Muttaqi and D. Sutanto, "An Approach for Online Assessment of Rooftop Solar PV Impacts on Low-Voltage Distribution Networks," *IEEE Transactions on Sustainable Energy*, vol. 5, no. 2, pp. 663-672, April 2014, doi: 10.1109/TSTE.2013.2280635.

[71] Deka, D., Chertkov, M., Backhaus, S.: ‘Topology estimation using graphical models in multi-phase power distribution grids’, arXiv preprint arXiv:180306531, 2018.

[72] Y. Liao, Y. Weng, G. Liu, Z. Zhao, C. Tan and R. Rajagopal, "Unbalanced multi-phase distribution grid topology estimation and bus phase identification", *IET Smart Grid*, vol. 2, no. 4, pp. 557-570, 2019. doi: 10.1049/iet-stg.2018.0291.

[73] L. Blakely, M. J. Reno, and W. C. Feng, “Spectral Clustering for Customer Phase Identification Using AMI Voltage Timeseries,” *2019 IEEE Power Energy Conf. Illinois (PECI)*, Champaign, IL, USA, 2019, pp. 1-7, doi: 10.1109/PECI.2019.8698780.

[74] C. M. Roberts, C. M. Shand, K. W. Brady, E. M. Stewart, A. W. McMor-ran and G. A. Taylor, "Improving distribution network model accuracy using impedance estimation from micro-synchrophasor data," *2016 IEEE Power and Energy Society General Meeting (PESGM)*, Boston, MA, 2016, pp. 1-5.

[75] S. Iakovlev, "NON-CONVEX OPTIMISATION IN MODERN POWER SYSTEMS AND ADVANCED ARRAY ANTENNAS," Ph.D. dissertation, The University of Melbourne, Australia, 2019.

[76] J. Peppanen, M. J. Reno, M. Thakkar, S. Grijalva and R. G. Harley, "Leveraging AMI Data for Distribution System Model Calibration and Situational Awareness," *IEEE Transactions on Smart Grid*, vol. 6, no. 4, pp. 2050-2059, July 2015.

[77] P. WONG, S. SPENCE and J. ZHONG, "THE APPLICATION OF ADVANCED DATA ANALYTICS TO SMART METER DATA", *25th International Conference on Electricity Distribution*, Madrid, 2019.

[78] A. J. Berrisford, "A tale of two transformers: An algorithm for estimating distribution secondary electric parameters using smart meter data," *2013 26th IEEE Canadian Conference on Electrical and Computer Engineering (CCECE)*, Regina, SK, 2013, pp. 1-6.

[79] S. Qin, B. Lang, L. Chen, W. Luan and S. Guo, "A Method for Distribution Line Impedance Calculation Based on Metering and Distribution Data Integration,"*2019 IEEE International Conference on Energy Internet (ICEI)*, Nanjing, China, 2019, pp. 59-63.

[80] S. Iakovlev, R. Evans and I. Mareels, "Low-Voltage Distribution Network Impedances Identification Based on Smart Meter Data", 2018.

[81] D. Kodaira, J. Park, S. Kim, S. Han and S. Han, "Impedance Estimation with an Enhanced Particle Swarm Optimization for Low-Voltage Distribution Networks", *Energies*, vol. 12, no. 6, p. 1167, 2019. Available: 10.3390/en12061167.

[82] J. Peppanen, S. Grijalva, M. Reno and R. Broderick, "Distribution system low-voltage circuit topology estimation using smart metering data", *2016 IEEE/PES Transmission and Distribution Conference and Exposition (T&D)*, 2016. Available: 10.1109/tdc.2016.7519985

[83] S. Park, D. Deka and M. Chcrtkov, “Exact Topology and Parameter Estimation in Distribution Grids with Minimal Observability,” *2018 Power Systems Computation Conference (PSCC)*, Dublin, Ireland, 2018.

[84] J. Watson, J. Welch and N. Watson, "Use of smart-meter data to determine distribution system topology", *The Journal of Engineering*, vol. 2016, no. 5, pp. 94-101, 2016.

[85] J. De La Ree, V. Centeno, J. S. Thorp, and A. G. Phadke, “Synchronized phasor measurement applications in power systems,” *IEEE Transactions on Smart Grid*, vol. 1, no. 1, pp. 20–27, 2010.

[86] C. S. Cheng and D. Shirmohammadi, "A three-phase power flow method for real-time distribution system analysis," *IEEE Transactions on Power Systems*, vol. 10, no. 2, pp. 671-679, May 1995, doi: 10.1109/59.387902.

[87] E. Namanya, "Voltage Calculation on Low Voltage Feeders with Distributed Generation", Master of Science in Engineering, University of Cape Town, 2014.

[88] J. A. Martinez and J. Mahseredjian, "Load flow calculations in distribution systems with distributed resources. A review," *2011 IEEE Power and Energy Society General Meeting*, Detroit, MI, USA, 2011, pp. 1-8, doi: 10.1109/PES.2011.6039172.

[89] Sellick, Rob & Gaunt, C.T., "Comparing methods of calculating voltage drop in low voltage feeders," *Transactions of the South African Institute of Electrical Engineers*, 1995.

[90] Powerconsultants. "LVDrop7 Low Voltage Drop Calculator configuration forum." Powerconsultants. http://www.powerconsultants.com.au/html/Software/LVDropForum/LVDrop7Forum.htm. (Accessed May. 29, 2020).

[91] G. Hall, "Distribution Design Standard-Underground Systems," TasNetwork, Tasmanian, Australia, 2016. [Online]. Available: https://www.tasnetworks.com.au/config/getattachment/e0eccf19-5e84-4a7b-aa82-e8f18a69148a/Distribution-Design-Standard-Underground-System.pdf

[92] FPL. "The Flow of Electricity," Fpl, n.d. [Online]. Available: https://www.fpl.com/reliability/flow-electricity/pdf/Flow_of_Electricity_English.pdf

[93] R. Ciric, A. Feltrin and L. Ochoa, "Power flow in four-wire distribution networks-general approach", *IEEE Transactions on Power Systems*, vol. 18, no. 4, pp. 1283-1290, 2003. Available: 10.1109/tpwrs.2003.818597.

[94] H. Hosseinian Yengejeh, F. Shahnia and S. Islam, "Disconnection of single-phase rooftop PVs after short-circuit faults in residential feeders", *Australian Journal of Electrical and Electronics Engineering*, vol. 13, no. 2, pp. 151-165, 2016. Available: 10.1080/1448837x.2016.1221637.

[95] W. Kersting, "Distribution system modeling and analysis," Boca Raton, Fla.: Taylor & Francis, 2007.

[96] L. Degroote, B. Renders, B. Meersman and L. Vandevelde, "Neutral-point shifting and voltage unbalance due to single-phase DG units in low voltage distribution networks", *2009 IEEE Bucharest PowerTech*, 2009. Available: 10.1109/ptc.2009.5281998.

[97] R. Stoicescu, K. Miu, C. O. Nwankpa, D. Niebur and Xiaoguang Yang, "Three-phase converter models for unbalanced radial power-flow studies" in *IEEE Transactions on Power Systems*, vol. 17, no. 4, pp. 1016-1021, Nov. 2002, doi: 10.1109/TPWRS.2002.804942.

[98] K. Miu, M. Kleinberg, "Impact Studies of Unbalanced Multi-Phase Distribution System Component Models", Proceedings of the 2010 IEEE PES General Meeting, Minneapolis, July 2010.

[99] D. F. Frame, G. W. Ault and S. Huang, "The uncertainties of probabilistic LV network analysis," *2012 IEEE Power and Energy Society General Meeting*, San Diego, CA, 2012, pp. 1-8, doi: 10.1109/PESGM.2012.6344587.

[100] C. Grudzien, D. Deka, M. Chertkov and S. Backhaus, "Structure- and Physics-Preserving Reductions of Power Grid Models", *Multiscale Modeling & Simulation*, vol. 16, no. 4, pp. 1916-1947, 2018. Available: 10.1137/17m1138054.

[101] F. OLIVIER, R. FONTENEAU and D. ERNST, "MODELLING OF THREE-PHASE FOUR-WIRE LOW-VOLTAGE CABLES TAKING INTO ACCOUNT THE NEUTRAL CONNECTION TO THE EARTH", presented at the CIRED Workshop, Ljubljana, 2018.

[102] W. H. Kersting and W. H. Phillips, "Distribution feeder line models," in *IEEE Transactions on Industry Applications*, vol. 31, no. 4, pp. 715-720, July-Aug. 1995.

[103] R. M. Ciric, L. F. Ochoa, A. Padilla-Feltrin and H. Nouri, "Fault analysis in four-wire distribution networks" in *IEEE Proceedings - Generation, Transmission and Distribution*, vol. 152, no. 6, pp. 977-982, 4 Nov. 2005.

[104] K. Miu and M. Kleinberg, "Impact studies of unbalanced multi-phase distribution system component models," *IEEE PES General Meeting*, Providence, RI, 2010, pp. 1-4, doi: 10.1109/PES.2010.5589570.

[105] J. Frost. "How to Choose Between Linear and Nonlinear Regression - Statistics By Jim." Statistics By Jim. https://statisticsbyjim.com/regression/choose-linear-nonlinear-regression/ (Accessed May. 29, 2020).

[106] NCSS. "Nonlinear Regression." NCSS, 2020. [Online]. Available: https://ncss-wpengine.netdna-ssl.com/wp-content/themes/ncss/pdf/Procedures/NCSS/Nonlinear_Regression.pdf

[107] M. Bremer, "Multiple Linear Regression." Cornell University, 2012. [Online]. Available: http://mezeylab.cb.bscb.cornell.edu/labmembers/documents/supplement%205%20-%20multiple%20regression.pdf

[108] M. Lacey, "Multiple Linear Regression." Yale University, 1997. [Online]. Available: http://www.stat.yale.edu/Courses/1997-98/101/linmult.htm

[109] C. Shalizi, "Lecture 14: Multiple Linear Regression", Carnegie Mellon University, 2015. [Online]. Available: https://www.stat.cmu.edu/~cshalizi/mreg/15/lectures/14/lecture-14.pdf

[110] F. Calero, "Mutual Impedance in Parallel Lines – Protective Relaying and Fault Location Considerations", in *34th Annual Western Protective Relay Conference*, 2007.

[111] Python. [Online]. Available: https://www.python.org

[112] R. C. Dugan and T. E. McDermott, "An open source platform for collaborating on smart grid research," in *Proc. 2011 IEEE Power and Energy Society General Meeting*, pp. 1-7.

[113] Electricity North West Limited, “Low Voltage Network Solutions: A First Tier LowCarbon Networks Fund Project,” ENWL, 2014. [Online]. Available:http://www.enwl.co.uk/docs/default-source/future-low-voltage/lv-network-solutionsclose-down-june-14-v4-1-final.pdf?sfvrsn=2

[114] I. Richardson, M. Thomson, D. Infield, and C. Clifford, “Domestic electricity use: A high-resolution energy demand model,” *Energy Build.*, vol. 42, no. 10, pp. 1878–1887, Oct. 2010.

Appendix

This section uses an example of a three-phase LV feeder (Figure 1) to analyse the impact of every impedance variable (i.e. Rs, Xs, Rm, and Xm) on customer voltages. The feeder is 200m, which feeds three end-customers. The cable conductor is obtained from Ausnet Services, and the actual self and mutual impedances are 39.733+j15.533mΩ and 14.333+j1.133mΩ, respectively.

To assess the impact of each impedance variable on the voltages, this study needs four groups of impedance variables. In each group, one impedance variable has a -50% error, and the other three impedance variables use their actual values. Thus, four groups have four different poorly estimated impedance variables. Assuming a balanced LV feeder, demands on the three phases are simultaneously increased from 10kW to 50kW, with a step size of 10kW. Under certain demand conditions, customer voltages are calculated by running power flow based on the four groups of impedance variables, and the values are called 'Estimated Voltage'.

The impact of the sole impedance variable on voltages is assessed by subtracting the actual voltages from the 'Estimated Voltage' in four groups. Here, actual voltages are determined by the actual impedances and the power flow engine. The voltage mismatch is shown in Figure 2, which shows that the contributions of four different impedance variables on voltages from large to small are listed as follows: Rs, Rm, Xs, and Xm.

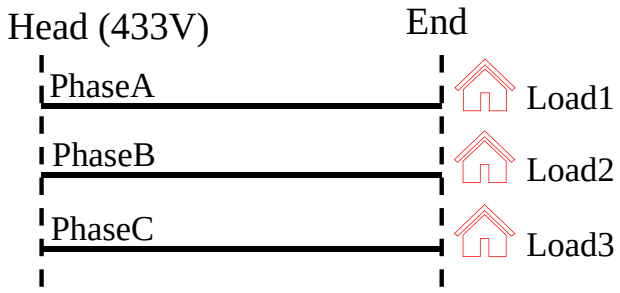

Figure A-1. Example LV feeder

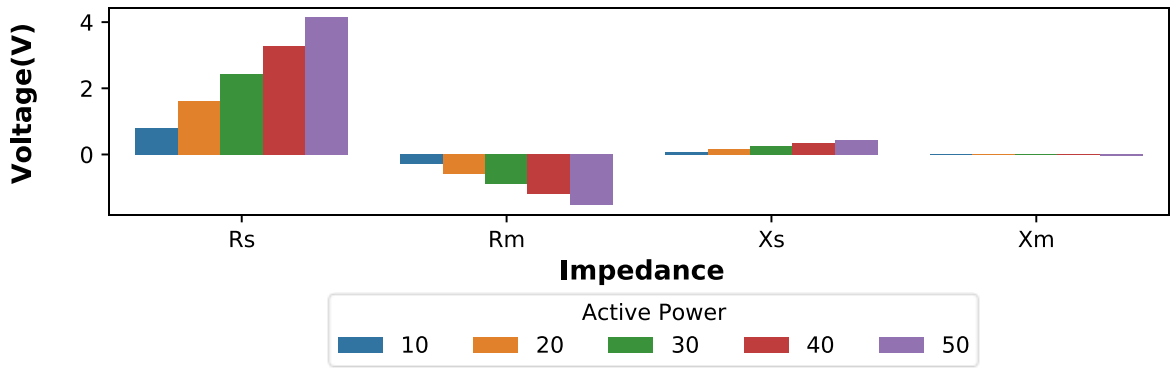

Figure A-2. The voltage mismatch of each load due to the sole impedance variable error (-50%)